Risø–R–615(EN)

The Cup Anemometer

and Other Exciting Instruments

Leif Kristensen

Risø National Laboratory, Roskilde, Denmark
April 1993

Denne afhandling er af Danmarks Tekniske Højskole antaget til forsvar for den tekniske doktorgrad.

Antagelsen er sket efter bedømmelse af den foreliggende afhandling og følgende tre artikler:

1. Busch, N.E. and Kristensen, L. (1976). Cup Anemometer Overspeeding. *J. Appl. Meteorol.*, **15**, 1328-1332.
2. Kristensen, L. and Lenschow, D.H. (1988). The Effect of Nonlinear Dynamic Forcing Response on Measured Means. *J. Atmos. Oceanic Technol.*, **5**, 34-43.
3. Kristensen, L., Casanova, M., Courtney, M.S. and Troen, I. (1991). In Search of a Gust Definition. *Boundary-Layer Meteorol.*, **55**, 91-107.

Lyngby, den 31. marts 1993

Hans Peter Jensen
Rektor

/

Henrik Moltke
Administrationschef

This thesis has been accepted by the Technical University of Denmark for public defence in fulfilment of the requirements for the degree of Doctor Technices.

The acceptance is based on this dissertation and the following three articles:

1. Busch, N.E. and Kristensen, L. (1976). Cup Anemometer Overspeeding. *J. Appl. Meteorol.*, **15**, 1328-1332.
2. Kristensen, L. and Lenschow, D.H. (1988). The Effect of Nonlinear Dynamic Forcing Response on Measured Means. *J. Atmos. Oceanic Technol.*, **5**, 34-43.
3. Kristensen, L., Casanova, M., Courtney, M.S. and Troen, I. (1991). In Search of a Gust Definition. *Boundary-Layer Meteorol.*, **55**, 91-107.

Lyngby, March 31, 1993

Hans Peter Jensen
President

/

Henrik Moltke
Secretary

ISBN 87–550–1796–7 (Second printing)
ISSN 0106–2840

Information Service Department · Risø · 1993

Contents

Abstract Nonlinear sensor dynamics is discussed in terms of differential equations in time with the input signal and the response as dependent variables. The cup anemometer response to the turbulent wind is analyzed in detail. Applying second-order perturbation theory, the so-called overspeeding, which is a bias in the measured mean wind speed due to fluctuations in the longitudinal wind component, is evaluated in terms of a phenomenological model of the wind forcing of the cup rotor. It is shown how the fluctuation in the other wind components give rise to three other types of bias and it is concluded that the positive bias in the mean wind speed due to wind-direction fluctuations is always largest and much larger than the overspeeding and can be as much as 18% whereas the overspeeding only in extreme cases exceeds about 2%. The differential equation describing the cup-anemometer dynamics is of only first order. However, the technique of evaluating the bias on the mean is generalized to apply to sensors with nonlinear dynamics and obeying second-order differential equations. It is then demonstrated how the bias in the mean due to random fluctuations can be determined for three other sensor, namely the Pitot tube, the thrust anemometer and the CSIRO liquid water probe. The last instrument will always have a negative bias. Returning to the discussion of the cup anemometer, it is shown how this instrument can be used together with a wind vane to reduce the bias due to wind direction fluctuations. Finally it is discussed how a precise definition of a gust can be implemented and how gusts can be determined by means of a cup anemometer.

1 Introduction

What makes cup anemometers interesting? Anybody understands intuitively why they are turning and that their rotation rate increases with increasing wind speed. So what is it?

The cup anemometer is a standard instrument, widely used for routine observations as well as for experimental field measurements. Judging from the literature since the 1920's (Kaganov and Yaglom, 1976, Wyngaard, 1981, Coppin, 1982), there has been a considerable interest in understanding the dynamics of the cup anemometer, in particular when it is exposed to a turbulent wind. It has been of great concern that the cup anemometer 'overspeeds', i.e. it responds more quickly to an increase in the wind than to a decrease of the same magnitude and thus tends 'to spend more time on the high side than on the low side of the mean' with the consequence that the measured mean wind speed will be too high. This is of particular importance in the determination of wind stress by measuring wind profiles. The overspeeding is probably the main reason that there has been such an interest in modelling the motion of cup anemometers.

A satisfactory solution to the overspeeding problem was obtained by Wyngaard *et al.* (1974), Kaganov and Yaglom (1976) and Busch and Kristensen (1976). Wyngaard *et al.* (1974) considered a general, phenomenological model of the torque on the cup rotor. They wrote the torque as a second-order expansion in the wind-and response perturbations. They were then able to determine the expansion coefficients by measuring the torque directly in a wind tunnel where they forced the cup anemometer to rotate with a speed which was not in equilibrium with the wind speed. Kaganov and Yaglom (1976) and Busch and Kristensen (1976) independently used this general theory to give an explicit expression for the overspeeding and quantify the corresponding bias in the mean in terms of the turbulence intensity and the cup anemometer distance constant. Their results showed how the quadratic (nonlinear) terms in the forcing were responsible for the overspeeding.

This raises the question whether other instruments have nonlinear forcing and whether this leads to systematic errors in the measured mean values if the input is random and turbulent. In Kristensen and Lenschow (1988) we addressed this question and derived a general theory for first-order systems, of which the cup anemometer may serve as a prototype, and for second-order systems such as thrust anemometers. We applied the theory to a Pitot tube, a thrust anemometer described by Smith (1980) and to the CSIRO liquid water probe (King, 1978).

The theme in the following will be the interpretation of signals from instruments with nonlinear forcing, exposed to a random, turbulent input. Although there is a vast amount of literature about the cup anemometer, this is not a review, but a general introduction to the phenomenological theory of instrument response. It would be possible to trace the history of the cup anemometer by starting with the review by Wyngaard (1981), supplemented by the text book by Middleton and Spilhaus (1953).

First we will deal with the cup anemometer in great detail; we will discuss first- and second-order perturbation equations of motion and the different types of overspeeding. A simple model for the forcing with five parameters will be evaluated, discussed and used to explain the dynamic properties of the cup anemometer. Then we will give an account of the theory of nonlinear forcing of first- and second-order systems by Kristensen and Lenschow (1988) and discuss its application to the Pitot tube, the thrust anemometer and the CSIRO liquid water probe. Since

the operation of this last instrument is based on a special application of a constant-temperature hot-wire anemometer, it would seem natural to include an analysis of this anemometer which, according to Freymuth (1977), has a nonlinear response to the fluctuating wind. Interesting as such an analysis certainly would be, I have decided that it is beyond the scope of this presentation to include a discussion of the hot-wire anemometer with all the details the subject would deserve.

Finally we return to the cup anemometer and show how to use it in conjunction with a wind vane in such a way as to reduce the bias in the measured mean wind velocity due to wind-direction fluctuations and at the same time obtain the mean and the variance of the wind direction. Then we demonstrate how the cup anemometer can be applied in gust measurements. The emphasis in this second application is more on definition and a practical way of predicting gusts.

I hope that the analysis given here will show the need to understand the interaction between instruments and the medium providing the input. Without such understanding, one cannot hope to obtain a correct interpretation of the output. At the same time it is my aspiration to illustrate the exciting response properties of seemingly dull instruments by developing the necessary mathematical tools.

2 The Cup Anemometer

As a field instrument and general-purpose anemometer for operational purposes the cup anemometer has three good properties.

Firstly, it is omnidirectional; when mounting the instrument, it is only necessary to make sure that the axis is pointing in the vertical direction.

Secondly, a good cup anemometer with a linear calibration filters the wind speed in space, along the wind direction, and not in time. This is a very useful property in turbulence measurements since turbulent fluctuations to a very high degree of accuracy (to that of Taylor's hypothesis) can be considered spatial rather than temporal phenomena. As we will see, the filter is of the simplest first-order type with a distance constant which is independent of the wind speed.

Finally, the cup anemometer is robust and easy to operate.

We assume that the cup anemometer is mounted with its axis vertical. In this case the equation for the rotation rate of the rotor can be written

$$\dot{\tilde{s}} = F(\tilde{s}, \sqrt{\tilde{u}^2 + \tilde{v}^2}, \tilde{w}), \tag{1}$$

where $\tilde{u}$, $\tilde{v}$ and $\tilde{w}$ are the instantaneous horizontal and vertical wind components and $\tilde{s}$ is the instantaneous rotation rate of the anemometer rotor in rad s^{-1}. The angular momentum of the rotor is proportional to $\tilde{s}$ and (1) just states that the rate of change* of the angular momentum is equal to the torque on the rotor. This torque is caused by the wind and the friction in the instrument bearings. For a real cup anemometer the right-hand side, the torque divided by the moment of inertia, is a function of $\tilde{s}$, the total horizontal wind component $\sqrt{\tilde{u}^2 + \tilde{v}^2}$ as well as the vertical wind component $\tilde{w}$.

*A dot over a variable signifies differentiation with respect to time. This convention is not used consistently. At certain places I use d/dt for clarity.

2.1 Calibration

When the anemometer is exposed to a horizontal wind speed which at a given time changes from one value to another there will be a non-zero torque on the rotor and $\dot{\tilde{s}}$ will be different from zero until $\tilde{s}$ has obtained such a magnitude that the torque is again zero. This steady-state situation is usually established in less than 1 s. The rotation rate will stay constant as long as the wind speed is constant. It is an increasing function of the wind speed and therefore $\tilde{s}$ is a measure of the wind speed.

The cup anemometer is usually calibrated in a wind tunnel which is operated with wind speeds in the range of interest.

In the steady state, with a constant horizontal wind speed U and a constant rotation rate S, (1) reduces to

$$F(S, U, 0) = 0. \tag{2}$$

Solving (2) for S we obtain the calibration equation

$$S = S(U). \tag{3}$$

Linear calibration

It is a well-known experience that the cup anemometer has a steady-state calibration curve which, for most purposes can be considered linear, i.e. $d^2S/dU^2 = 0$. This means that we can write (3) as

$$S = \frac{U - U_0}{\ell}. \tag{4}$$

Offset speed

Here U_0 is a positive *offset speed*. It is no more than about 0.1 m s^{-1} for a good cup anemometer. Often it is called the starting speed, but that is really a misnomer; when the wind speed is very small—less than 1 m s^{-1}, say—the contribution to the total torque from the friction in the bearings becomes significant and the steady-state calibration expression is no longer close to being linear. Also, experience shows that the real starting speed is in general larger than U_0 (Busch *et al.*, 1980). This means that the cup anemometer is unsuited to operate in very light winds. If the wind speed is just a few meters per second U_0 can be neglected in most applications.

Calibration distance

The quantity ℓ is a length scale which, when $U_0 \ll U$, can be visualized as the length of the column of air which has blown through the anemometer when the rotor has turned one radian. We shall call it the *calibration distance*.

Most cup anemometers are designed such that they have linear calibrations for wind speeds exceeding a few meters per second. Middleton and Spilhaus (1953) cite Brazier (1914) for having discovered that to minimize the second-and higher-order terms in the calibration, the ratio of the cup diameter to the diameter of the circle described by the cup centers must be 0.5. The discovery that shorter cup arms improve the linearity of the calibration is supported by the findings of Patterson (1926). The linearity of the calibration is of importance if we want to use the cup anemometer as described in section 4.

2.2 First-Order Perturbation

In operation the cup anemometer will be exposed to a wind velocity which fluctuates in magnitude and direction. We assume that the mean wind velocity is

horizontal and that the fluctuations are small compared to the mean wind speed U. We decompose the instantaneous wind velocity as

$$\left\{ \begin{array}{c} \tilde{u} \\ \tilde{v} \\ \tilde{w} \end{array} \right\} = \left\{ \begin{array}{c} U+u \\ v \\ w \end{array} \right\}, \tag{5}$$

letting the direction of the mean wind define the x axis.

Denoting averaging by $\langle\ \rangle$, we see that (5) implies

$$\langle u \rangle = \langle v \rangle = \langle w \rangle = 0. \tag{6}$$

Correspondingly, we write the instantaneous rate of rotation as

$$\tilde{s} = S + s, \tag{7}$$

where S is the steady-state calibration given in (3).

The way in which $\tilde{s}$ is decomposed does not guarantee that $\langle s \rangle$ is zero; in fact, $\langle s \rangle \neq 0$ is a manifestation of the so-called overspeeding as we shall see later.

First, however, we will derive a first-order perturbation equation for the rotation rate in u, v, w and s. The overspeeding is caused by the nonlinearity of the function F and can therefore not be determined from this first-order analysis.

Substituting (5) and (7) in (1) and expanding to first order we get

$$\dot{s} = \frac{\partial F}{\partial S} s + \frac{\partial F}{\partial U} u + \frac{\partial F}{\partial W} w, \tag{8}$$

where the derivatives are taken at the point $(S(U), U, 0)$. We note that there are no terms proportional to v; since

$$\begin{aligned} \sqrt{\tilde{u}^2 + \tilde{v}^2} &= \sqrt{(U+u)^2 + v^2} \\ &= U\sqrt{1 + 2\frac{u}{U} + \frac{u^2}{U^2} + \frac{v^2}{U^2}} \\ &= U\left\{ 1 + \frac{1}{2}\left(2\frac{u}{U} + \frac{u^2}{U^2} + \frac{v^2}{U^2} \right) \right. \\ &\qquad \left. - \frac{1}{8}\left(2\frac{u}{U} \right)^2 + \text{higher-order terms} \right\} \\ &\approx U + u + \frac{v^2}{2U}, \end{aligned} \tag{9}$$

the first term containing v in the expansion of $\sqrt{\tilde{u}^2 + \tilde{v}^2}$ is proportional to v^2.

Equation (8) tells us that the angular acceleration of the rotor, $\dot{s}$, is proportional to the instantaneous longitudinal and vertical velocity deviations u and w from the mean and to the deviation of the angular velocity s from S, given by (3).

In order to understand (8), let us first consider a situation in which $w = 0$, so that there is only a horizontal velocity perturbation. Let this be positive—a little step change in speed from U to $U+u$. We know from experience that this will make the rotor turn faster, i.e. $\dot{s} > 0$, and eventually settle at a rotation rate corresponding to the new speed $U + u$. The implication is that $\partial F/\partial U$ must be positive. But then $\partial F/\partial S$, the coefficient in front of s, must be negative. Otherwise the rotation rate will keep growing.

First-order constraint

We can see this in another, more formal way, by differentiating (2) with respect to U, keeping in mind that S is a function of U. The result of this operation is the following constraint

$$\frac{\partial F}{\partial S}\frac{dS}{dU} + \frac{\partial F}{\partial U} = 0. \tag{10}$$

Here dS/dU and $\partial F/\partial U$ are both positive. Consequently, $\partial F/\partial S$ must be negative.

A glance at (8) shows that $\partial F/\partial S$ has the physical dimension of a reciprocal time. We therefore define the time scale

$$\tau_0 = -\left(\frac{\partial F}{\partial S}\right)^{-1}. \tag{11}$$

This time scale will in general be a function of U.

With the help of (10) and (4) we can express $\partial F/\partial U$ in terms of τ_0 and the calibration distance ℓ:

$$\frac{\partial F}{\partial U} = \frac{1}{\tau_0}\frac{dS}{dU} = \frac{1}{\tau_0 \ell}. \tag{12}$$

The first-order perturbation equation (8) can then be reformulated as

$$\dot{s} + \frac{s}{\tau_0} = \frac{1}{\ell}\frac{u}{\tau_0} + \frac{\partial F}{\partial W}w. \tag{13}$$

The right-hand side contains the external forcing, consisting of terms in which the input variables u and w are multiplied by the respective sensitivities of the instrument. The left-hand side is the reaction of the cup anemometer.

Let us consider a situation with a horizontal input $u(t)$ only. Then the first-order perturbation equation for the rotor motion reads

$$\dot{s} + \frac{s}{\tau_0} = \frac{1}{\ell}\frac{u}{\tau_0}. \tag{14}$$

Response to step input

This is the linear response equation of a first-order system with one input $u(t)$. It can be studied in a number of ways. One simple and illuminating diagnostic tool is a study of its response to a step function given by

$$u = \begin{cases} 0 & \text{for } t < 0 \\ \\ \Delta U & \text{for } t \geq 0 \end{cases}. \tag{15}$$

In this case, the response will be

$$s(t) = \frac{\Delta U}{\ell}(1 - \mathrm{e}^{-t/\tau_0}) \tag{16}$$

—the classical response of a first-order system to a step function. Figure 1 shows how the response adjusts to the new equilibrium value of the input. It grows such that when $t = \tau_0$ it has attained 63% of its terminal value $s(\infty)$. The time scale τ_0 is a measure of the time the system needs to respond to a sudden change in the input.

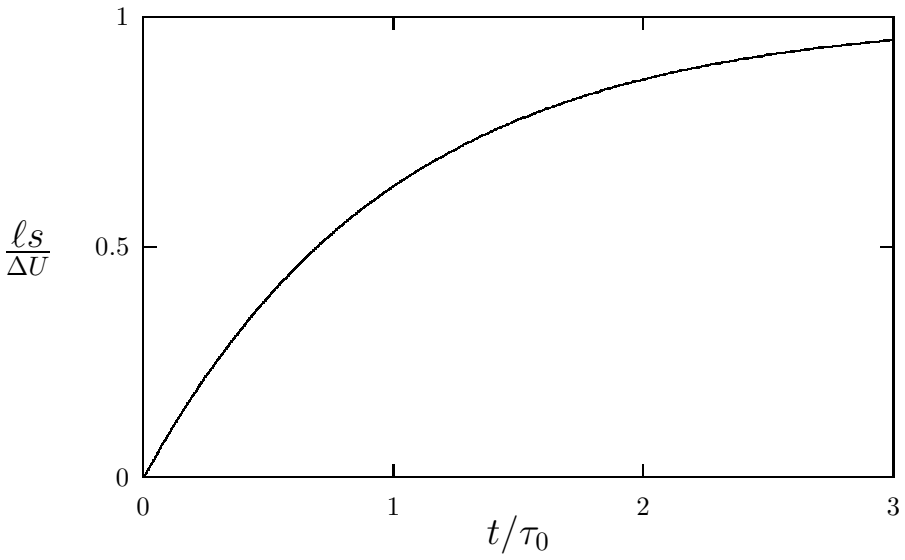

Figure 1. The first-order response (16) of a cup anemometer to a step input ΔU.

Let us return to the more general equation (13). We saw that the coefficient of u was determined by (4), (10) and (11). How can we relate the coefficient $\partial F/\partial W$ to observed cup-anemometer characteristics? The answer is that this quantity is connected with the first-order *angular response* of the cup anemometer. First, however, we must specify what we understand by the term angular response.

Angular response, definition

We define it in terms of a constant wind velocity $\mathbf{U}$ which forms an angle ϑ with the rotor plane. Such a situation can be obtained in a wind tunnel, operated at constant speed U, by tilting the anemometer the angle ϑ from vertical. When the anemometer is tilted towards the flow, this corresponds to a downward or negative velocity component as seen from the anemometer; in that case we consider ϑ negative. Conversely, tilting the anemometer away from the flow gives a positive angle of attack ϑ. Figure 2 illustrates how the cup anemometer is mounted in the wind tunnel in the case when a positive vertical wind component is simulated.

The total speed is $U = |\mathbf{U}|$ and we denote the component perpendicular to the rotor plane w_ϑ. The component in the rotor plane is the sum of U and the perturbation u_ϑ, which of course is zero when w_ϑ is zero. With these definitions, simple geometrical considerations lead to

$$(U + u_\vartheta)^2 + w_\vartheta^2 = U^2. \tag{17}$$

and, solving (17) for u_ϑ, we get

$$u_\vartheta = -\left(U - \sqrt{U^2 - w_\vartheta^2}\right). \tag{18}$$

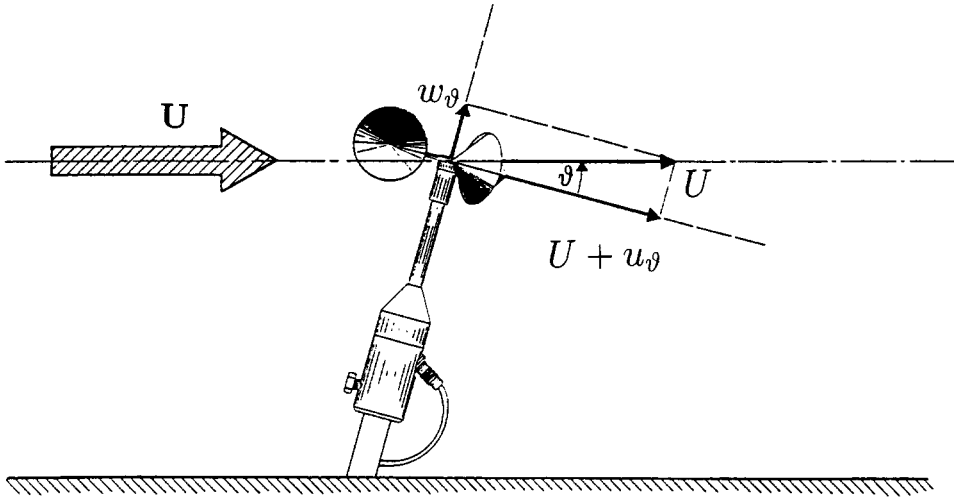

Figure 2. A cup anemometer mounted in a wind tunnel for angular response determination.

The angle of attack becomes

$$\vartheta = \arcsin\Big(\frac{w_\vartheta}{U}\Big)\,. \tag{19}$$

The steady-state response of the cup anemometer S is in this situation a function of ϑ and U and we define the angular response as $g(\vartheta, U)$ as

$$g(\vartheta, U) = \frac{S(\vartheta, U)}{S(0, U)}. \tag{20}$$

Busch *et al.* (1980) show the angular response of the Risø-70 model. The data were obtained in a wind tunnel with wind speeds U in the interval from 7 to 18 m s^{-1}. The curve they show represents an average from which the individual curves do not deviate more than 0.001 in the interval from $-45°$ to $+45°$. On basis of this result we assume that the angular response of a cup anemometer in general can be assumed independent of the wind speed.

We are in general interested only in the case $|w_\vartheta| \ll U$ and then (18) and (19) become

$$u_\vartheta \approx -\frac{w_\vartheta^2}{2U} \tag{21}$$

and

$$\vartheta \approx \frac{w_\vartheta}{U}. \tag{22}$$

Equation (21) shows that the constant perturbation w_ϑ of the vertical velocity component implies a perturbation in horizontal velocity component of second order in w_ϑ.

First-order angular response

Denoting the anemometer perturbation response s_ϑ and applying (13) to this

situation, we get

$$s_\vartheta = \tau_0 \frac{\partial F}{\partial W} w_\vartheta, \tag{23}$$

since $\dot{s_\vartheta} = 0$ for a constant input. The u_ϑ-term is of order w_ϑ^2 and must consequently be left out in first-order considerations.

Applying (4) to the horizontal wind component $U + u_\vartheta \approx U$ and assuming that U_0 can be neglected, we recast (23) in the form

$$\frac{s_\vartheta}{S} = \ell\tau_0 \frac{\partial F}{\partial W} \frac{w_\vartheta}{U} = \ell\tau_0 \frac{\partial F}{\partial W} \vartheta. \tag{24}$$

The angular response to the first order in ϑ thus becomes

$$g(\vartheta) = \frac{S + s_\vartheta}{S} = 1 + \ell\tau_0 \frac{\partial F}{\partial W} \vartheta. \tag{25}$$

The function $g(\vartheta)$ is assumed independent of U, and the coefficient

$$\mu_1 = \ell\tau_0 \frac{\partial F}{\partial W} \tag{26}$$

in front of ϑ is therefore also independent of U. As shown here, the value of μ_1 can be determined in a wind tunnel.

Going back to (20), we see that the linear calibration (4) with $U_0 = 0$ implies that

$$S(\vartheta, U) = \frac{U}{\ell} g(\vartheta). \tag{27}$$

Ideally, we would like the cup anemometer to be sensitive only to the wind component in the rotor plane. This requires that $g(\vartheta) = \cos(\vartheta)$. For small angles we have to second order in ϑ

$$\cos(\vartheta) \approx 1 - \frac{\vartheta^2}{2}.$$

In other words, for a good cup anemometer, the angular response should not contain a term proportional to ϑ. This is the case in (25) if μ_1 is not zero. In the next subsection, where we discuss second-order perturbations, we return to a more complete description of the angular response and at that occasion we will include all terms of second order in w_ϑ.

After having introduced the constant μ_1, we rewrite the first-order perturbation equation (13) as

$$\dot{s} + \frac{s}{\tau_0} = \frac{1}{\ell} \left\{ \frac{u}{\tau_0} + \mu_1 \frac{w}{\tau_0} \right\}. \tag{28}$$

With the initial condition $s(-\infty) = 0$, the solution to this equation is *First-order solution*

$$s(t) = \frac{1}{\ell} \int_0^\infty \{u(t-\tau) + \mu_1 w(t-\tau)\} \exp(-\tau/\tau_0) \frac{d\tau}{\tau_0}. \tag{29}$$

This result will be an important ingredient when we are going to discuss second-order perturbations and overspeeding.

Before we leave the subject of first-order perturbations, we will briefly return to first-order constraints, but in a little more general way.

Two first-order constraints

We imagine a steady-state condition in which W can be different from zero. Then

$$F(S(U,W),U,W) = 0. \tag{30}$$

In other words, the rotation rate S must be considered a function of both U and W.

We are dealing with this function in the neighborhood of the point $(S(U,W),U,W) = (S(U,0),U,0)$ and therefore S is the same linear function of U as that given by (4), i.e.

$$\frac{\partial S}{\partial U} = \frac{1}{\ell}. \tag{31}$$

Taking the partial derivative of (30) with respect to U we get

$$\frac{\partial F}{\partial S}\frac{1}{\ell} + \frac{\partial F}{\partial U} = 0. \tag{32}$$

This equation is equivalent to (10).

Taking the derivative of (30) with respect to W yields

$$\frac{\partial F}{\partial S}\frac{\partial S}{\partial W} + \frac{\partial F}{\partial W} = 0. \tag{33}$$

Applying (11) and (26) to (33), we see that $\partial S/\partial W$ given by

$$\frac{\partial S}{\partial W} = \frac{\mu_1}{\ell}. \tag{34}$$

Since μ_1 and ℓ by assumption are independent of U in the neighborhood of $(S(U,W),U,W) = (S(U,0),U,0)$, the derivatives of (31) and (34) with respect to U are zero in the point $(S(U,0),U,0)$, i.e.

$$\frac{\partial^2 S}{\partial U^2} = \frac{\partial^2 S}{\partial U \partial W} = 0. \tag{35}$$

However, there are no a priori reason that the second derivative of S with respect to W is zero in this point.

The constraints (32) and (33) will, together with (29), be important for the evaluation of overspeeding.

2.3 Second-Order Perturbation

We now turn to the second-order expansion of (1) in the neighborhood of the equilibrium point $(S(U),U,0)$.

We have to be careful with the second argument of the forcing function because it contains the lateral component v to the second power; however, there is no second-order term in u as (9) shows.

Expanding $F(\tilde{s},\sqrt{\tilde{u}^2+\tilde{v}^2},\tilde{w})$ in the neighborhood of $(S(U),U,0)$ and collecting terms of the same order, we get

$$\begin{aligned}\dot{s}+\frac{s}{\tau_0} &= \frac{1}{\ell\tau_0}u+\frac{\mu_1}{\ell\tau_0}w+\frac{1}{\ell\tau_0}\frac{v^2}{2U}\\ &\quad+\frac{1}{2}\left\{\frac{\partial^2 F}{\partial U^2}u^2+2\frac{\partial^2 F}{\partial U\partial W}uw+\frac{\partial^2 F}{\partial W^2}w^2\right\}\\ &\quad+\frac{1}{2}\left\{\frac{\partial^2 F}{\partial S^2}s^2+2\frac{\partial^2 F}{\partial S\partial U}su+2\frac{\partial^2 F}{\partial W\partial S}ws\right\}. \end{aligned} \tag{36}$$

This is a very 'nasty', nonlinear differential equation if we were going to find an exact solution as we did with the first-order perturbation equation (28). In the next section we will see that it is not necessary to find the solution to (36) in order to obtain expressions for the overspeeding.

Three second-order constraints

However, before we turn to this subject we will derive three more constraints between the second derivatives of $F(S(U,W),U,W)$ in the point $(S(U,W),U,W) = (S(U,0),U,0)$.

Taking the derivatives of (32) and (33) with respect to U and W at this point, we obtain, after using (34) to replace $\partial S/\partial W$,

$$\frac{\partial^2 F}{\partial S^2}\frac{1}{\ell^2}+2\frac{\partial^2 F}{\partial S\partial U}\frac{1}{\ell}+\frac{\partial^2 F}{\partial U^2}=0, \tag{37}$$

$$\frac{\partial^2 F}{\partial S^2}\frac{\mu_1}{\ell^2}+\frac{\partial^2 F}{\partial S\partial U}\frac{\mu_1}{\ell}+\frac{\partial^2 F}{\partial W\partial S}\frac{1}{\ell}+\frac{\partial^2 F}{\partial U\partial W}=0 \tag{38}$$

and

$$\frac{\partial^2 S}{\partial W^2}\frac{\partial F}{\partial S}+\frac{\partial^2 F}{\partial S^2}\frac{\mu_1^2}{\ell^2}+2\frac{\partial^2 F}{\partial W\partial S}\frac{\mu_1}{\ell}+\frac{\partial^2 F}{\partial W^2}=0. \tag{39}$$

We note that (39) has a term proportional to the second derivative $\partial^2 S/\partial W^2$. As was the case with the first derivative, it is possible to obtain information about $\partial^2 S/\partial W^2$ by determining the the angular response to the second order in w_ϑ.

Second-order angular response

Proceeding as in last subsection and, once again, applying (21), we get from (36)

$$\begin{aligned}\frac{s_\vartheta}{\tau_0} &= -\frac{w_\vartheta^2}{2\ell U\tau_0}+\mu_1\frac{w_\vartheta}{\ell\tau_0}\\ &\quad+\frac{1}{2}\left\{\frac{\partial^2 F}{\partial U^2}\left(-\frac{w_\vartheta^2}{2U}\right)^2+2\frac{\partial^2 F}{\partial U\partial W}\left(-\frac{w_\vartheta^3}{2U}\right)+\frac{\partial^2 F}{\partial W^2}w_\vartheta^2\right\}\\ &\quad+\frac{1}{2}\left\{\frac{\partial^2 F}{\partial S^2}s_\vartheta^2+2\frac{\partial^2 F}{\partial S\partial U}s_\vartheta\left(-\frac{w_\vartheta^2}{2U}\right)+2\frac{\partial^2 F}{\partial W\partial S}w_\vartheta s_\vartheta\right\}. \end{aligned} \tag{40}$$

Noting from this equation that s_ϑ is of the order w_ϑ to at least the first power and, retaining terms of no higher than second order in w_ϑ, we rewrite (40) as

$$\frac{1}{2}\frac{\partial^2 F}{\partial S^2}s_\vartheta^2-\frac{1}{\tau_0}\left\{1-\tau_0\frac{\partial^2 F}{\partial W\partial S}w_\vartheta\right\}s_\vartheta+\mu_1\frac{w_\vartheta}{\ell\tau_0}+\frac{1}{2\tau_0}\left\{\frac{\partial^2 F}{\partial W^2}-\frac{1}{\ell U}\right\}w_\vartheta^2=0. \tag{41}$$

This is a quadratic equation in s_ϑ. Substitution of $\mu_1 w_\vartheta/\ell$ for s_ϑ in the first term of (41) yields the solution †

$$s_\vartheta = \mu_1 \frac{w_\vartheta}{\ell} + \frac{\tau_0}{2}\left\{\frac{\partial^2 F}{\partial S^2}\frac{\mu_1^2}{\ell^2} + 2\frac{\partial^2 F}{\partial W \partial S}\frac{\mu_1}{\ell} + \frac{\partial^2 F}{\partial W^2} - \frac{1}{\ell U \tau_0}\right\} w_\vartheta^2. \tag{42}$$

Comparing the coefficient of w_ϑ^2 with (39), we see that (42) can also be written

$$s_\vartheta = \mu_1 \frac{w_\vartheta}{\ell} + \frac{1}{2}\left\{\frac{\partial^2 S}{\partial W^2} - \frac{1}{\ell U}\right\} w_\vartheta^2, \tag{43}$$

where we have used (11) to replace $\partial F/\partial S$ with $-1/\tau_0$.

Ignoring the offset speed, i.e. using the approximation $U \approx \ell S$, the angular response now becomes

$$\begin{aligned} g(\vartheta) &\approx g\Big(\frac{w}{U}\Big) = 1 + \frac{s_\vartheta}{S} \\ &\approx 1 + \mu_1 \frac{w_\vartheta}{U} + \frac{1}{2}\left\{\ell U \frac{\partial^2 S}{\partial W^2} - 1\right\}\frac{w_\vartheta^2}{U^2} \\ &= 1 - \frac{w_\vartheta^2}{2U^2} + \mu_1 \frac{w_\vartheta}{U} + \frac{1}{2}\mu_2 \frac{w_\vartheta^2}{U^2} \\ &\approx \cos(\vartheta) + \mu_1 \vartheta + \frac{1}{2}\mu_2 \vartheta^2, \end{aligned} \tag{44}$$

where we have defined the quantity μ_2 by

$$\mu_2 = \ell U \frac{\partial^2 S}{\partial W^2}. \tag{45}$$

Again, based on measurements (Busch *et al.*, 1980), we assume that the angular response is independent of the wind speed U. Consequently, μ_2 must also be independent of U.

We see from (44) that the cup anemometer has a cosine angular response only when both μ_1 and μ_2 are zero.

The constraint (39) can now be reformulated in terms of the new constant μ_2 as

$$\frac{\partial^2 F}{\partial S^2}\frac{\mu_1^2}{\ell^2} + 2\frac{\partial^2 F}{\partial W \partial S}\frac{\mu_1}{\ell} + \frac{\partial^2 F}{\partial W^2} = \frac{\mu_2}{\ell U \tau_0}. \tag{46}$$

Wind tunnel measurements

Wyngaard *et al.* (1974) were the first to formulate a general equation of motion in terms of the first and second derivatives of $F(S,U,W)$ for $(S(U,W),U,W) = (S(U,0),U,0)$ and to determine these quantities in a wind tunnel for one particular cup anemometer‡. Leaving out the lateral velocity fluctuations, they reformulated (36) in terms of $s' = s/S$, $u' = u/U$ and $w' = w/U$ in the following way

† A quadratic equation has of course two solutions. The other solution contains a term of order w_ϑ^0, i.e. a constant, and is therefore not realistic since s_ϑ must be zero when w_ϑ is zero.

‡ Wyngaard (1991, private communication) believes, without being completely certain, that the cup assembly is identical to that used in the Kansas Windy Acres 1968 field experiment (Haugen *et al.*, 1971 and Businger *et al.*, 1971).

$$
\begin{aligned}
s' + \tau_0 \dot{s}' \quad = \quad & a_1 u' + a_2 w' \\
& + a_3 {s'}^2 + a_4 {u'}^2 + a_5 {w'}^2 \\
& + a_6 u' s' + a_7 u' w' + a_8 s' w'. \qquad (47)
\end{aligned}
$$

Comparing with (36) we can state their results in both their and our notation as follows

$$
\left\{ \begin{array}{c} a_1 \\ a_2 \\ a_3 \\ a_4 \\ a_5 \\ a_6 \\ a_7 \\ a_8 \end{array} \right\} \equiv \left\{ \begin{array}{c} 1 \\ \mu_1 \\ \frac{1}{2}\frac{\partial^2 F}{\partial S^2}\frac{U\tau_0}{\ell} \\ \frac{1}{2}\frac{\partial^2 F}{\partial U^2}\ell U\tau_0 \\ \frac{1}{2}\frac{\partial^2 F}{\partial W^2}\ell U\tau_0 \\ \frac{\partial^2 F}{\partial S \partial U} U\tau_0 \\ \frac{\partial^2 F}{\partial U \partial W}\ell U\tau_0 \\ \frac{\partial^2 F}{\partial W \partial S} U\tau_0 \end{array} \right\} = \left\{ \begin{array}{rr} 1.03 & < \pm 10\% \\ 0.06 & \pm 0.1 \\ -0.23 & < \pm 10\% \\ 0.96 & < \pm 10\% \\ 0.67 & \pm 0.1 \\ -0.73 & < \pm 10\% \\ 0.04 & \pm 0.1 \\ -0.12 & \pm 0.1 \end{array} \right\}. \qquad (48)
$$

Here we have again assumed that $U = \ell S$ and in that case the condition

$$a_1 = 1 \qquad (49)$$

must be fulfilled.

Further, the constraints (37) and (38) imply

$$a_3 + a_4 + a_6 = 0 \qquad (50)$$

and

$$2a_2(a_3 + a_6) + a_7 + a_8 = 0. \qquad (51)$$

The three tests (49), (50) and (51) are fulfilled well within the experimental uncertainty.

We can use the measurements by Wyngaard *et al.* (1974) and the constraint (46) to determine the constant μ_2 for their anemometer. The result is

$$\mu_2 = 2(a_2^2 a_3 + a_2 a_8 + a_5) \approx 2a_5 = 1.3. \qquad (52)$$

Coppin (1982) determined a_1, a_3, a_4, a_5 and a_6 for a number of different cup anemometers. He also found that (50) was satisfied within the accuracy of the measurements and that a_5 ranged from 0.47 to 0.90. Unfortunately, Coppin (1982) does not present results concerning a_2, a_7 or a_8. It seems that he assumes, on basis

of arguments and measurements by Wyngaard *et al.* (1974), that these three quantities safely can be set equal to zero. We can therefore not check if his data fulfil (51). However, assuming that a_2 is in fact zero, or at least very small compared to one, we conclude from (52) that

$$\frac{\partial^2 F}{\partial W^2} = \frac{2a_5}{\ell U \tau_0} \approx \frac{\mu_2}{\ell U \tau_0}. \tag{53}$$

This equation implies, together with (26), that we can determine *the torque* as a function of the vertical velocity component, by measuring the angular response and determining the two parameters μ_1 and μ_2. Later, we will show how it is possible to use a simple model for the response to the horizontal wind to express the torque as a function of this wind component in terms of ℓ and two more instrument parameters.

2.4 Overspeeding

With the second-order perturbation equation (36) we are also equipped to study and discuss overspeeding. But first we will try to understand why a cup anemometer must be expected to give a positive bias to the mean in a turbulent wind. We follow the line of arguments by Wyngaard (1981).

The wind force on one cup depends not only on the magnitude of the wind speed relative to the cup. It also depends on the angle of attack. For the same relative wind speed, the force is larger when the wind blows into the cup than when it blows on its outside. Intuitively, this seems obvious, but it is also confirmed experimentally by Patterson (1926), who measured the force as a function of the angle of attack. In both cases the force is in the direction of the relative wind speed and is proportional to its square.

In a constant wind with speed U, the cup speed U_c will also be constant. The cup speed will be smaller that U. Otherwise the relative wind will blow on the same side of the cup, no matter where it is in its motion around the rotor axis; there will then be a net torque, forcing the rotor to slow down until the condition $U_c < U$ is fulfilled. When the cup moves in the direction of the wind, the average force on the cup will roughly be $K_+(U - U_c)^2$, where K_+ is a positive constant. When it moves against the wind the force will be $K_-(U + U_c)^2$, where K_- is another positive constant.

The total average torque F on the rotor, made up by the contributions from each cup, must be zero when U and U_c are constant, viz.

$$F = rA(N_c)\{K_+(U - U_c)^2 - K_-(U + U_c)^2\} = 0. \tag{54}$$

In (54) r is the radius of the rotor, N_c the number of cups and $A(N_c)$ an unknown (positive) function which of course would be equal to N_c if the cups were not in each others wake most of the time. In these semiquantitative arguments we neglect the effect of the friction in the bearings.

Equation (54) implies that $K_+ > K_-$.

If there is a sudden change in the wind speed from U to $U + u$, the torque will initially be

$$F = rA(N_c)\{K_+(U + u - U_c)^2 - K_-(U + u + U_c)^2\}$$

$$= \quad rA(N_c)\{[K_+ - K_-]u^2 + 2[K_+(U - U_c) - K_-(U + U_c)]u\}, \qquad (55)$$

where we have used (54). The coefficient of u^2 is positive. The coefficient of u must also be positive when U and U_c are different from zero since (54) implies, not only that $K_+ > K_-$, but also that

$$\sqrt{K_+}(U - U_c) = \sqrt{K_-}(U + U_c). \qquad (56)$$

If the left-hand side of (56) is multiplied by $\sqrt{K_+}$ and the right-hand side by $\sqrt{K_-}$, we obtain the inequality

$$K_+(U - U_c) > K_-(U + U_c), \qquad (57)$$

which shows that the coefficient of u is positive. A sudden increase u of the wind speed will then give a torque which is numerically larger than a sudden decrease $-u$ of the same magnitude. Since the rotation rate is not in equilibrium with the turbulent wind, which constantly has many small and fast changes up and down, the rotor will on average tend to run too fast with respect to the mean wind and thus give a positive bias.

Kaganov and Yaglom (1976) and Busch and Kristensen (1976) independently analyzed this phenomenon quantitatively and arrived at the same result, the last authors with arguments which we will present here in a somewhat different and expanded form.

Turning now to this more rigorous analysis, we consider a situation where the wind velocity is horizontal in the mean and stationary so that $\langle u \rangle = \langle v \rangle = \langle w \rangle = 0$. Taking the average of (36) and normalizing by $S = S(U)$, we obtain

$$\begin{aligned} \frac{\langle s \rangle}{S} \quad = \quad & \frac{\langle v^2 \rangle}{2U^2} \\ & + \frac{\ell\tau_0}{2U}\left\{\frac{\partial^2 F}{\partial U^2}\langle u^2\rangle + 2\frac{\partial^2 F}{\partial U \partial W}\langle uw\rangle + \frac{\partial^2 F}{\partial W^2}\langle w^2\rangle\right\} \\ & + \frac{\ell\tau_0}{2U}\left\{\frac{\partial^2 F}{\partial S^2}\langle s^2\rangle + 2\frac{\partial^2 F}{\partial S \partial U}\langle su\rangle + 2\frac{\partial^2 F}{\partial W \partial S}\langle ws\rangle\right\}. \end{aligned} \qquad (58)$$

where we have used the linear calibration (4) and neglected the offset U_0[§].

The right-hand side of this equation is in general not zero, but will be dependent on the turbulent properties of the atmosphere in the measuring period. Since the cup anemometer is calibrated in a constant, laminar wind field in a wind tunnel, this means that $\langle s \rangle$ will be interpreted as an addition to the measured mean wind speed if we use the calibration expression (3) or (4).

Four bias types

According to (58) the relative bias $\langle s \rangle / S$ gets contributions from the three different velocity components. There are terms proportional to the variances $\langle u^2 \rangle$, $\langle v^2 \rangle$ and $\langle w^2 \rangle$ and one term proportional to the covariance $\langle uw \rangle$, the so-called stress. The last line of (58) shows terms where the response s enters, either as its variance or as its covariances with u and w. These last three terms make the study of

[§]I could easily take the offset into account, but the clarity of the presentation of overspeeding would suffer without any significant information being added. It is probably advisable to include the offset in an actual instrument investigation if the wind speed is low.

overspeeding very interesting. They will be determined by means of the first-order solution (29) and shown to get all their contributions from low-frequency variances and covariance of u and w. The total bias can therefore be partitioned according to origin—whether it is the variance of u, v or w, or the covariance of u and w. We will call them u-bias, v-bias, w-bias and stress-bias, respectively, and denote them δ_u, δ_v, δ_w and δ_*.

v-bias

The v-bias

$$\delta_v = \frac{\langle v^2 \rangle}{2U^2},$$

stands out by itself. It is not 'mixed up' with any of the other velocity components or with the response. Obviously, there would be no v-bias if there were no wind-direction fluctuations. The bias is there because the cup anemometer responds, not only to the longitudinal velocity component $\tilde{u}$, but to the *total* horizontal wind component $\sqrt{\tilde{u}^2 + \tilde{v}^2}$. Therefore there will be a contribution which corresponds exactly to the third term in the last line of (9). If we were interested in the mean of the total horizontal wind speed we would not call v-bias a bias at all¶.

$\langle s^2 \rangle$, $\langle su \rangle$ and $\langle ws \rangle$

Now we evaluate $\langle s^2 \rangle$, $\langle su \rangle$ and $\langle ws \rangle$ in (58) by means of the first-order solution (29). Introducing the covariance functions

$$R_u(\tau) = \langle u(t)u(t+\tau) \rangle, \tag{59}$$

$$R_{uw}(\tau) = \langle u(t)w(t+\tau) \rangle \tag{60}$$

and

$$R_w(\tau) = \langle w(t)w(t+\tau) \rangle, \tag{61}$$

we get, using (29),

$$\langle su \rangle = \frac{1}{\ell} \int_0^\infty \{R_u(\tau) + \mu_1 R_{uw}(-\tau)\} \exp(-\tau/\tau_0) \frac{d\tau}{\tau_0} \tag{62}$$

and

$$\langle ws \rangle = \frac{1}{\ell} \int_0^\infty \{R_{uw}(\tau) + \mu_1 R_w(\tau)\} \exp(-\tau/\tau_0) \frac{d\tau}{\tau_0}. \tag{63}$$

Noting that s to the first order is a stationary time series for which

$$0 = \frac{d\langle s^2 \rangle}{dt} = 2\langle s\dot{s} \rangle, \tag{64}$$

we can determine $\langle s^2 \rangle$ from (62) and (63) by multiplying the first-order perturbation equation (28) by s and averaging. This procedure results in

$$\begin{aligned} \langle s^2 \rangle &= \frac{1}{\ell}\{\langle us \rangle + \mu_1 \langle ws \rangle\} \\ &= \frac{1}{\ell^2} \int_0^\infty \{R_u(\tau) + \mu_1[R_{uw}(\tau) + R_{uw}(-\tau)] + R_w(\tau)\} \\ &\qquad \times \exp(-\tau/\tau_0) \frac{d\tau}{\tau_0}. \end{aligned} \tag{65}$$

¶This bias is known in the literature under the name 'DP-error' (MacCready, 1966), which stands for data-processing error.

It turns out to be convenient to express the biases in terms of the power spectra, $S_u(\omega)$ and $S_w(\omega)$, and the cross-spectrum $S_{uw}(\omega)$. Therefore we write the covariances as

$$R_u(\tau) = \int_{-\infty}^{\infty} S_u(\omega) \exp(i\omega\tau) d\omega \tag{66}$$

$$R_{uw}(\tau) = \int_{-\infty}^{\infty} S_{uw}(\omega) \exp(i\omega\tau) d\omega \tag{67}$$

and

$$R_w(\tau) = \int_{-\infty}^{\infty} S_w(\omega) \exp(i\omega\tau) d\omega, \tag{68}$$

where

$$S_u(\omega) = \frac{1}{2\pi} \int_{-\infty}^{\infty} R_u(\tau) \exp(-i\omega\tau) d\tau, \tag{69}$$

$$S_{uw}(\omega) = \frac{1}{2\pi} \int_{-\infty}^{\infty} R_{uw}(\tau) \exp(-i\omega\tau) d\tau \tag{70}$$

and

$$S_w(\omega) = \frac{1}{2\pi} \int_{-\infty}^{\infty} R_w(\tau) \exp(-i\omega\tau) d\tau. \tag{71}$$

The cross-spectrum $S_{uw}(\omega)$ is in general complex and is traditionally expressed in terms of the even cospectrum $Co_{uw}\omega$ and the odd quadrature-spectrum $Q_{uw}(\omega)$ as

$$S_{uw}(\omega) = Co_{uw}(\omega) + i\, Q_{uw}(\omega). \tag{72}$$

Substituting (66), (67) and (68) into (62), (63) and (65), we get

$$\langle su \rangle = \frac{1}{\ell} \int_{-\infty}^{\infty} \frac{S_u(\omega)}{1 + \omega^2 \tau_0^2} d\omega + \frac{\mu_1}{\ell} \int_{-\infty}^{\infty} \frac{Co_{uw}(\omega) + \omega\tau_0 Q_{uw}(\omega)}{1 + \omega^2 \tau_0^2} d\omega, \tag{73}$$

$$\langle ws \rangle = \frac{\mu_1}{\ell} \int_{-\infty}^{\infty} \frac{S_w(\omega)}{1 + \omega^2 \tau_0^2} d\omega + \frac{1}{\ell} \int_{-\infty}^{\infty} \frac{Co_{uw}(\omega) - \omega\tau_0 Q_{uw}(\omega)}{1 + \omega^2 \tau_0^2} d\omega \tag{74}$$

and

$$\langle s^2 \rangle = \frac{1}{\ell^2} \int_{-\infty}^{\infty} \frac{S_u(\omega)}{1 + \omega^2 \tau_0^2} d\omega + \frac{\mu_1^2}{\ell^2} \int_{-\infty}^{\infty} \frac{S_w(\omega)}{1 + \omega^2 \tau_0^2} d\omega + \frac{\mu_1}{\ell^2} \int_{-\infty}^{\infty} \frac{2\, Co_{uw}(\omega)}{1 + \omega^2 \tau_0^2} d\omega. \tag{75}$$

Equations (73), (74) and (75) show that most of the contributions to the covariances $\langle su \rangle$ and $\langle ws \rangle$ and to the variance $\langle s^2 \rangle$ come from the low-frequency part of the variances $\langle u^2 \rangle$ and $\langle w^2 \rangle$ and the covariance $\langle uw \rangle$. As we shall see, it will be convenient to decompose these last quantities in their low-frequency and high-frequency parts according to

$$\langle u^2 \rangle = R_u(0) = \int_{-\infty}^{\infty} \frac{S_u(\omega)}{1 + \omega^2 \tau_0^2} d\omega + \int_{-\infty}^{\infty} \frac{\omega^2 \tau_0^2}{1 + \omega^2 \tau_0^2} S_u(\omega) d\omega, \tag{76}$$

$$\langle uw\rangle = R_{uw}(0) = \int_{-\infty}^{\infty} \frac{Co_{uw}(\omega)}{1+\omega^2\tau_0^2} d\omega + \int_{-\infty}^{\infty} \frac{\omega^2\tau_0^2}{1+\omega^2\tau_0^2} Co_{uw}(\omega) d\omega \tag{77}$$

and

$$\langle w^2\rangle = R_w(0) = \int_{-\infty}^{\infty} \frac{S_w(\omega)}{1+\omega^2\tau_0^2} d\omega + \int_{-\infty}^{\infty} \frac{\omega^2\tau_0^2}{1+\omega^2\tau_0^2} S_w(\omega) d\omega. \tag{78}$$

It is now in principle easy to evaluate (58) by substituting (73) through (78) and by applying the constraints (37), (38) and (46). However, let us go a little slow in the beginning.

u-bias

Imagine for a moment that there are no w-fluctuations. Then $\langle w^2\rangle = \langle uw\rangle = 0$ and $\langle ws\rangle = 0$. Further, each of the equations (73) and (75) have only one term on the right-hand side, namely that containing $S_u(\omega)$. In this case, where there are only contributions from fluctuations in u, the entire relative bias $\langle s\rangle/S$ is equal to δ_u. Evaluation of (58) yields

$$\begin{aligned}
\delta_u &= \frac{\ell\tau_0}{2U}\left\{\frac{\partial^2 F}{\partial S^2}\langle s^2\rangle + 2\frac{\partial^2 F}{\partial S\partial U}\langle su\rangle + \frac{\partial^2 F}{\partial U^2}\langle u^2\rangle\right\} \\
&= \frac{\ell\tau_0}{2U}\left\{\frac{\partial^2 F}{\partial S^2} + 2\frac{\partial^2 F}{\partial S\partial U} + \frac{\partial^2 F}{\partial U^2}\right\}\int_{-\infty}^{\infty}\frac{S_u(\omega)}{1+\omega^2\tau_0^2}d\omega \\
&\quad + \frac{\ell\tau_0}{2U}\frac{\partial^2 F}{\partial U^2}\int_{-\infty}^{\infty}\frac{\omega^2\tau_0^2}{1+\omega^2\tau_0^2}S_u(\omega)d\omega \\
&= \frac{\ell U\tau_0}{2}\frac{\partial^2 F}{\partial U^2}\frac{1}{U^2}\int_{-\infty}^{\infty}\frac{\omega^2\tau_0^2}{1+\omega^2\tau_0^2}S_u(\omega)d\omega,
\end{aligned} \tag{79}$$

where we have used (37) to obtain the last line.

Equation (79) shows that the u-bias is proportional to the integral of the product of the spectrum $S_u(\omega)$ and the high-pass filter

$$H(\omega) = \frac{\omega^2\tau_0^2}{1+\omega^2\tau_0^2}, \tag{80}$$

i.e. the high-frequency u-variance, divided by U^2. Going back to (48), we identify as the factor in front of $1/U^2$ as the coefficient a_4, introduced by Wyngaard *et al.* (1974). We may therefore also write (79) as

$$\delta_u = \frac{a_4}{U^2}\int_{-\infty}^{\infty}\frac{\omega^2\tau_0^2}{1+\omega^2\tau_0^2}S_u(\omega)d\omega. \tag{81}$$

This final result makes intuitively a lot of sense. We expect the u-bias to be larger for larger relative turbulence intensities $\sqrt{\langle u^2\rangle}/U$. Since the power spectrum $S_u(\omega)$ is in fact proportional to the variance of the longitudinal velocity component, (79) or (81) shows that δ_u is proportional to the square of the relative turbulence intensity. The integral picks out the high-frequency part of the spectrum as the part of the variance which contributes. Fluctuations faster than the reciprocal of the time constant τ_0 contribute whereas the anemometer is fast enough to follow fluctuations slower than $1/\tau_0$, so that these are correctly contributing to the mean.

Integral time scale

Figure 3 shows the situation. A typical power spectrum of $u(t)$, normalized by the

variance $\langle u^2 \rangle$, is shown as a function of the dimensionless frequency $\omega \mathcal{T}_u$, where

$$\mathcal{T}_u = \int_0^\infty \frac{R_u(\tau)}{R_u(0)} d\tau \tag{82}$$

is the so-called integral time scale of the time series $u(t)$—a measure of the 'memory' of $u(t)$ in the sense that $R_u(\tau)$ for $\tau = \mathcal{T}_u$ has decreased to a value numerically 'small' compared to $R_u(0)$. The typical spectrum has a low-frequency part $|\omega| \lesssim \mathcal{T}_u^{-1}$ where it does not vary much and a high-frequency part where it decreases as a power law.

The high-pass filter function $H(\omega)$ is shown for three different values of the ratio $\tau_0/\mathcal{T}_u$.

We see that if the anemometer is slow ($\tau_0 \gg \mathcal{T}_u$) we get more u-bias than when it is fast ($\tau_0 \ll \mathcal{T}_u$).

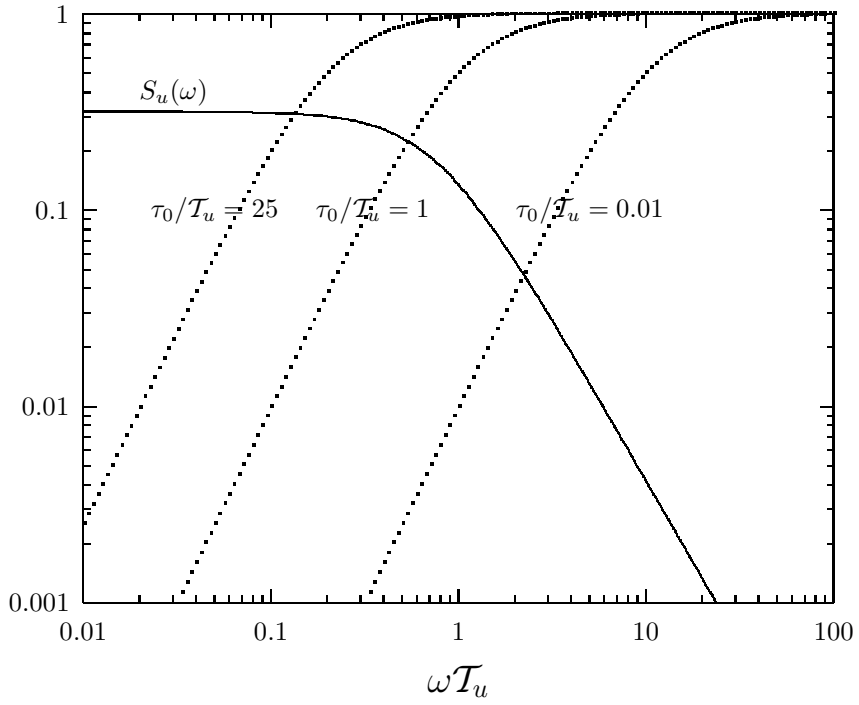

Figure 3. The spectrum $S_u(\omega)$ (solid line) and the high-pass filter $H(\omega)$, given in (80) (dotted lines), for three different values of the ratio $\tau_0/\mathcal{T}_u$.

w-bias

Now we imagine that there are no u-fluctuations. Proceeding as in the case of the u-bias, we obtain

$$\delta_w = \frac{\mu_2}{2} \frac{1}{U^2} \int_{-\infty}^{\infty} \frac{S_w(\omega)}{1 + \omega^2 \tau_0^2} d\omega + \frac{\ell U \tau_0}{2} \frac{\partial^2 F}{\partial W^2} \frac{1}{U^2} \int_{-\infty}^{\infty} \frac{\omega^2 \tau_0^2}{1 + \omega^2 \tau_0^2} S_w(\omega) d\omega. \tag{83}$$

In this case there is both a low-frequency and a high-frequency term. Again, using (48), we see that (83) can be written

$$\delta_w = \frac{\mu_2}{2U^2} \int_{-\infty}^{\infty} \frac{S_w(\omega)}{1 + \omega^2 \tau_0^2} d\omega + \frac{a_5}{U^2} \int_{-\infty}^{\infty} \frac{\omega^2 \tau_0^2}{1 + \omega^2 \tau_0^2} S_w(\omega) d\omega. \tag{84}$$

This result can be simplified even further if we assume the validity of (53). In that case

$$\delta_w \approx a_5 \frac{\langle w^2 \rangle}{U^2} \approx \frac{\mu_2}{2} \frac{\langle w^2 \rangle}{U^2}. \tag{85}$$

In other words, the w-bias is, apart from the coefficient a_5, simply equal to the squared, relative turbulence intensity of w. By looking back at the expression (44), we note that if the anemometer has a cosine angular response, which implies $\mu_2 = 0$, the w-bias is zero.

Stress-bias

Finally, when there are both u-and w-fluctuations, the last bias contribution, the stress-bias, is

$$\begin{aligned}
\delta_* &= \ell U \tau_0 \frac{\partial^2 F}{\partial U \partial W} \frac{1}{U^2} \int_{-\infty}^{\infty} \frac{\omega^2 \tau_0^2}{1+\omega^2\tau_0^2} Co_{uw}(\omega) d\omega \\
&\quad + U\tau_0 \left\{ \mu_1 \frac{\partial^2 F}{\partial S \partial U} - \frac{\partial^2 F}{\partial W \partial S} \right\} \frac{1}{U^2} \int_{-\infty}^{\infty} \frac{\omega\tau_0}{1+\omega^2\tau_0^2} Q_{uw}(\omega) d\omega \\
&= \frac{a_7}{U^2} \int_{-\infty}^{\infty} \frac{\omega^2\tau_0^2}{1+\omega^2\tau_0^2} Co_{uw}(\omega) d\omega \\
&\quad + \frac{\mu_1 a_6 - a_8}{U^2} \int_{-\infty}^{\infty} \frac{\omega\tau_0}{1+\omega^2\tau_0^2} Q_{uw}(\omega) d\omega.
\end{aligned} \tag{86}$$

We see that measuring the coefficients $a_1 \ldots a_8$ and the angular response of a cup anemometer in a wind tunnel, we can quantify the entire overspeeding if we know the second-order characteristics of the velocity turbulence, including spectra and cross-spectra of u and w.

From an application point of view, this is very satisfactory. It would, from a more theoretical point of view, be even better if we could relate all these coefficients and second derivatives to a few parameters characterizing the instrument. In the next section we shall see how this is possible by constructing a simple, phenomenological model for the torque exerted on the cup rotor by the wind field.

2.5 Modelling Wind Forcing

In last subsection we discussed a very simple model of the torque from the wind on a cup-anemometer rotor. It was based on the assumption that the cup is a moving drag-element with a drag coefficient depending on the orientation of the cup with respect to the direction of the wind. We did this in order to understand qualitatively why the cup anemometer overspeeds and not underspeeds. Here I suggest a model which is not only based on the assumption that the torque is a second-order polynomial in the wind speed and the cup-rotor speed, but also takes into account what we know about the calibration and the first-order response to a change in the wind speed.

Introducing for convenience the notation

$$\tilde{h} = \sqrt{\tilde{u}^2 + \tilde{v}^2} \tag{87}$$

for the instantaneous, total horizontal wind speed component, we hypothesize with many others [see e.g., Kaganov and Yaglom (1976) or Coppin (1982)] a form of the

function $F(\tilde{s}, \tilde{h}, 0)$ based on the assumption that the torque of the turbulent wind is a homogeneous, second-order polynomial in $\tilde{s}$ and $\tilde{h}$. We add the constraint that the two roots in $F(S, U, 0) = 0$ must have opposite sign. Otherwise there would be no unambiguous calibration $S = U/\ell$. The possibility that $S = U/\ell$ is a double root must be ruled out because it implies that not only $F(S, U, 0)$, but also $\partial F/\partial S$ is zero, corresponding to an infinite time scale τ_0 according to (11). With this in mind, I suggest the following form

Constraints on torque expression

$$F(\tilde{s}, \tilde{h}, 0) = \frac{1}{2}\rho C \frac{Ar}{I}(\tilde{h} - \ell\tilde{s})(\tilde{h} + \Lambda\tilde{s}). \tag{88}$$

Here C is a dimensionless constant, ρ the density of air, A an effective cup area, r an effective radius of the cup rotor and I its moment of inertia. The quantity Λ is some positive instrument length scale, the significance of which will be explained later.

Kondo *et al.* (1971) found a similar expression for $F(\tilde{s}, \tilde{h}, 0)$, but they inferred from measurements by Brevoort and Joyner (1935) that the equivalent of Λ should be negative. This could be an indication that Λ is so small compared to ℓ that it is difficult to determine experimentally.

Busch (1965) [see also Busch *et al.* (1980)] suggested a somewhat more general expression which is not limited to being a second-order polynomial in $\tilde{s}$ and $\tilde{h}$. This model also implies that S is proportional to U if the friction can be neglected.

The first useful result we can derive from (88) is an expression for the time constant τ_0 which we introduced with (11). Taking the derivative with respect to $\tilde{s}$, we get

$$\tau_0 = -\left(\frac{\partial F}{\partial S}\right)^{-1} = \frac{1}{U}\frac{2I}{\rho C A r(\ell + \Lambda)}. \tag{89}$$

We note that the time constant is inversely proportional to U with a factor of proportionality which is determined entirely by the densities of air and the rotor material and by the rotor geometry. Instead of using a time constant for a cup anemometer it is more natural to use a *distance constant*

Distance constant

$$\ell_0 = U\tau_0 = \frac{2I}{\rho C A r(\ell + \Lambda)}, \tag{90}$$

because this quantity is a true instrument constant which does not depend on the wind speed. The fact that a cup anemometer response is characterized by a distance constant rather than a time constant has been confirmed experimentally (MacCready, 1965).

Since the moment of inertia I is proportional to the rotor density ρ_r and to the fifth power of its linear dimensions ($\propto r$) we conclude from (90) that the distance constant is proportional to ρ_r/ρ and $r^2/(\ell + \Lambda)$. The calibration distance ℓ is independent of the moment of inertia, i.e. of the density of the rotor material, and determined entirely by the rotor geometry. It is proportional to r and usually of the same order. If we assume that Λ scales with r, just like ℓ does, we conclude that the distance constant is proportional to r. The rotor of the Risø-70 model (Busch *et al.*, 1980) is made of carbon reinforced plastic with a density ρ_r of about 1.5 g cm^{-3}. The radius r is 0.07 m and the distance constant ℓ_0 was determined to be 1.7 m. This is a rather typical modern, sturdy cup anemometer, which is used for routine measurements of mean wind speed by Risø National Laboratory. Older models are typically made of steel and they are often larger, with radii of about 0.15 m. They have distance constants of about 20 m and reacts

consequently much slower than newer models of standard cup anemometers. The smallest distance constant is reported Frenzen (1988). His miniature instrument which is designed for turbulence measurements and is quite fragile and unsuited for routine operations, has $\ell_0 = 0.25$ m. The rotor is made of styrofoam and has a radius of only 0.01 m.

Applying (90) the forcing function may now be rewritten as

$$F(\tilde{s}, \tilde{h}, 0) = \frac{(\tilde{h} - \ell\tilde{s})(\tilde{h} + \Lambda\tilde{s})}{\ell_0(\ell + \Lambda)}. \tag{91}$$

We see that the forcing by the *horizontal* wind can be specified by means of the three length scales, ℓ, ℓ_0 and Λ.

I showed in the preceeding subsections how the first- and second derivatives of the forcing function enter the second-order perturbation equation of motion and the biases. All the derivatives with respect to S and U in the point $(S(U), U, 0)$ can now be expressed in terms of U, ℓ, ℓ_0 and Λ as

$$\left\{ \begin{array}{c} \dfrac{\partial F}{\partial S} \\ \dfrac{\partial F}{\partial U} \end{array} \right\} = \left\{ \begin{array}{c} -\dfrac{U}{\ell_0} \\ \dfrac{U}{\ell_0 \ell} \end{array} \right\} \tag{92}$$

and

$$\left\{ \begin{array}{c} \dfrac{\partial^2 F}{\partial S^2} \\ \dfrac{\partial^2 F}{\partial S \partial U} \\ \dfrac{\partial^2 F}{\partial U^2} \end{array} \right\} = \left\{ \begin{array}{c} -2\dfrac{\ell\Lambda}{\ell_0(\ell + \Lambda)} \\ -\dfrac{\ell - \Lambda}{\ell_0(\ell + \Lambda)} \\ 2\dfrac{1}{\ell_0(\ell + \Lambda)} \end{array} \right\}. \tag{93}$$

Equation (92) is consistent with (11), (12) and (90), as expected. More interesting is the interpretation of the first three terms on the right-hand side in the first line of (79). In the light of (93), the third term, proportional to $\langle u^2 \rangle$, is *always* positive as already pointed out by more qualitative arguments. The first term, proportional to $\langle s^2 \rangle$, is *always* negative. This means that the instrument response s will not only damp, i.e. low-pass filter, the input through the first-order term, but also try to counteract the overspeeding through the second-order term. The second term, proportional to $\langle su \rangle$, can have either sign, depending on the length scale Λ's magnitude compared to ℓ: if $\Lambda < \ell$ the covariance $\langle su \rangle$ will help the first term counteract the overspeeding and if $\Lambda > \ell$ it will help the third term enhancing it.

Translating (93) to the coefficients $a_1 \ldots a_8$ introduced by Wyngaard *et al.* (1974), we get by using (48) the identity $U\tau_0 = \ell_0$,

$$\left\{ \begin{array}{c} a_3 \\ a_4 \\ a_6 \end{array} \right\} = \left\{ \begin{array}{c} \frac{1}{2}\dfrac{\partial^2 F}{\partial S^2}\dfrac{\ell_0}{\ell} \\ \frac{1}{2}\dfrac{\partial^2 F}{\partial U^2}\ell\ell_0 \\ \dfrac{\partial^2 F}{\partial S \partial U}\ell_0 \end{array} \right\} = \left\{ \begin{array}{c} -\dfrac{\Lambda}{\ell + \Lambda} \\ \dfrac{\ell}{\ell + \Lambda} \\ -\dfrac{\ell - \Lambda}{\ell + \Lambda} \end{array} \right\}. \tag{94}$$

We see that the model fulfills (50). However, our model predicts still another constraint,

$$a_4 - a_3 = 1, \tag{95}$$

and the condition

$$a_4 < 1. \tag{96}$$

Wyngaard *et al.* (1974) found $a_4 - a_3 = 1.19 \pm 14\%$. Coppin (1982) got corresponding values between 1.08 and 1.29.

The inequality (96) is, according to (48), fulfilled by the data by Wyngaard *et al.* (1974). Coppin (1982), on the other hand, found that six out of the seven anemometers he investigated had values of a_4 larger than one. At the same time he found that a_1 was larger than one by about 0.2 for all seven anemometers. Our model predicts that a_1 is exactly one and the only possible way to understand the results by Coppin (1982) in our framework is to accept that the offset speed U_0 is significant. It is possible to take U_0 into account in our model and one result of this generalization is that a_4 must be divided by a_1^2 before comparison with the inequality (96). When this 'normalization' is carried out all his values of a_4 fall well below one.

These two tests of the model seems to be fulfilled only moderately well, but I feel that the agreement is such that it is justified to apply the model to reformulate the bias expressions in terms of its parameters.

Inserting (93) in (38) and (46), these relations take the forms

$$\frac{1}{\ell}\frac{\partial^2 F}{\partial W \partial S} + \frac{\partial^2 F}{\partial U \partial W} = \frac{\mu_1}{\ell \ell_0} \tag{97}$$

and

$$2\frac{\mu_1}{\ell}\frac{\partial^2 F}{\partial W \partial S} + \frac{\partial^2 F}{\partial W^2} = \frac{\mu_2}{\ell \ell_0} + \frac{\mu_1^2}{\ell \ell_0}\frac{2\Lambda}{\ell + \Lambda}. \tag{98}$$

Eliminating $\partial^2 F/\partial W \partial S$ from (97) and (98), we get

$$\frac{\partial^2 F}{\partial W^2} = \frac{\mu_2}{\ell \ell_0} + 2\mu_1 \frac{\partial^2 F}{\partial U \partial W} - \frac{2\mu_1^2}{\ell_0(\ell + \Lambda)}, \tag{99}$$

which is more general than (53).

Forcing by the vertical wind component

At this point it is tempting to formulate a model for the torque which includes the dependence on the vertical velocity component $\tilde{w}$. We will do it by securing that the constraints (97) and (98) are fulfilled.

We note, by looking back at (31) and (34), that a small, vertical wind component W has the same effect on the rotation rate as the increase $\mu_1 W$ in the horizontal wind component. The first thing to do would therefore be to replace $\tilde{h}$ in (91) by $\tilde{h} + \mu_1 \tilde{w}$. This is sufficient to fulfil (97), but not (98). To accomplish that, without violating (97) or any other constraints we have used, all we have to do is to add a term proportional to $\tilde{w}^2$. It is easily seen that the expression

$$F(\tilde{s}, \tilde{h}, \tilde{w}) = \frac{(\tilde{h} + \mu_1 \tilde{w} - \ell \tilde{s})(\tilde{h} + \mu_1 \tilde{w} + \Lambda \tilde{s})}{\ell_0(\ell + \Lambda)} + \frac{\mu_2 \tilde{w}^2}{2\ell_0 \ell} \tag{100}$$

meets all our requirements.

With this equation for the torque we can now establish the complete translation table between the coefficients $a_1 \ldots a_8$ and the model parameters. Carrying out all the differentiations of $F(\tilde{s}, \tilde{h}, \tilde{w})$ to second order and then setting $(\tilde{s}, \tilde{h}, \tilde{w}) = (U/\ell, U, 0)$, we get the result

$$\left\{\begin{array}{c} a_1 \\ a_2 \\ a_3 \\ a_4 \\ a_5 \\ a_6 \\ a_7 \\ a_8 \end{array}\right\} \equiv \left\{\begin{array}{r} 1 \\ \mu_1 \\ \frac{1}{2}\frac{\partial^2 F}{\partial S^2}\frac{\ell_0}{\ell} \\ \frac{1}{2}\frac{\partial^2 F}{\partial U^2}\ell\ell_0 \\ \frac{1}{2}\frac{\partial^2 F}{\partial W^2}\ell\ell_0 \\ \frac{\partial^2 F}{\partial S \partial U}\ell_0 \\ \frac{\partial^2 F}{\partial U \partial W}\ell\ell_0 \\ \frac{\partial^2 F}{\partial W \partial S}\ell_0 \end{array}\right\} = \left\{\begin{array}{rl} 1 & \\ \mu_1 & \\ -\frac{\Lambda}{\ell+\Lambda} & \\ \frac{\ell}{\ell+\Lambda} & \\ \frac{\mu_1^2 \ell}{\ell+\Lambda} & + \frac{\mu_2}{2} \\ -\frac{\ell-\Lambda}{\ell+\Lambda} & \\ \frac{2\mu_1\ell}{\ell+\Lambda} & \\ -\mu_1\frac{\ell-\Lambda}{\ell+\Lambda} & \end{array}\right\}. \tag{101}$$

Our phenomenological model shows that the dynamic behavior of a cup anemometer can be described to second order in perturbations around a calibration point $(S, U, W) = (U/\ell, U, 0)$ by five independent parameters. The four of them are those which traditionally are specified. They are the calibration distance ℓ, which specifies the translation from signal to wind speed, the distance constant ℓ_0 characterizing the low-pass filtering of the anemometer and the two dimensionless parameters μ_1 and μ_2 accounting for the sensitivity to the vertical wind component. They can obtained by use of a low-turbulence wind tunnel. This is obvious what ℓ, μ_1 and μ_2 are concerned. The distance constant can be determined by holding and releasing the cup rotor in a constant wind (cf. discussion about response to step input on page 10). The last parameter, the length scale Λ, I have not been able to interpret so far. It does not manifest itself in the steady-state calibration or in the first-order dynamics as is the case with the other four parameters. Looking at the translation table (101), we see that we can determine Λ by measuring the second derivatives of the torque F with respect to the response S and U.

We will now see how the parameters introduced here enter the expressions for the biases δ_u, δ_w and δ_*.

2.6 Overspeeding Revisited

In this subsection we will apply the results from the simple phenomenological model we have just discussed to overspeeding. In the following subsection we will quantify the four types of biases δ_u, δ_v, δ_w and δ_* by means of the measurements by Wyngaard *et al.* (1974) and surface-layer parameters describing the spectra.

The simplest contribution to the overspeeding is the u-bias. Applying (94) to (81), we get *u-bias*

$$\delta_u = \frac{\ell}{\ell+\Lambda}\frac{1}{U^2}\int_{-\infty}^{\infty}\frac{\omega^2(\ell_0/U)^2}{1+\omega^2(\ell_0/U)^2}S_u(\omega)d\omega. \tag{102}$$

Taylor's hypothesis

At this point it seems appropriate to apply Taylor's hypothesis which states that all fluctuations of a turbulent quantity at a fixed point can be attributed to 'frozen' turbulence being carried past a fixed point by the mean wind. This is of course an idealization because the eddies move themselves around, even statistically, but the characteristic time it takes an eddy to 'complete a revolution' is long compared to the time it takes to carry it by the observing point. This time is dependent on the mean wind speed U; the larger it is the better Taylor's hypothesis works. It is easily seen that the most important 'number of merit' by which to judge the validity of this hypothesis is the relative turbulence intensity $\sqrt{u^2}/U$. If this number is very small, Taylor's hypothesis works very well. Lumley and Panofsky (1964) discuss it in quite some detail. They state the result that if $\sqrt{u^2}/U \lesssim 1/3$ it is not experimentally possible in a field situation to detect deviations from the hypothesis up to 90 m. This means in a semiquantitative language that eddies with linear dimensions up to 90 m then will pass an observation point with speed U without changing shape noticeably. The condition that the relative turbulence intensity has to be small compared to one must be fulfilled in any case for our perturbation theory to work.

In frequency domain Taylor's hypothesis works statistically as the simplest possible *dispersion relation* between frequency ω and wave number k, defined as 2π divided by the wavelength:

$$\omega = kU. \tag{103}$$

This means that we can simply change variables to k by using the relation

$$S_u(k) = F_u(k)\frac{dk}{d\omega} = \frac{1}{U}F_u(k), \tag{104}$$

where $F_u(k)$ is the longitudinal spectrum in wave-number domain. Over the years—and in particular since the nineteen sixties—a lot of experimental information has been compiled about $F_u(k)$, information which will help us quantify the overspeeding, as we shall see.

We reformulate (102) in terms of $F_u(k)$ with the result

$$\delta_u = \frac{\ell}{\ell+\Lambda}\frac{1}{U^2}\int_{-\infty}^{\infty}\frac{k^2\ell_0^2}{1+k^2\ell_0^2}F_u(k)dk. \tag{105}$$

We see how convenient this formulation is in case of a cup anemometer: the turbulence is a 'frozen', random spatial structure, with a characteristic linear dimension $\mathcal{L}_u = U\mathcal{T}_u$, being carried through the cup anemometer, which probes it with a linear low pass filter with a length constant equal to ℓ_0, along the mean wind direction. At the same time, the cup anemometer measures the mean wind speed with a bias, which is proportional to the area under the spectrum, after this has been multiplied by the high-pass filter,

$$G(k) = \frac{k^2\ell_0^2}{1+k^2\ell_0^2} = 1 - \frac{1}{1+k^2\ell_0^2}. \tag{106}$$

Incidentally, this filter is exactly 'complementary' to the low-pass filter $1-G(k) = 1/(1+k^2\ell_0^2)$ through which the anemometer 'sees' the turbulence. Instead of comparing the anemometer time constant τ_0, which is not an instrument constant, but inversely proportional to U, with the integral time scale $\mathcal{T}_u$ (82), which is also inversely proportional to U for frozen turbulence, we compare length with length,

ℓ_0 with $\mathcal{L}_u$, when we want to understand and interpret the cup anemometer signal and estimate the u-bias.

Figure 4, which is a 'Taylor-translation' of Figure 3 to wave-number domain illustrates what is going on in (105). The u-bias is an increasing function of $\ell_0/\mathcal{L}_u$ and, eventually, when this ratio goes to infinity, the integral becomes equal to the variance $\langle u^2 \rangle$.

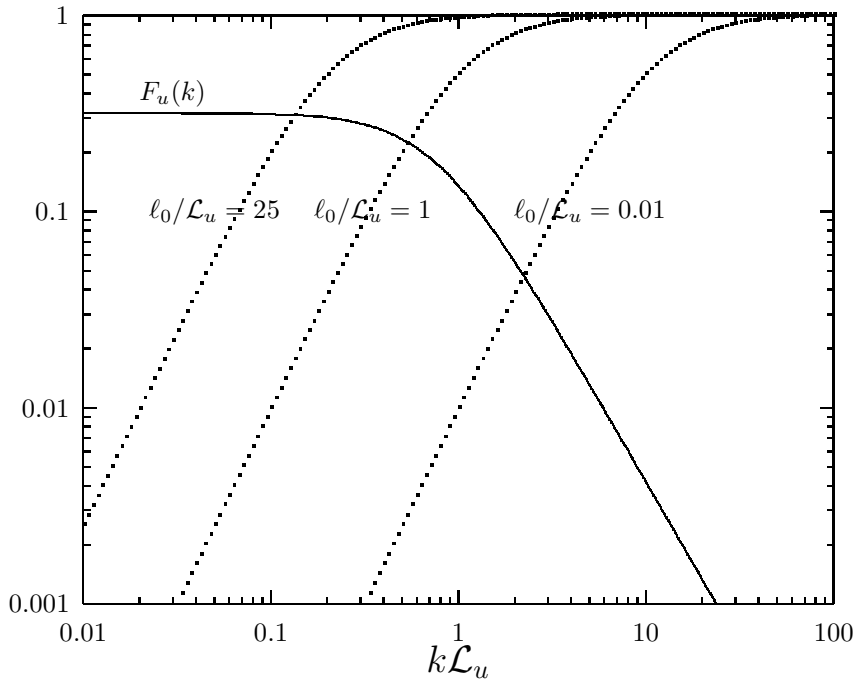

Figure 4. The spectrum $F_u(k)$ (solid line) and the high-pass filter $G(k)$, given in (106) (dotted lines) for three different values of the ratio $\ell_0/\mathcal{L}_u$.

Based on (105), we see that the upper limit to δ_u is the square of the turbulence intensity $\sqrt{\langle u^2 \rangle}/U$; the factor $\ell/(\ell + \Lambda)$ in front of the integral is less than unity and the integral is equal to the fraction of the variance of those eddies which are smaller in linear dimensions than ℓ_0.

Using (101), we can now formulate the w-bias, (84), and the stress bias, (86), as *w-bias and stress-bias*

$$\delta_w = \frac{\mu_2}{2}\frac{\langle w^2 \rangle}{U^2} + \frac{\mu_1^2 \ell}{\ell + \Lambda}\frac{1}{U^2}\int_{-\infty}^{\infty} \frac{k^2\ell_0^2}{1 + k^2\ell_0^2} F_w(k)dk \tag{107}$$

and

$$\delta_* = \frac{2\mu_1 \ell}{\ell + \Lambda}\frac{1}{U^2}\int_{-\infty}^{\infty} \frac{k^2\ell_0^2}{1 + k^2\ell_0^2} Co(k)dk, \tag{108}$$

where, just as in (104), we have applied Taylor's hypothesis to translate the spectra $S_w(\omega)$ and $Co_{uw}(\omega)$ in frequency domain to their counterparts $F_w(k)$ and $Co(k)$ in wave-number domain.

It is a consequence of our model for the torque that the coefficient $\mu_1 a_6 - a_8$ in front of the integral containing the quadrature spectrum in (108) is zero. The measurements (48) by Wyngaard *et al.* (1974) render this quantity 0.08 ± 0.14, consistent with the model prediction.

We note that there are two terms in the w-bias, one proportional to the entire variance and one proportional to the high-frequency variance of $\tilde{w}$. The last term is analogous to the u-bias—remember, a small deviation w from zero of the vertical velocity component is equivalent to a small deviation in the horizontal velocity component equal to $\mu_1 w$. The term is the variance of small scale fluctuations of $\tilde{w}$ and therefore the parameter μ_1 enters as μ_1^2.

According to (48), $\mu_1^2 \ell/(\ell + \Lambda) = a_2^2 a_5$ is about 0.004 and therefore quite small compared to $\mu_2/2 \approx a_5 = 0.67$. Further, the first term contains the entire variance of $\tilde{w}$ whereas the second contains only the high-wave number part of the variance. On basis of this, we will neglect the second term in the following.

While the u-bias is always positive and the sign of the w-bias is given by the sign μ_2, it is difficult to tell whether the stress-bias is positive or negative. The low wave-number bulk of the cospectrum is negative under normal conditions in the atmospheric surface layer; the atmosphere transfers momentum to the surface so that u and w are anti-correlated[‖]. In the high wave-number part, corresponding to k-values of the order of magnitude of the reciprocal height, the cospectrum is numerically very small and it is hard to tell if it sometimes is positive. Kaimal *et al.* (1972) find, on experimental basis, that it is reasonable to assume the $Co(k)$ is negative for all values of k. Assuming this, the integral in (108) is negative. Consequently, stress-bias will have the opposite sign of μ_1 in the surface layer.

We can interpret this result qualitatively by considering what the downward momentum transport consists of. At a particular position it consists of series of small bursts of downward transport of positive momentum ($u > 0$ and $w < 0$), termed *sweeps*, and upward transport of negative momentum ($u < 0$ and $w > 0$), *ejections* (see e.g., Robinson, 1991). If we have a negative value of $\mu_1 = \ell\ell_0 \partial F/\partial W/U$, the sweeps will be enhanced and the ejections suppressed. The net result is in this case a positive stress-bias.

We see that if the anemometer has cosine angular response then, according to (44), $\mu_1 = \mu_2 = 0$ with the consequence that $\delta_w = \delta_* = 0$.

The four biases δ_u, δ_v, δ_w and δ_*, making up the overspeeding by addition, can be said to be of two types according to the scale of the variance entering. Whereas δ_u and δ_* according to (105) and (108) contain only the small scale variance, δ_v and δ_w are both proportional to the variance from all scales. As we shall see in next section, this has very important consequences for the relative contributions of the four biases.

2.7 Overspeeding in the Surface Layer

As noted earlier, the v- and w-bias are of different character than u-bias and the stress-bias. Here we will treat these first.

u-bias

It is possible to evaluate the integral determining δ_u in (105) if the turbulent length scale $\mathcal{L}_u$ of u is much larger than ℓ_0. Since a cup anemometer will typically have a distance constant ℓ_0 of about 1 m and $\mathcal{L}_u$ is several times the height, this condition is often met. In that case we can approximate the spectrum in the entire integration domain by [see e.g., Kaimal *et al.* (1972)]

$$F_u(k) = \frac{1}{2}\alpha_1 \varepsilon^{2/3} |k|^{-5/3}, \tag{109}$$

[‖]Kaimal *et al.* (1972) find that at numerically very low wave numbers $|k| \sim 0.003$ rad s^{-1} there is a tendency for the cospectrum to be become positive in erratically scattered intervals on the k-axis. This phenomenon is observed only under unstable conditions.

where ε is the rate of dissipation of specific kinetic energy and $\alpha_1 \simeq 0.56$ the Kolmogorov constant for the longitudinal spectrum. The value of this constant is chosen in accordance with the discussion by Kristensen *et al.* (1989)**. The reason that this approach works is that the integral (105) is actually convergent when we apply (109) to the entire integration interval. Since

$$\int_0^\infty \frac{\xi^{1/3}}{1+\xi^2} d\xi = \frac{\pi}{\sqrt{3}}, \tag{110}$$

we get

$$\delta_u = \frac{\pi}{\sqrt{3}} \alpha_1 \frac{\ell}{\ell+\Lambda} \frac{(\varepsilon \ell_0)^{2/3}}{U^2}. \tag{111}$$

Equation (111) overestimates the u-bias because the low-wave number part of the spectrum is overestimated by (109). In Appendix A, I show that the resulting overestimation of the u-bias is very small.

Stress-bias

The basis for the spectrum (109) is that the turbulence in the wave-number domain $|k| \gtrsim \mathcal{L}_u$ can be considered locally isotropic, yet not affected by the dissipation. We mean isotropic in the statistical sense and one consequence is that the correlation between velocity components must be zero. This is of course an approximation because it would mean that the cospectrum $Co(k)$ would be identically zero in the inertial subrange. The measured cospectrum of $\tilde{u}$ and $\tilde{w}$ does indeed fall off very rapidly in the inertial subrange. Wyngaard and Coté (1972) found, on basis of the data presented by Kaimal *et al.* (1972) and dimensional analysis, that it was well represented by

$$Co(k) = -\frac{1}{2} \zeta_1 \frac{dU}{dz} \varepsilon^{1/3} |k|^{-7/3}, \tag{112}$$

where $\zeta_1 \sim 0.15$ is a constant.

Using this form in the entire range of k, the integral (108) is convergent. The result of the integration is

$$\begin{aligned} \delta_* &= -\frac{2\mu_1 \ell}{\ell+\Lambda} \zeta_1 \frac{dU}{dz} \varepsilon^{1/3} \frac{1}{U^2} \int_0^\infty \frac{k^2 \ell^2}{1+k^2\ell_0^2} k^{-7/3} dk \\ &= -\frac{\pi}{\sqrt{3}} \frac{2\mu_1 \ell}{\ell+\Lambda} \zeta_1 \frac{1}{U^2} \frac{dU}{dz} \ell_0 (\varepsilon \ell_0)^{1/3}. \end{aligned} \tag{113}$$

As in the case of the u-bias, (113) will give a numerical overestimation of the stress-bias because the low-wave number part of the cospectrum is incorrectly represented by (112).

Surface layer results

The two types of biases (111) and (113) have in common that they are limited in the sense that only eddies smaller than the distance constant play a role. We can evaluate them in the surface layer by using the Monin-Obukhov scaled expressions for $U(z)$, dU/dz and $\varepsilon(z)$ [see e.g., Panofsky and Dutton (1984)]. The constant ζ_1 is according to Wyngaard and Coté (1972) also a function of height, but it does not vary much (perhaps by 30%), so we will treat it as a constant for convenience.

**There has to be a factor 1/2 in front because α_1 traditionally is defined for 'one-sided' spectra whereas we let k go from $-\infty$ to ∞.

In the surface layer, which is that part of the atmosphere which is so close to the ground that the variation of the friction velocity

$$u_* = \sqrt{-\langle uw \rangle} \tag{114}$$

with height can be neglected, an important characteristic length scale to describe profiles of first and higher moments of velocities and scalars is the Monin-Obukhov length

$$L = -\frac{u_*^2}{\kappa g}\frac{T}{T_*}. \tag{115}$$

Here κ is the von Kármán constant, equal to about 0.4 according to Zhang *et al.* (1988), g the acceleration of gravity, T the mean temperature of the surface layer and

$$T_* = \frac{\langle w\theta \rangle}{u_*} \tag{116}$$

the upward turbulent flux of potential temperature θ divided by the friction velocity (114).

The ratio z/L is proportional to the ratio between the production of specific turbulent kinetic energy by buoyancy and shear. Panofsky and Dutton (1984) have a full discussion of all these concepts and also the expressions we are going to use.

In a neutrally stratified surface layer the gradient dU/dz of the mean wind speed is proportional to the friction velocity u_* and inversely proportional to the height z. This can be seen in different ways—by first-order closure theory (see e.g., Panofsky and Dutton, 1984) or by first-order matching of wind profiles in the boundary layer (Tennekes and Lumley, 1972 and Tennekes, 1981). When the surface layer is not neutral, the extra scaling length L makes it impossible to maintain such a simple assumption about the gradient. In this case we write

$$\frac{dU}{dz} = \frac{u_*}{\kappa z}\varphi_m\Big(\frac{z}{L}\Big), \tag{117}$$

where $\varphi_m(z/L)$ is the so-called diabatic correction. If there is no buoyancy production of turbulence, i.e. if the surface layer is neutrally stratified, the argument z/L is zero and the function $\varphi_m(z/L)$ one. In that case the gradient of U is inversely proportional to the height z and $U(z)$ consequently logarithmic.

Integrating the general expression (117) with respect to z we obtain

$$U(z) = \frac{u_*}{\kappa}\left\{\ln\Big(\frac{z}{z_0}\Big) - \psi_m\Big(\frac{z}{L}\Big)\right\}, \tag{118}$$

where z_0 is the roughness length and

$$\psi_m\Big(\frac{z}{L}\Big) = \int_{z_0/L}^{z/L}\{1-\varphi_m(\zeta)\}\frac{d\zeta}{\zeta} \approx \int_0^{z/L}\{1-\varphi_m(\zeta)\}\frac{d\zeta}{\zeta}. \tag{119}$$

The rate of dissipation of specific kinetic energy is in general also a function of z/L and is written

$$\varepsilon(z) = \frac{u_*^3}{\kappa z}\varphi_\varepsilon\Big(\frac{z}{L}\Big). \tag{120}$$

With all these parameters describing the profiles of the wind speed, the wind-speed gradient and the dissipation rate, we can reformulate the u-bias and the stress-bias as follows

$$\delta_u = \frac{\pi}{\sqrt{3}} \frac{\ell}{\ell + \Lambda} \alpha_1 \kappa^{4/3} \chi_u\left(\frac{z}{z_0}, \frac{z}{L}\right) \left(\frac{\ell_0}{z}\right)^{2/3} \tag{121}$$

and

$$\delta_* = -\frac{\pi}{\sqrt{3}} \frac{2\mu_1 \ell}{\ell + \Lambda} \zeta_1 \kappa^{2/3} \chi_*\left(\frac{z}{z_0}, \frac{z}{L}\right) \left(\frac{\ell_0}{z}\right)^{4/3} . \tag{122}$$

We have introduced the two functions

$$\chi_u\left(\frac{z}{z_0}, \frac{z}{L}\right) = \left\{\ln\left(\frac{z}{z_0}\right) - \psi_m\left(\frac{z}{L}\right)\right\}^{-2} \varphi_\varepsilon^{2/3}\left(\frac{z}{L}\right) \tag{123}$$

and

$$\chi_*\left(\frac{z}{z_0}, \frac{z}{L}\right) = \left\{\ln\left(\frac{z}{z_0}\right) - \psi_m\left(\frac{z}{L}\right)\right\}^{-2} \varphi_m\left(\frac{z}{L}\right) \varphi_\varepsilon^{1/3}\left(\frac{z}{L}\right), \tag{124}$$

which are shown in Figures 5 and 6 for unstable stratification and values of z/z_0 representing the end points of a typical interval of this quantity.

Following Carl *et al.* (1973), we have here chosen

$$\varphi_m\left(\frac{z}{L}\right) = \left(1 - 16\frac{z}{L}\right)^{-1/3}, \tag{125}$$

thus obtaining

$$\psi_m\left(\frac{z}{L}\right) = \frac{3}{2} \ln\left(\frac{1 + \xi + \xi^2}{3}\right) - \sqrt{3} \arctan\left(\frac{1}{\sqrt{3}} \frac{\xi - 1}{\xi + 1}\right), \tag{126}$$

where

$$\xi = \left(1 + 16\left|\frac{z}{L}\right|\right)^{1/3}, \tag{127}$$

and

$$\varphi_\varepsilon\left(\frac{z}{L}\right) = 1 - \frac{z}{L}. \tag{128}$$

Qualitatively the u-bias and the stress-bias differ in their dependence on the ratio of the distance constant to the height. The first contains the ratio to the power 2/3, the second to the power 4/3. Further, $\chi_*(z/z_0, z/L)$ is an order of magnitude smaller than $\chi_u(z/z_0, z/L)$. Finally, the constant $\alpha_1 \kappa^{4/3}$ in the expression for δ_u is much larger than the corresponding constant $2\mu_1\zeta_1$ in that for δ_*. The first constant, the so-called K-von K product (Kolmogorov and von Kármán), is, according to Frenzen and Hart (1983) [see also Kristensen *et al.* (1989)] 0.165, whereas $2\mu_1\zeta_1\kappa^{2/3}$ with the data (48) by Wyngaard *et al.* (1974) becomes 0.01.

In a very unstable situation with $L = -10$ m, the u-bias becomes about 1.6%, if we are conservative and assume that Λ is much smaller than ℓ, and measure in the height $z = 10$ m with a cup anemometer with a distance constant $\ell_0 = 2$ m

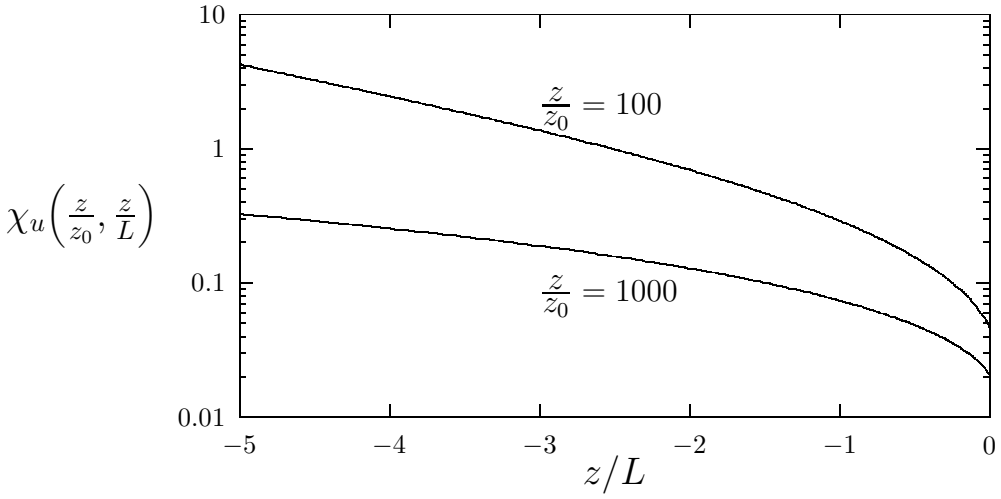

Figure 5. The function $\chi_u(z/z_0, z/L)$ for negative values of z/L.

over a terrain with $z_0 = 0.1$ m. Of course, if we measure with a heavy, large cup anemometer with $\ell_0 = 10$ m we get $\delta_u = 4.6\%$, but even this instrument will only give rise to a u-bias of about 1.4% under neutral conditions.

As shown, the stress-bias will, unless the ratio ℓ_0/z is much larger than one, be at least one order of magnitude smaller.

We can easily calculate the u-bias and the stress-bias in stable stratification, but the variance $\langle u^2 \rangle$ and the covariance $\langle uw \rangle$ are much smaller in the inertial subrange than in neutral and unstable situations and consequently the u-bias and the stress-bias are also much smaller.

v- and w-bias

The v-bias and the w-bias enter unfiltered by the anemometer as shown in (58) and (107). They are

$$\delta_v = \frac{\langle v^2 \rangle}{2U^2} \tag{129}$$

and

$$\delta_w = \mu_2 \frac{\langle w^2 \rangle}{2U^2}. \tag{130}$$

Taking $\mu_2/2 = a_5 = 0.67$ [see (48) and (94)] as a typical value the two biases δ_v and δ_w look as if they were similar in magnitude. This, however, is not always the case and in particular not when the surface layer cannot be assumed neutral.

w-bias

The w-bias is usually smaller than the v-bias and occasionally much smaller. This is so because the size of the eddies of vertical velocity and, consequently, their contribution to the variance of $\tilde{w}$ is limited by the height. In the surface layer this variance increases with decreasing z/L and Panofsky and Dutton (1984) suggest that its square root under unstable conditions can be written

$$\frac{\sqrt{\langle w^2 \rangle}}{u_*} = \varphi_3\left(\frac{z}{L}\right) = 1.25 \left\{1 - 3\frac{z}{L}\right\}^{1/3}. \tag{131}$$

Employing (131) together with (118) in (130) we get

$$\delta_w = \mu_2 \frac{\kappa^2}{2} \left\{ \ln\left(\frac{z}{z_0}\right) - \psi_m\left(\frac{z}{L}\right) \right\}^{-2} \varphi_3^2\left(\frac{z}{L}\right). \tag{132}$$

With $L = -10$ m, $z = 10$ m, $z_0 = 0.1$ m and $\mu_2 = 2a_5 = 1.34$, we get $\delta_w \approx 0.016\mu_2 \approx 2.1\%$. In the same height and with the same roughness length, the w-bias is $\delta_w \approx 0.006\mu_2 \approx 0.8\%$ for neutral stratification.

v-bias

The expression (129) for the v-bias contains no parameters from the cup anemometer [which is strictly speaking an approximation because it is based on the assumption that U_0 is zero in (4)]; it is simply half of the square of the relative turbulence intensity of $\tilde{v}$. In contrast to the variance of $\tilde{w}$ the variance of $\tilde{v}$ is not limited by the height (Kaimal *et al.*, 1976) anywhere in the convective boundary layer, including the surface layer. It does not scale with z/L, but rather with z_i/L, where z_i is the depth of the convective boundary layer and it can become quite large compared to $\langle w^2 \rangle$. Panofsky and Dutton (1984) support this statement concerning the surface layer and observe that also under neutral and stable conditions (Smith and Abbott, 1961) will there occasionally be large values of $\langle v^2 \rangle$. Depending on the averaging time the wind-direction fluctuations can be as large as 25° and this means that δ_v can be 10% under both unstable and stable conditions.

According to Panofsky and Dutton (1984)

$$\frac{\sqrt{\langle v^2 \rangle}}{u_*} = \frac{\sqrt{\langle u^2 \rangle}}{u_*} = \varphi_1\left(\frac{z_i}{L}\right) = \left\{12 - 0.5\frac{z_i}{L}\right\}^{1/3} \tag{133}$$

fits observed data well under unstable conditions. The v-bias then becomes

$$\delta_v = \frac{\kappa^2}{2} \left\{ \ln\left(\frac{z}{z_0}\right) - \psi_m\left(\frac{z}{L}\right) \right\}^{-2} \varphi_1^2\left(\frac{z_i}{L}\right). \tag{134}$$

With $L = -10$ m, $z = 10$ m, $z_i = 1000$ m and $z_0 = 0.1$ m, (134) yields $\delta_v \approx 12\%$.

The Kansas Experiment

Kaganov and Yaglom (1976) present in their interesting introduction an account for the controversies about overspeeding which has always meant u-bias in my terminology. Kondo *et al.* (1971) find that it is small—less than a few percent—whereas Izumi and Barad (1970) concluded that, based on comparison with sonic anemometers, it amounted to no less than 10% in the 1968 Kansas Windy Acres field experiment (Haugen *et al.*, 1971 and Businger *et al.*, 1971). All the cup anemometer measurements of mean wind speeds were consequently corrected down by 10% in this famous field experiment. In field experiments there are occasionally still large systematic differences between wind speeds measured by cup anemometers and by sonic anemometers (Frenzen, 1991, private communication).

What was the situation in Kansas in 1968 then?

We can safely assume that the roughness length z_0 was about 0.02 m as it is for uncut grass (Panofsky and Dutton, 1984). The lowest measuring height was $z = 5.66$ m. The most unstable run had $z/L = -2$. We do not know the depth of the boundary layer, but a typical value would be $z_i = 1000$ m. Let us further assume that the distance constant ℓ_0 was 2 m and that $(\mu_1, \mu_2) = (a_2, 2a_5) = (0.06, 1.34)$. With this information we can estimate all the four biases, assuming $\Lambda \ll \ell$. We

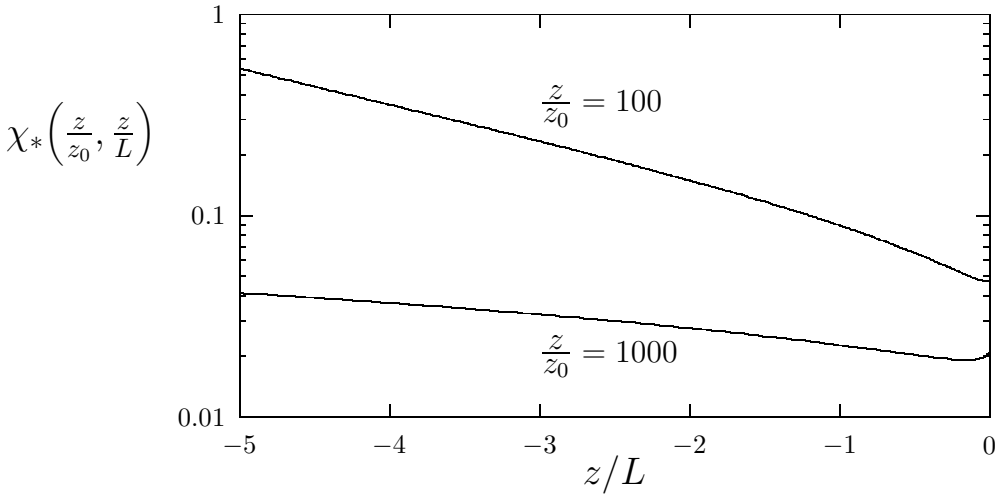

Figure 6. The function $\chi_*(z/z_0, z/L)$ for negative values of z/L.

get

$$\left\{\begin{array}{c}\delta_u\\ \delta_v\\ \delta_w\\ \delta_*\end{array}\right\} = \left\{\begin{array}{r}2.2\%\\ 18.3\%\\ 1.8\%\\ -0.01\%\end{array}\right\}. \tag{135}$$

We see that the v-bias under convective conditions is by far the most important systematic error if the cup anemometer signal is interpreted as the mean of $\tilde{u}$. It may be that we have assumed a too large value of z_i, but even if z_i were only 500 m, δ_v would still be 12%.

Under neutral stratification even δ_v becomes quite small; with the same height and roughness we get, using $\sqrt{\langle v^2\rangle}/u_* = 1.92$ from Panofsky and Dutton (1984), $\delta_v \sim 1\%$.

Izumi and Barad (1970) 'emulated' the cup anemometer signal from the sonic signal by calculating the total horizontal wind speed 20 times per second and averaging this quantity over 15 minutes. This average wind speed, now containing the instrument independent v-bias, was compared to the 15 minutes average of the cup anemometer signal. Their conclusion was that it was between 8 and 16% smaller than the mean wind speed obtained from the cup anemometer. Since the v-bias is the same for the sonic and the cup anemometer and since the effect of different exposures has been accounted for, the implication of the investigation by Izumi and Barad (1970) is that the sum of δ_u, δ_w and δ_* must be 8 to 16%. This contradicts (135) which states that this sum hardly amounts to more than 4%. The most likely explanation is that the cup anemometers and the sonics were exposed differently as also pointed out by Wieringa (1980) [see also the discussion between Wyngaard *et al.* (1982) and Wieringa (1982)]. The overspeeding problem

in the Kansas experiment can probably not be solved.

There is a method to avoid v-bias by using the cup anemometer in conjunction with a wind vane as we shall see later in section 4.

2.8 Afterthoughts

I have now come to the end of the discussion of the cup anemometer. Using a phenomenological model, augmented by a more physical model based on assumptions about the wind force on the rotor and about the linearity of the calibration, my main conclusion is that cup-anemometer overspeeding is seldom a problem. Only the v-bias can at times be large, but, as I will show in section 4, it is very easy to remove this bias operationally.

However, there is a minor point I would like to take up before we leave this subject.

Irregular rotation

Until now we have tacitly assumed that the output $\tilde{s}$ of the anemometer is a 'smooth', low-pass filtered picture of the wind speed. This is not correct. The rotor does not turn with a constant angular velocity in a constant wind. It *wobbles* because the rotor is not in itself axisymmetric so that the wind does not constantly attack the same cup configuration. For example, a three-cup rotor has only a 120° rotation symmetry which means that $\tilde{s}$ is at best a periodic signal with a period equal to one third of the full time Δt of one rotor revolution. This is shown experimentally by Coppin (1982) who has measured the torque $F = \dot{\tilde{s}}$ in a wind tunnel with a temporal resolution much smaller than Δt. In order to eliminate the effect of the uneven angular velocity of the rotor we must filter $\tilde{s}$ over at least one period. This is done by measuring the time Δt for each revolution. The implication is that the cup anemometer operates as not only a first-order filter, characterized by the distance constant ℓ_0, but as a combination of this filter and an unweighted average over one revolution, corresponding to a line average of length $2\pi\ell$ along the wind direction. This combined low-pass filter has the transfer function

$$H(k) = \frac{\mathrm{sinc}^2(\pi k\ell)}{1 + k^2\ell_0^2}, \tag{136}$$

which is shown in Figure 7 for the Risø-70 model and in the limit $\ell/\ell_0 \to 0$.

As the figure shows, the extra low-pass filtering from averaging over one full rotor resolution is only of consequence for the Risø-70 model when $k\ell_0 \gtrsim 1$ at which point the transfer function already has fallen down to 0.5. The equation (136) shows that if $\ell \approx \ell_0$ the cup anemometer cannot be considered a simple first-order filter.

3 Dynamics of Nonlinear Sensors

The nonlinear forcing theory of cup anemometers can be generalized to any first- or higher-order sensor system. In Kristensen and Lenschow (1988) we analyzed first- and second-order systems and applied our theory to predict the systematic error in the measured mean for three different sensors with nonlinear forcing.

Our 1988-analysis was simpler than that of the cup anemometer because the sensors were assumed to respond to only one input and not to two or more as is the case with the cup anemometer: if the angular response is not ideal, i.e. not a cosine response, it has two independent input, the horizontal wind component and the

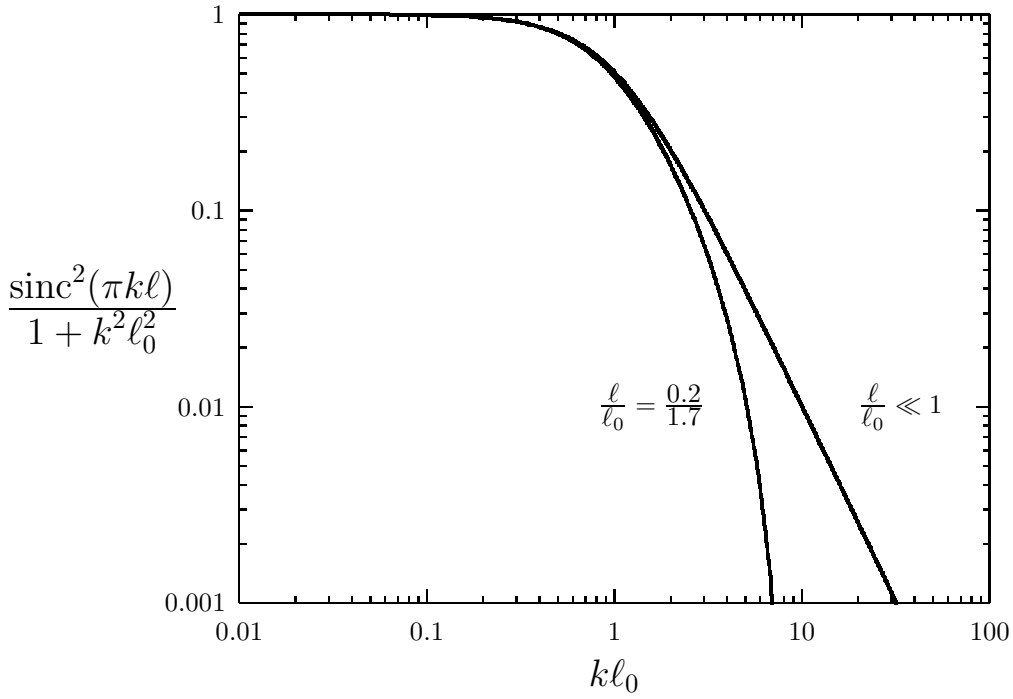

Figure 7. The transfer function $H(k)$ as given by (136) for the Risø-70 model with $\ell = 0.2$ m and $\ell_0 = 1.7$ m and for a hypothetical cup anemometer with $\ell/\ell_0 = 0$.

vertical wind component. On the other hand, we relaxed the condition that the steady-state calibration should be linear.

First-order systems

A first-order system with input $\tilde{x}$ and response $\tilde{y}$ follows the equation

$$\dot{\tilde{y}} = F(\tilde{y}, \tilde{x}), \tag{137}$$

where the function $F(\tilde{y}, \tilde{x})$ is a general forcing function of the input and the response.

Just as in the case of the cup anemometer, the steady-state calibration is obtained by letting the input $\tilde{x}$ stay constant until the system does not change its state anymore, viz. $\dot{\tilde{y}}$ is zero. In this situation the input X and the response Y satisfy the equation

$$F(Y, X) = 0, \tag{138}$$

which allows us to determine $Y = Y(X)$ as a function of X.

Since the function $F(Y, X)$ has such a form that the $F(Y(X), X)$ is always zero, the first and second derivatives of $F(Y(X), X)$ with respect to X are also zero[††].

In other words,

$$\frac{\partial F}{\partial Y}\frac{dY}{dX} + \frac{\partial F}{\partial X} = 0 \tag{139}$$

[††]The same argument implies of course that all higher derivatives are zero. Considering only second-order perturbations, however, we need not to worry about higher derivatives than the second.

and

$$\frac{\partial F}{\partial Y}\frac{d^2Y}{dX^2} + \frac{\partial^2 F}{\partial Y^2}\left[\frac{dY}{dX}\right]^2 + 2\frac{\partial^2 F}{\partial Y \partial X}\frac{dY}{dX} + \frac{\partial^2 F}{\partial X^2} = 0. \tag{140}$$

We note that (140) has a term proportional to d^2F/dX^2 because we include sensors with nonlinear calibration in our investigation.

Following the procedure we used when we analyzed the dynamics of the cup anemometer, the input is written

$$\tilde{x} = X + x, \tag{141}$$

while the output is decomposed according to

$$\tilde{y} = Y(X) + y. \tag{142}$$

Substituting in (137) and expanding to second order in x and y in the neighborhood of $(X, Y(X))$, we get in analogy to (36)

$$\dot{y} + \frac{y}{\tau_0} = \frac{dY}{dX}\frac{x}{\tau_0} + \frac{1}{2}\left\{\frac{\partial^2 F}{\partial Y^2}y^2 + 2\frac{\partial^2 F}{\partial Y \partial X}xy + \frac{\partial^2 F}{\partial X^2}x^2\right\}, \tag{143}$$

where

$$\tau_0 = -\left(\frac{\partial F}{\partial Y}\right)^{-1} \tag{144}$$

is the time constant, which in general is a function of X. As in the case of the cup anemometer, $\partial F/\partial Y = -1/\tau_0$ must be positive; otherwise the system would be unstable for a small change x in the input (cf. the discussion of the response to a step function on page 10).

To obtain the form of the first term on the right-hand side of (143) the first-order constraint (139) was applied.

Following almost the same procedure as in the case of the cup anemometer, we, Kristensen and Lenschow (1988), found that if the input $\tilde{x}$ to a first-order system is not constant, the systematic error $\langle y \rangle$ of the measured mean is given by

$$\begin{aligned} \langle y \rangle &= \frac{1}{2}\frac{\partial^2 F}{\partial X^2}\tau_0 \int_{-\infty}^{\infty} \frac{\omega^2\tau_0^2}{1+\omega^2\tau_0^2} S_x(\omega) d\omega \\ &\quad + \frac{1}{2}\frac{d^2Y}{dX^2}\int_{-\infty}^{\infty} \frac{S_x(\omega)}{1+\omega^2\tau_0^2} d\omega, \end{aligned} \tag{145}$$

where $S_x(\omega)$ is the power spectrum of $\tilde{x}$.

There are two terms in (145). The first corresponds exactly to the u-bias (81) of the cup anemometer. The second accounts for the non-linearity of the calibration of the system. It is proportional to the second derivative of $Y(X)$, i.e. the curvature of the calibration curve, and to the low frequency part of the variance.

We can, as we pointed out in Kristensen and Lenschow (1988), understand in what way this second term describes a systematic error if we imagine that the

time constant τ_0 is very small compared to the integral time scale of the process $x(t)$. In that case the first term is zero and the second becomes

$$\lim_{\tau_0 \to 0}(\langle y \rangle) = \frac{1}{2}\frac{d^2Y}{dX^2}\int_{-\infty}^{\infty} S_x(\omega)d\omega = \frac{1}{2}\frac{d^2Y}{dX^2}\langle x^2 \rangle. \tag{146}$$

We could have arrived at this result directly by neglecting the finite response time of the system and averaging the calibration function with a fluctuating argument:

$$\begin{aligned} \langle \tilde{y} \rangle &= \langle Y(\tilde{x}) \rangle = \langle Y(X+x) \rangle \\ &\approx \left\langle Y(X) + \frac{dY}{dX}x + \frac{1}{2}\frac{d^2Y}{dX^2}x^2 \right\rangle = Y + \frac{1}{2}\frac{d^2Y}{dX^2}\langle x^2 \rangle, \end{aligned} \tag{147}$$

We see that our second-order perturbation theory, leading to (145) retrieves the well-known effect of nonlinear calibration on measured means.

Second-order systems

We will now generalize our second-order perturbation theory to second-order systems. Just like a first-order system is described mathematically by a first-order differential equation like (137), the dynamic behavior of second-order system follows a second-order differential equation, i.e.

$$\ddot{\tilde{y}} = F(\tilde{y}, \dot{\tilde{y}}, \tilde{x}). \tag{148}$$

As in the case of a first-order system, the steady-state calibration is determined by letting the input $\tilde{x}$ stay constant until the response $\tilde{y}$ has become constant. In this situation, both the first and the second time derivatives of $\tilde{y}$ are zero and the input X and the response Y must fulfil the equation

$$F(Y, 0, X) = 0. \tag{149}$$

Again, solving this equation for Y, we obtain a calibration expression $Y = Y(X)$ and, just as in the case of a first-order system, the two constraints (139) and (140) follow immediately.

Decomposing according to (141) and (142), and expanding (148) to the second order in the neighborhood of $(\tilde{y}, \dot{\tilde{y}}, \tilde{x}) = (Y(X), 0, X)$, we get

$$\begin{aligned} \ddot{\tilde{y}} &\equiv \ddot{y} = F(Y+y, \dot{y}, X+x) \\ &\approx \frac{\partial F}{\partial Y}y + \frac{\partial F}{\partial \dot{Y}}\dot{y} + \frac{\partial F}{\partial X}x \\ &\quad + \frac{1}{2}\left\{ \frac{\partial^2 F}{\partial Y^2}y^2 + \frac{\partial^2 F}{\partial \dot{Y}^2}\dot{y}^2 + \frac{\partial^2 F}{\partial X^2}x^2 \right\} \\ &\quad + \frac{\partial^2 F}{\partial Y \partial \dot{Y}}y\dot{y} + \frac{\partial^2 F}{\partial \dot{Y} \partial X}\dot{y}x + \frac{\partial^2 F}{\partial X \partial Y}xy, \end{aligned} \tag{150}$$

where, according to the convention we use here, $\partial/\partial Y$, $\partial/\partial \dot{Y}$ and $\partial/\partial X$ mean partial differentiation with respect to $\tilde{y}$, $\dot{\tilde{y}}$ and $\tilde{x}$, respectively, in the point $(Y(X), 0, X)$.

Natural frequency

Since second-order systems must also be stable, both $\partial F/\partial Y$ and $\partial F/\partial \dot{Y}$ must

be negative and we can introduce the *natural* frequency ω_0 and the (positive) *damping coefficient* ζ by

Damping coefficient

$$\frac{\partial F}{\partial Y} = -\omega_0^2 \tag{151}$$

and

$$\frac{\partial F}{\partial \dot{Y}} = -2\zeta\omega_0. \tag{152}$$

Equation (151) together with (139) implies that

$$\frac{\partial F}{\partial X} = \omega_0^2 \frac{dY}{dX}, \tag{153}$$

so that we can reformulate (150) as

$$\begin{aligned} \ddot{y} + 2\zeta\omega_0\dot{y} + \omega_0^2 y &= \frac{dY}{dX}\omega_0^2 x(t) \\ &\quad + \frac{1}{2}\left\{\frac{\partial^2 F}{\partial Y^2}y^2 + \frac{\partial^2 F}{\partial \dot{Y}^2}\dot{y}^2 + \frac{\partial^2 F}{\partial X^2}x^2\right\} \\ &\quad + \frac{\partial^2 F}{\partial Y \partial \dot{Y}}y\dot{y} + \frac{\partial^2 F}{\partial \dot{Y}\partial X}\dot{y}x + \frac{\partial^2 F}{\partial X \partial Y}xy. \end{aligned} \tag{154}$$

Keeping only the first-order terms on the right-hand side, (154) is a linear, second-order differential equation describing a damped oscillator, i.e. a second-order filter, with the natural frequency ω_0 and the damping coefficient ζ, subjected to the forcing $dY/dX\omega_0^2 x(t)$.

As in the case of a first-order filter like (14) we can imagine that the input $x(t)$ is a step function given by

Response to step input

$$x = \begin{cases} 0 & \text{for } t < 0 \\ \Delta X & \text{for } t \geq 0 \end{cases}. \tag{155}$$

The output from the linear filter (154) is

$$y(t) = \frac{dY}{dX}\Delta X \begin{cases} 1 - \exp(-\zeta\omega_0 t)\left\{\cos\left(\sqrt{1-\zeta^2}\,\omega_0 t\right) \right. \\ \qquad \left. + \dfrac{\zeta}{\sqrt{1-\zeta^2}}\sin\left(\sqrt{1-\zeta^2}\,\omega_0 t\right)\right\}, & 0 \leq \zeta < 1 \\ 1 - \exp(-\omega_0 t)\left\{1 + \omega_0 t\right\}, & \zeta = 1 \\ 1 - \exp(-\zeta\omega_0 t)\left\{\cosh\left(\sqrt{\zeta^2-1}\,\omega_0 t\right) \right. \\ \qquad \left. + \dfrac{\zeta}{\sqrt{\zeta^2-1}}\sinh\left(\sqrt{\zeta^2-1}\,\omega_0 t\right)\right\}, & 1 < \zeta < \infty \end{cases}, \tag{156}$$

shown in Figure 8 for four different values of ζ.

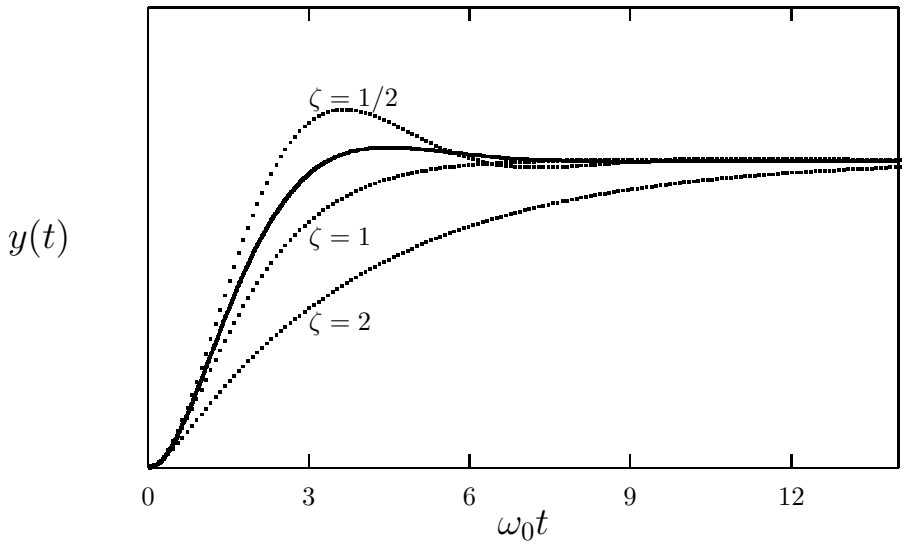

Figure 8. The functions $y(t)$, given by (156) for ζ =0.5, 1 and 2 (dots) and for $\zeta = 1/\sqrt{2}$.

When $\zeta \geq 1$ the solution (156) is an increasing function of time whereas it becomes a damped oscillation for $0 < \zeta < 1$. In Figure 8, I have chosen to show the response $y(t)$ with the value $\zeta = 1/\sqrt{2}$ because, in a certain sense, which is explained below, this damping coefficient provides the best compromise between a fast response and minimal 'overshoot'.

The first-order solution to (154) with the initial conditions $y(-\infty) = 0$ and $\dot{y}(-\infty) = 0$ is

$$y(t) = \frac{dY}{dX} \frac{\omega_0}{\sqrt{1-\zeta^2}} \int_0^\infty x(t-t') \mathrm{e}^{-\zeta\omega_0 t'} \sin\left(\sqrt{1-\zeta^2}\,\omega_0 t'\right) dt', \tag{157}$$

where the damping coefficient is assumed limited to the interval $0 < \zeta < 1$. If $\zeta > 1$, all we have to do is to replace 'sin' by 'sinh' and $\sqrt{1-\zeta^2}$ by $\sqrt{\zeta^2-1}$; in the special case $\zeta = 1$ (157) has a well-defined limit.

Second-order transfer function

If $x(t)$ is a stationary time series, the power spectrum $S_y(\omega)$ of $y(t)$ can be expressed in terms of the power spectrum $S_x(\omega)$ of $x(t)$ simply by

$$S_y(\omega) = K(\omega) S_x(\omega), \tag{158}$$

where

$$K(\omega) = \left(\frac{dY}{dX}\right)^2 \frac{\omega_0^4}{(\omega^2-\omega_0^2)^2 + 4\zeta^2\omega_0^2\omega^2} \tag{159}$$

is the transfer function for a second-order, linear filter. A discussion of this low-pass filter, its response to a step input (157) and the transfer function (159) can be found in Larsen and Busch (1974) in connection with the description of their wind vane. In Figure 9 we have shown $K(\omega)$ for the same four values of ζ as in Figure 8.

Butterworth filters

Figure 9 illustrates why the value $\zeta = 1/\sqrt{2}$ is an advantageous choice of the

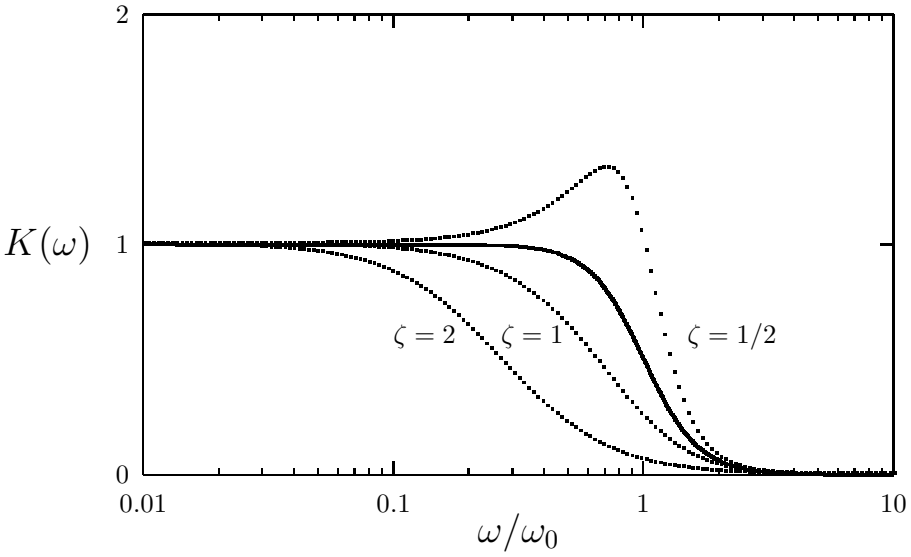

Figure 9. The transfer function $K(\omega)$, given by (159) for ζ =0.5, 1 and 2 (dots) and for $\zeta = 1/\sqrt{2}$.

damping coefficient of a second-order, linear filter: we usually prefer that the low-pass filtered signal $y(t)$ is attenuated as little as possible with respect to $x(t)$ to as high frequencies as possible and then 'rolls off' fast with increasing frequency. We see that when the damping coefficient is greater than one, the transfer function decreases rather slowly with the frequency. $K(\omega)$ decreases faster with frequency the smaller the damping coefficient. When ζ is small compared to one, $K(\omega)$ will have a maximum, which is usually undesirable. It turns out that the 'roll off' is steepest, without $K(\omega)$ having a maximum, when $\zeta = 1/\sqrt{2}$. The filter is then a so-called Butterworth filter of second order (e.g. Stearns and David, 1988). It is often said that a Butterworth filter has 'maximum flatness'. The general form of the transfer function $B_n(\omega)$ of a Butterworth filter of order n is

$$B_n(\omega) = \left(\frac{dY}{dX}\right)^2 \frac{\omega_0^{2n}}{\omega_0^{2n} + \omega^{2n}}. \tag{160}$$

Phase delay

In this context it is sometimes important to look at the phase delay. The filter has the property—as is also the case with a first-order filter like the cup anemometer—that it can only 'look back' in time. By this I mean that it is the present and the past of the input $x(t)$ which determines the output $y(t)$. This means that $y(t)$ is 'delayed' with respect to $x(t)$. The delay will depend on how rapid the input varies as compared to the natural frequency ω_0 of the filter: if it varies comparatively slowly, the delay will be unimportant and if it varies fast, the delay can be of considerably consequence. Formally the delay can be defined by letting $x(t)$ be a harmonic function of time, i.e.

$$x(t) = \Delta X \cos(\omega t). \tag{161}$$

Writing the output $y(t)$ as the phase-shifted cosine,

$$y(t) = \sqrt{K(\omega)}\frac{dY}{dX}\Delta X \cos(\omega t - \beta_{xy}), \tag{162}$$

where $K(\omega)$ is given by (159) and $\beta_{xy}(\omega)$ the delay, a necessary and sufficient condition that (161) and (162) fulfil the linear part of (154) is that the phase-shift is given by

$$\beta_{xy}(\omega) = \arctan\left(2\zeta\frac{\omega\omega_0}{\omega_0^2-\omega^2}\right). \tag{163}$$

This can been seen directly by substituting (161) and (162) in (154). The delay $\beta_{xy}(\omega)$ which, as expected, is a function of the frequency ω of the harmonic input, is shown in Figure 10. We see that irrespective the value of the damping coefficient ζ, the phase delay, or the phase distortion, is equal to $\pi/2$ when $\omega = \omega_0$. What is important is that when the damping coefficient is small, the phase delay stays small closer to $\omega = \omega_0$ than when it is large. Again, if we demand that the transfer function $K(\omega)$ is monotonic and decreasing the best compromise is to let $\zeta = 1/\sqrt{2}$.

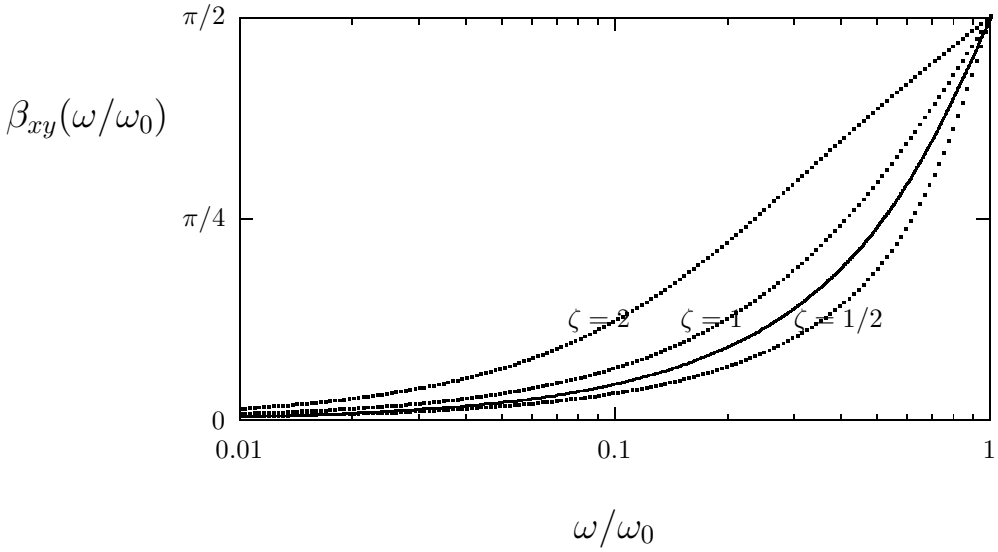

Figure 10. The phase delay $\beta_{xy}(\omega)$, given by (163) for ζ =0.5, 1 and 2 (dots) and for $\zeta = 1/\sqrt{2}$.

Taking the average of (154), we get an expression for the systematic error $\langle y\rangle$ due to non-linear forcing,

$$\begin{aligned}\omega_0^2\langle y\rangle &= \frac{1}{2}\left\{\frac{\partial^2 F}{\partial Y^2}\langle y^2\rangle + \frac{\partial^2 F}{\partial \dot{Y}^2}\langle \dot{y}^2\rangle\right.\\ &\qquad \left. +2\frac{\partial^2 F}{\partial \dot{Y}\partial X}\langle \dot{y}x\rangle + 2\frac{\partial^2 F}{\partial X\partial Y}\langle xy\rangle + \frac{\partial^2 F}{\partial X^2}\langle x^2\rangle\right\}.\end{aligned} \tag{164}$$

We have assumed that $x(t)$ is stationary so that $y(t)$ to the first order is also stationary. This implies that the term $\partial^2 F/\partial Y\partial\dot{Y}\langle y\dot{y}\rangle$ is identically zero and has consequently been left out of (164).

Using the first-order solution (157) and its first derivative, Kristensen and Lenschow (1988) determined the second-order moments on the right-hand side of

(164). We used the two constraints (139) and (140) and should have arrived at the following result

$$\langle y \rangle = \int_{-\infty}^{\infty} \frac{H_0(\omega) + H_2(\omega) + H_4(\omega)}{(\omega^2 - \omega_0^2)^2 + 4\zeta^2\omega_0^2\omega^2} S_x(\omega) d\omega, \tag{165}$$

where

$$H_0(\omega) = \frac{\omega_0^4}{2} \frac{d^2Y}{dX^2}, \tag{166}$$

$$\begin{aligned} H_2(\omega) \quad = \quad & \omega^2 \left\{ \frac{1}{2} \frac{\partial^2 F}{\partial \dot{Y}^2} \omega_0^2 \left[\frac{dY}{dX} \right]^2 \right. \\ & \left. + \left[2 \frac{\partial^2 F}{\partial \dot{Y} \partial X} \zeta\omega_0 - \frac{\partial^2 F}{\partial X \partial Y} \right] \frac{dY}{dX} + 2 \frac{\partial^2 F}{\partial X^2} \left[\zeta^2 - \frac{1}{2} \right] \right\} \end{aligned} \tag{167}$$

and

$$H_4(\omega) = \frac{\omega^4}{2\omega_0^2} \frac{\partial^2 F}{\partial X^2}. \tag{168}$$

Unfortunately, we set $H_4(\omega) = 0$ by mistake.

The first of these functions is really a constant and will give rise to a bias which is due to the non-linearity of the calibration $Y = Y(X)$. This bias is proportional to the low-frequency part of the variance of the input.

The second function is proportional to the square of the frequency and in (165) the corresponding part of the systematic error can best be described as a bias due to a band-passed part of the input variance.

The last function $H_4(\omega)$ will, combined with the denominator in (165), be a high-pass filter of the variance and it is consequently this term which corresponds most closely to the first term in (145) for first-order systems.

In Kristensen and Lenschow (1988) we applied first- and second-order forcing theory on three examples: the Pitot tube (Lenschow, 1986), the thrust anemometer (Smith, 1980) and the CSIRO liquid water probe (King *et al.*, 1978). The first has first-order forcing, the two last second-order forcing. In the next three subsections we will give an account of our analysis. However, it will not be nearly as detailed as the discussion of the cup anemometer in section 2.

3.1 The Pitot Tube

This instrument is commonly used to measure air-flow speed in wind tunnels and from aircraft. It measures the pressure difference $\tilde{q}$ between the so-called total pressure (static pressure plus the kinetic energy density) and the static pressure. In a constant wind $\tilde{u}$ the relation between the measured pressure difference and $\tilde{u}$ is

$$\tilde{q} = \frac{1}{2} \rho \tilde{u}^2, \tag{169}$$

where ρ is the air density.

This equation is true only when $\tilde{u}$ and $\tilde{q}$ are constant. In a fluctuating wind there is an imbalance, approximately described by (Kristensen and Lenschow, 1988)

$$\dot{\tilde{q}} = \frac{1}{\tau_0}\left\{\frac{1}{2}\rho\tilde{u}^2 - \tilde{q}\right\}. \tag{170}$$

The time scale τ_0 characterizes the pressure transmission time and is directly proportional to the length of the pressure tubes.

Let us first consider $\tilde{q}$ as the response. This means that the forcing, by definition [see (137)] is

$$F(\tilde{q},\tilde{u}) = \frac{1}{\tau_0}\left\{\frac{1}{2}\rho\tilde{u}^2 - \tilde{q}\right\}. \tag{171}$$

Being a bit repetitious, the steady-state calibration between the constant input U and the constant response Q can be determined by the equation

$$F(Q,U) = \frac{1}{\tau_0}\left\{\frac{1}{2}U^2 - Q\right\} = 0 \tag{172}$$

with the result

$$Q = \frac{1}{2}\rho U^2. \tag{173}$$

Decomposing input and response according to

$$\left\{\begin{array}{c}\tilde{u}\\ \\ \tilde{q}\end{array}\right\} = \left\{\begin{array}{c}U+u\\ \\ Q+q\end{array}\right\}, \tag{174}$$

we obtain the second-order perturbation equation

$$\dot{q} + \frac{q}{\tau_0} = \rho U\frac{u}{\tau_0} + \frac{\rho}{2\tau_0}u^2. \tag{175}$$

We note that the response q does not enter the right-hand side. This means that in this case there is no second-order *feedback*.

Applying (145), we see that the first term, as a consequence of this missing feedback, is zero and that the bias simply becomes

$$\frac{\langle q\rangle}{Q} = \frac{\langle u^2\rangle}{U^2}, \tag{176}$$

i.e. the square of the relative turbulence intensity.

If we interpret $\tilde{q}$ as an instantaneous estimate $\tilde{v}$ of the wind speed by *Linearization*

$$\tilde{v} = \sqrt{\frac{2\tilde{q}}{\rho}}, \tag{177}$$

the dynamic equation for the output $\tilde{v}$ becomes

$$\dot{\tilde{v}} = \frac{1}{2\tau_0}\left(\frac{\tilde{u}^2}{\tilde{v}} - \tilde{v}\right). \tag{178}$$

The signal interpretation is called *linearization* and will of course lead to the linear calibration.

The calibration with the instantaneous interpretation of $\tilde{q}$ of course leads to the linear calibration

$$V = V(U) = U. \tag{179}$$

The overspeeding becomes, again with the aid of (145),

$$\frac{\langle v \rangle}{V} = \frac{1}{U^2} \int_{-\infty}^{\infty} \frac{\omega^2 \tau_0^2}{1 + \omega^2 \tau_0^2} S_u(\omega) d\omega. \tag{180}$$

While the cup anemometer (and other rotation anemometers) are characterized by a distance constant the Pitot tube has a time constant. However, if we for a given mean wind speed compare the overspeeding of the linearized signal from a Pitot tube to that of the cup anemometer and assume a mean wind speed such that the two time constants are the same, we see by comparing with (102) that the Pitot tube has an overspeeding which is about the same as the u-bias of the cup anemometer.

The maximum overspeeding is, according to (176) and (180) $\langle u^2 \rangle / (U^2)$, no matter whether the signal is linearized or not. In an aircraft where typical values are $\sqrt{\langle u^2 \rangle} \sim 1$ m s^{-1} and $U \gtrsim 50$ m s^{-1} Pitot tube overspeeding is hardly of any concern.

3.2 The Thrust Anemometer

Measurement of wind speed by a thrust anemometer is obtained by measuring the drag force on a reference body, held in elastic suspension, so that its displacement becomes proportional to the drag force.

In Kristensen and Lenschow (1988) we discuss the thrust anemometer developed at Pennsylvania State University (Norman *et al.*, 1976). This instrument has a cylindrical styrofoam drag element mounted coaxially on the end of a thin ceramic rod, which is fixed in the opposite end and thus provides the elastic suspension force. Part of this rod is submerged in silicon oil for damping. The drag element is 0.048 m long and has a diameter of 0.016 m. The length and diameter of the ceramic rod are 0.012 m and 0.0025 m, respectively. In Kristensen and Lenschow (1988) a sketch shows the anemometer and its geometrical dimensions.

The equation describing the displacement $\tilde{\delta}$ in one direction is a second-order differential equation

$$\ddot{\tilde{\delta}} = F(\tilde{\delta}, \dot{\tilde{\delta}}, \tilde{u}). \tag{181}$$

In vacuum the anemometer would, if it were set in motion, describe a damped oscillation, characterized by the frequency ω_1 which is proportional to the square root of the restoring force, and the damping coefficient η. Most of the damping could be ascribed to the damping oil.

In the wind the drag force is proportional to the square of the relative velocity $\dot{\tilde{\delta}} - \tilde{u}$ of the drag element compared to the wind and the total forcing function can be written

$$F(\tilde{\delta}, \dot{\tilde{\delta}}, \tilde{u}) = -2\eta\omega_1 \dot{\tilde{\delta}} - \omega_1^2 \tilde{\delta} + \frac{1}{\ell_t} \{\tilde{u} - \dot{\tilde{\delta}}\}^2, \tag{182}$$

where ℓ_t is an instrument length scale.

Again, the calibration is determined by

$$F(\Delta, 0, U) = 0, \tag{183}$$

so that

$$\Delta \equiv \Delta(U) = \frac{U^2}{\ell_t \omega_1^2}. \tag{184}$$

With this equation and the theory for the bending and oscillations of a beam (the ceramic rod), which is clamped in one end, it is possible to give a physical interpretation of the length ℓ_t. According to standard literature such as Sommerfeld (1964) or Feynman *et al.* (1964), the displacement Δ is under steady-state conditions given by

$$\Delta = \frac{1}{3}\frac{F_D}{E\mathcal{I}}\lambda^3, \tag{185}$$

where F_D is the drag force on the drag element and where λ is the length, E Young's modulus (ratio between stress and strain) and $\mathcal{I}$ the cross-sectional moment of inertia (dimension length to the fourth power) of the rod. The drag force is, with the same notation as that used in (88) for the cup anemometer,

$$F_D = \frac{1}{2}\rho C A U^2. \tag{186}$$

The area A is here the projected area of the cylindrical drag element. Since the Reynolds number based on the diameter of the this drag element is of the order 10^4, the drag coefficient C is approximately one (Feynman *et al.*, 1964).

Following Clough and Penzien (1975) and the arguments by Panofsky and Dutton (1984), the frequency ω_1 of the free oscillation of a clamped rod is given by E, $\mathcal{I}$ and the mass M as

$$\omega_1^2 \approx 3.516\frac{E\mathcal{I}}{M\lambda^3}. \tag{187}$$

Substituting (186) in (185) and multiplying the result with (187), we can reproduce (184) in the form

$$M\Delta\omega_1^2 \approx 0.6\rho C A U^2. \tag{188}$$

The left-hand side is the mass of the rod times the acceleration in free oscillation of its top, whereas the right-hand side is the forcing by the wind. Equation (188) is the overall description of the motion the rod would perform, if we imagine that the air with wind speed U suddenly disappeared so that there is vacuum around the anemometer.

We see that the characteristic length ℓ_t is proportional to the length of the rod λ and the ratio between the density ρ_c of ceramic and that of air ρ; since $M = \rho_c A\lambda$ we may combine (184) and (188) to obtain the approximate relation

$$\ell_t \approx \frac{M}{0.6\rho C A} \approx \lambda\frac{\rho_c}{\rho}. \tag{189}$$

To determine ω_0 and ζ, we differentiate (184) once and twice with respect to U. These derivatives become

$$\frac{d\Delta}{dU} = \frac{2U}{\ell_t \omega_1^2} \tag{190}$$

and

$$\frac{d^2\Delta}{dU^2} = \frac{2}{\ell_t \omega_1^2}. \tag{191}$$

In this case

$$\omega_0 \equiv \sqrt{-\frac{\partial F}{\partial \Delta}} = \omega_1 \tag{192}$$

and

$$\zeta \equiv -\frac{1}{2\omega_0}\frac{\partial F}{\partial \dot{\Delta}} = \eta + \frac{U}{\ell_t \omega_1} \tag{193}$$

and we note that the damping gets an extra term due to the effect of the drag element moving air in front of it.

There are only three second derivatives different from zero. They are

$$\frac{\partial^2 F}{\partial U^2} = \frac{\partial^2 F}{\partial \dot{\Delta}^2} = -\frac{\partial^2 F}{\partial \dot{\Delta} \partial U} = \frac{2}{\ell_t}. \tag{194}$$

The three functions (166), (167) and (168) become

$$H_0(\omega) = \frac{\omega_1^2}{\ell_t}, \tag{195}$$

$$H_2(\omega) = \frac{4\omega^2}{\ell_t}\left(\eta^2 - \frac{1}{2}\right) \tag{196}$$

and

$$H_4(\omega) = \frac{\omega^4}{\ell_t \omega_1^2}. \tag{197}$$

Thus the relative bias is

$$\frac{\delta}{\Delta} = \frac{1}{U^2}\int_{-\infty}^{\infty} \frac{(\omega^2 - \omega_1^2)^2 + 4\eta^2\omega_1^2\omega^2}{(\omega^2 - \omega_1^2)^2 + 4\zeta^2\omega_1^2\omega^2} S_u(\omega) d\omega \tag{198}$$

Equation (193) tells us that the total damping coefficient ζ always is greater than η. The coefficient in front of the spectrum in (198) is therefore always smaller than one. Again we conclude that the upper limit to the relative bias is the square of the turbulence intensity.

Linearization

As we did in the case of the Pitot tube, we can remove the bias due to non-linearity of the calibration ($H_0(\omega)$) by making an on-line, instantaneous interpretation of $\tilde{\delta}(t)$ by the relation

$$\tilde{v} = \omega_1 \sqrt{\ell_t \tilde{\delta}} \tag{199}$$

and, in this way, evaluate the systematic error $\langle v \rangle$ of the 'apparent' wind speed.

We now have

$$\ddot{\tilde{v}} = F(\tilde{v}, \dot{\tilde{v}}, \tilde{u}) \tag{200}$$

with the somewhat more complicated forcing

$$F(\tilde{v}, \dot{\tilde{v}}, \tilde{u}) = -2\eta\omega_1\dot{\tilde{v}} - \frac{\omega_1^2}{2}\left\{\tilde{v} - \frac{\tilde{u}^2}{\tilde{v}}\right\} - \frac{2}{\ell_t}\tilde{u}\dot{\tilde{v}} - \frac{\dot{\tilde{v}}^2}{\tilde{v}} + 2\frac{\tilde{v}\dot{\tilde{v}}^2}{\ell_t^2\omega_1^2}. \tag{201}$$

In this case we have of course

$$V \equiv V(U) = U. \tag{202}$$

The frequency ω_0 and the damping ζ are the same as those given by (192) and (193) and the rest of the expressions necessary to determine the systematic error are

$$\frac{\partial^2 F}{\partial U^2} = -\frac{\partial^2 F}{\partial U \partial V} = \frac{\omega_1^2}{U}, \tag{203}$$

$$\frac{\partial^2 F}{\partial \dot{V} \partial U} = -\frac{2}{\ell_t} \tag{204}$$

and

$$\frac{\partial^2 F}{\partial \dot{V}^2} = 4\frac{U}{\ell_t^2\omega_1^2} - \frac{2}{U}. \tag{205}$$

We have here designed $H_0(\omega) = 0$. The two other weighting functions are

$$H_2(\omega) = 2\eta^2\frac{\omega_1^2\omega^2}{U} \tag{206}$$

and

$$H_4(\omega) = \frac{\omega^4}{2U}. \tag{207}$$

With the instant interpretation of $\tilde{\delta}$ the relative bias becomes

$$\frac{\langle v \rangle}{V} = \frac{1}{2U^2}\int_{-\infty}^{\infty} \frac{\omega^4 + 4\eta^2\omega_1^2\omega^2}{(\omega^2 - \omega_1^2)^2 + 4\zeta^2\omega_1^2\omega^2} S_u(\omega) d\omega. \tag{208}$$

Comparing (208) with (198) we find that $\langle \delta \rangle/\Delta > \langle v \rangle/V$ when $\eta > 1/\sqrt{2}$, irrespective of the spectrum. When $\eta \leq 1/\sqrt{2}$, we can not in general predict which of the total systematic errors is largest although, a priori, it seems likely that $\langle \delta \rangle/\Delta > \langle v \rangle/V$ for most spectra since the bulk of the velocity variance is likely to be concentrated at low frequencies.

To be more specific, the Penn State thrust anemometer has $\eta \approx 0.7$, $\omega_1 \approx 210$ rad s^{-1} and $\ell_t \approx 12$ m (John Norman, 1986, private communication). Therefore the contribution $U/(\omega_1\ell_t)$ to the total damping is negligible in comparison with η. The implication of $\zeta = \eta$ is that (198) becomes

$$\frac{\langle \delta \rangle}{\Delta} = \frac{\langle u^2 \rangle}{U^2}. \tag{209}$$

According to (133) and (129), the bias $\langle\delta\rangle/\Delta$ in (209) is twice that of δ_v, given by (134), under unstable conditions. It can consequently quite easily become large, perhaps more than 10%.

If we assume that the spectrum

$$S_u(\omega) = \frac{1}{2}\alpha_1(\varepsilon U)^{2/3}|\omega|^{-5/3}, \tag{210}$$

corresponding to (109) in the frequency domain, it is possible to evaluate the bias (208).

It becomes

$$\frac{\langle v\rangle}{V} = \alpha_1\frac{(\varepsilon U/\omega_1)^{2/3}}{2U^2}\left\{h(\zeta) + 4\eta^2 g(\zeta)\right\}, \tag{211}$$

where

$$g(\zeta) = \int_0^\infty \frac{s^{1/3}}{(s^2-1)^2 + 4\zeta^2 s^2}ds \tag{212}$$

and

$$h(\zeta) = \int_0^\infty \frac{s^{7/3}}{(s^2-1)^2 + 4\zeta^2 s^2}ds. \tag{213}$$

These functions can be expressed in terms of well-known standard functions as (Gradshteyn and Ryzhik, 1980)

$$g(\zeta) = \frac{\pi}{\sqrt{3}}\frac{\sin\left(\frac{1}{3}\arccos(2\zeta^2-1)\right)}{2\zeta\sqrt{1-\zeta^2}} \tag{214}$$

and

$$h(\zeta) = \frac{\pi}{\sqrt{3}}\frac{\sin\left(\frac{2}{3}\arccos(2\zeta^2-1)\right)}{2\zeta\sqrt{1-\zeta^2}}. \tag{215}$$

They are displayed in Figure 11.

We can use the diabatic functions (126) and (128) in subsection 2.7 to evaluate (211) in unstable stratification by means of (118) and (120):

$$\frac{\langle v\rangle}{V} = \frac{1}{2}\alpha_1\kappa^{2/3}\chi_t\left(\frac{z}{z_0},\frac{z}{L}\right)\left(\frac{u_*}{z\omega_1}\right)^{2/3}\left\{h(\zeta) + 4\eta^2 g(\zeta)\right\}, \tag{216}$$

where

$$\chi_t\left(\frac{z}{z_0},\frac{z}{L}\right) = \left\{\ln\left(\frac{z}{z_0}\right) - \psi_m\left(\frac{z}{L}\right)\right\}^{-4/3}\varphi_\varepsilon^{2/3}\left(\frac{z}{L}\right), \tag{217}$$

displayed in Figure 12.

Under rather unstable situations with $L = -10$ m, $z = 10$ m, $z_0 = 0.1$ m and $u_* = 0.5$ m s^{-1}, the Penn State thrust anemometer will have an overspeeding of about 0.1%. It will be even less for neutral and stable stratification.

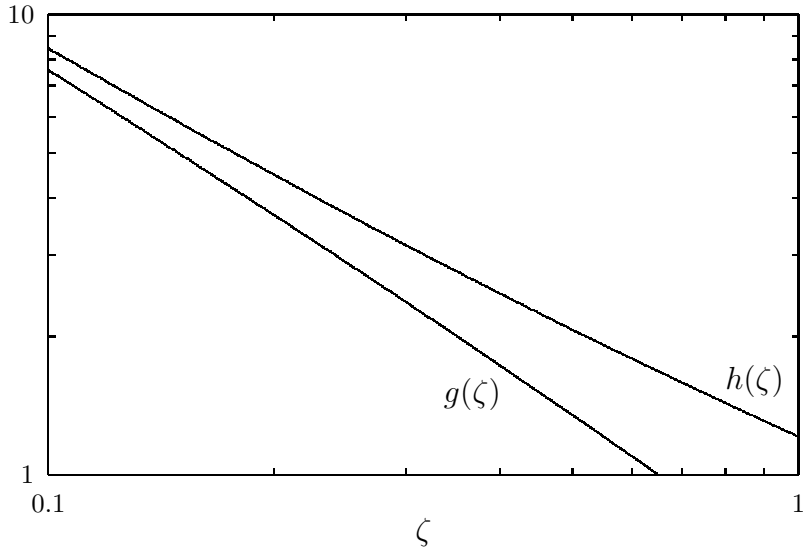

Figure 11. The functions $g(\zeta)$ and $h(\zeta)$, given by (214) and (215).

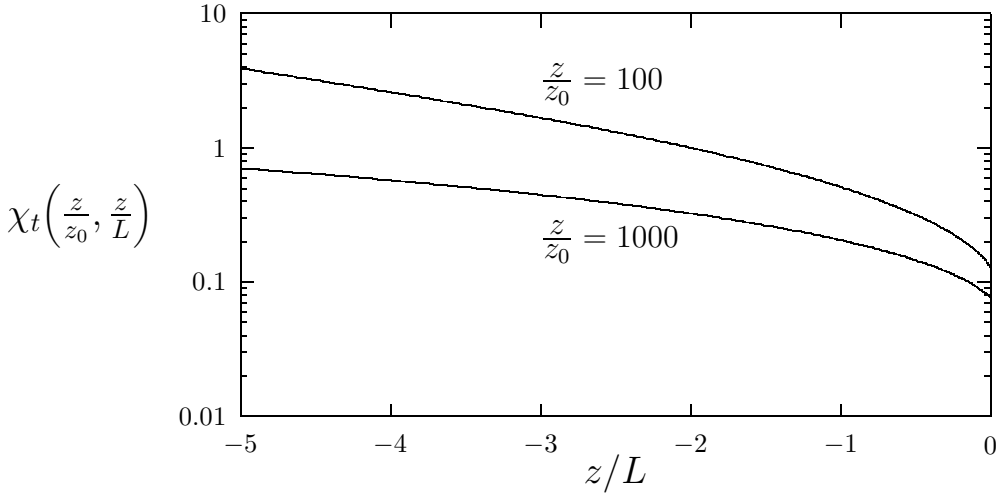

Figure 12. The function $\chi_t(z/z_0, z/L)$ for negative values of z/L.

It seems therefore advantageous to perform instantaneous, on-line interpretation of $\tilde{\delta}$ as prescribed by (199). It may reduce the systematic error due to nonlinear forcing quite considerably. Qualitatively, it is quite obvious why this is the case: when $H_0(\omega)$ is zero in (165), the low frequency part of the turbulence is excluded from contributing to the bias.

The section discussing the thrust anemometer in Kristensen and Lenschow (1988) is unfortunately haunted by errors. As a consequence of the missing term, proportional to ω^4 in [53][‡‡], [76] is in error. Further, there are errors independent of

[‡‡]References to equations in other texts are indicated by the equation numbers in square

this mistake in [88], [90] and [94]. The last equation becomes the same function as (214) if divided by η.

3.3 The CSIRO Liquid Water Probe

King *et al.* (1978) describe a liquid water probe which uses a constant-temperature hot-wire element exposed to the airstream to measure in-cloud, total liquid water concentration $\tilde{w}$ from an aircraft. Bradley and King (1979) show that when the fluctuations in liquid water concentration are small compared to the mean, the output signal $\tilde{w}_s$, normalized to concentration units, obeys the equation

$$\ddot{\tilde{w}}_s = \omega_d^2(1+r\tilde{w}_s)(\tilde{w}-\tilde{w}_s) - 2\zeta_d\omega_d(1+r\tilde{w}_s)^{-1/2}\dot{\tilde{w}}_s + r(1+r\tilde{w}_s)^{-1}\dot{\tilde{w}}_s^2, \quad (218)$$

where ω_d and ζ_d are the natural frequency and damping coefficient, respectively, for zero liquid water concentration and r the ratio between "wet" and "dry" cooling power for $\tilde{w} = 1$ g m^{-3}.

The wire evaporates the droplets it encounters. In clouds, the cooling will in general be dominated by this evaporating and if the density of water is more than about $\tilde{w} = 1$ g m^{-3}, both the natural frequency and the damping coefficient will be modified, as the dynamic equation (218) shows.

The calibration, the natural frequency and the damping coefficient are

$$W_s = W, \quad (219)$$

$$\omega_0 = \omega_d\sqrt{1+rW} \quad (220)$$

and

$$\zeta = \frac{\zeta_d}{1+rW}. \quad (221)$$

The error setting $H_4(\omega) = 0$ in general in (165) has fortunately no consequence in this case because $\partial^2 F/\partial X^2$ is zero so that $H_4(\omega) = 0$. The linear calibration implies that $H_0(\omega)$ is also zero. $H_2(\omega)$ is different from zero and given by

$$H_2(\omega) = -2\omega_d^2\omega^2 \quad (222)$$

and the relative bias becomes

$$\frac{\langle w_s\rangle}{W_s} = -2\frac{r}{W}\int_{-\infty}^{\infty}\frac{\omega_d^2\omega^2}{(\omega^2-\omega_0^2)^2+4\zeta^2\omega_0^2\omega^2}S_w(\omega)d\omega. \quad (223)$$

We note that this systematic error is negative.

In order to evaluate the magnitude of the relative bias, we (Kristensen and Lenschow, 1988) chose data from a flight with the NCAR Electra aircraft in marine stratocumulus off the California coast. The time series we selected was obtained from a flight leg at the top of the stratocumulus cloud layer, where the fluctuation level of the liquid water concentration is higher than within the cloud layer.

We found that the spectrum of liquid water concentration was proportional to the frequency to the minus one power, and consistent with the spectrum determined by NCAR's FSSP probe (Knollenberg, 1981).

parentheses.

It can be written in the form

$$S_w(\omega) = C\langle w^2\rangle/|\omega|, \tag{224}$$

where C is a dimensionless constant.

Assuming that the spectral shape does not change with the mean concentration W and that $\sqrt{\langle w^2\rangle}$ is always proportional to W, we get the following result

$$\frac{\langle w_s\rangle}{W_s} = -2\frac{C\langle w^2\rangle}{W^2}\,\frac{rW}{1+rW} I\left(\frac{\zeta_d}{1+rW}\right). \tag{225}$$

The function $I(\zeta)$ is

$$I(\zeta) = \int_0^\infty \frac{ds}{(1-s)^2 + 4\zeta^2 s} \tag{226}$$

which, after simple manipulations can be expressed in terms of well-known functions as

$$I(\zeta) = \frac{1}{2\zeta}\begin{cases} \left[\pi - \arctan\left(\dfrac{2\zeta\sqrt{1-\zeta^2}}{1-2\zeta^2}\right)\right]/\sqrt{1-\zeta^2}, & 0 < \zeta < 1/\sqrt{2} \\ \arctan\left(\dfrac{2\zeta\sqrt{1-\zeta^2}}{2\zeta^2-1}\right)/\sqrt{1-\zeta^2}, & 1/\sqrt{2} \le \zeta < 1 \\ \ln\left(2\zeta^2 - 1 + 2\zeta\sqrt{\zeta^2-1}\right)/\sqrt{\zeta^2-1}, & 1 \le \zeta < \infty \end{cases} \tag{227}$$

Figure 13 shows this function. For very small values of ζ it becomes asymptotically equal to $\pi/(2\zeta)$. This was unfortunately not what we showed in Figure 4 in Kristensen and Lenschow (1988); we made the mistake of letting the second line in (227) cover the entire interval from $0 < \zeta \le 1$, although it is clear that the integral (226) is divergent when $\zeta = 0$.

The time series analysis showed that the mean concentration was $W \approx 0.2$ g m^{-3} and $C\langle w^2\rangle \approx 2.5 \times 10^{-3}$ g^2 m^{-6}. According to Warren D. King (1986, private communication) and consistent with Bradley and King (1979), $r \approx 1$ g^{-1} m^3 and $\zeta_d = 2$. Inserting these values in (225) the relative bias can be determined as function of the mean concentration W. The result is shown in Figure (14).

We see that when the mean concentration is 2 g m^{-3}, which is a typical value in a cloud, the relative bias due to the nonlinear forcing is about -10%.

4 Cup and Vane

The almost linear calibration of the cup anemometer, its simple filtering characteristics and its simplicity in operation makes it well suited for routine measurements in meteorological services such as data recording for weather forecasting and airport briefings of pilots.

Combined with a wind vane, which incidentally is also omnidirectional, it can very easily provide information about wind speed and direction, wind direction variance $\langle\delta\phi^2\rangle$, and with a little more effort wind speed variance and consequently also, as we shall see, gust information.

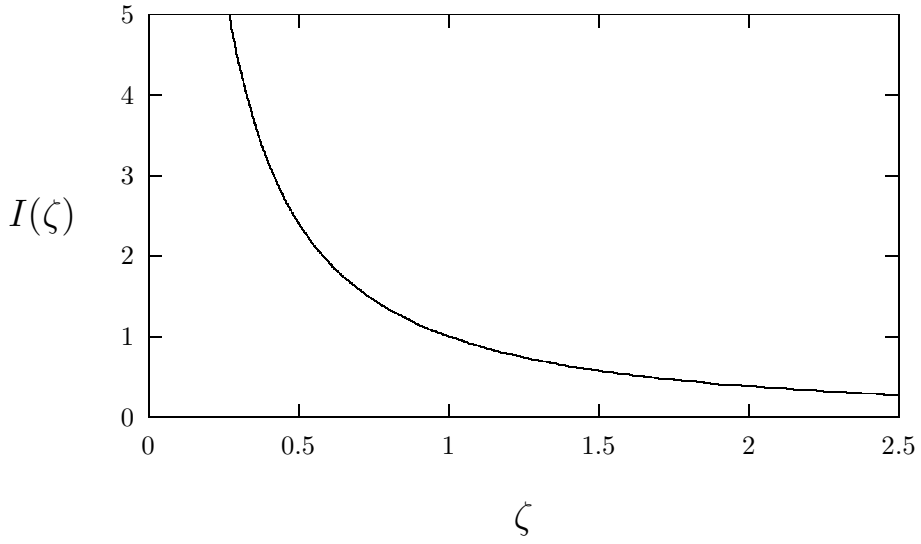

Figure 13. The function $I(\zeta)$.

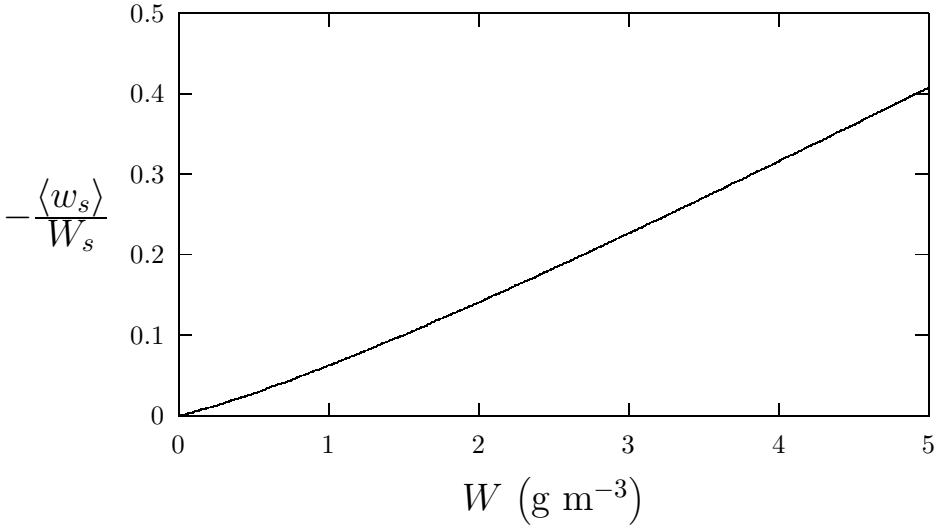

Figure 14. The relative bias of the CSIRO Liquid Water Probe as function of the mean concentration.

Wind vane

The common wind vane, which has been discussed in some detail by Wyngaard (1981), is well described as a second-order linear filter. Let $\alpha(t) \approx v/U$ be the instantaneous wind direction in a coordinate system where the mean wind direction defines the x-axis [see (5)] and ϕ the measured wind direction. Then

$$\ddot{\phi} + 2\zeta\omega_0\dot{\phi} + \omega_0^2\phi = \omega_0^2\alpha(t), \tag{228}$$

where ω_0 and ζ are the natural frequency and the damping coefficient, respectively.

We have already in section 3 shown how such a system reacts to a sudden change in the input [see (156)] and how in frequency domain the amplitude and the phase

of the output is related to the input.

Vane distance constant

As shown by Wyngaard (1981), the natural frequency ω_0 is proportional to the mean wind speed U, whereas the damping coefficient is independent of U. We can therefore introduce a *distance constant* ℓ_v by

$$\ell_v = \frac{U}{\omega_0} \tag{229}$$

and rewrite (228) as a differential equation in the coordinate x by using Taylor's hypothesis:

$$\frac{d^2\phi}{dx^2} + 2\frac{\zeta}{\ell_v}\frac{d\phi}{dx} + \frac{\phi}{\ell_v^2} = \frac{\alpha}{\ell_v^2}. \tag{230}$$

The transfer function and the phase delay now become functions of wave number k rather than frequency so that instead of (159) and (163) we have

$$K_v(k) = \frac{1}{(1-k^2\ell_v^2)^2 + 4\zeta^2 k^2 \ell_v^2} \tag{231}$$

and

$$\beta_v(k) = \arctan\left(\frac{2\zeta}{1-k^2\ell_v^2}\right). \tag{232}$$

Vane Butterworth filter

We see that the vane, like the cup anemometer, is a filter which operates in space along the mean wind direction. Again, in order for this filter to have the *maximum flatness* it should have a damping coefficient equal to $1/\sqrt{2}$, i.e. be a Butterworth filter (of second order). Larsen and Busch (1974) have shown how in practice it is possible to obtain this value over a large range of wind speeds by choosing a proper length of the vane arm.

Matching of distance constants

It is most advantageous to match the distance constant ℓ_v to that of the cup anemometer ℓ_0. In that way simultaneous outputs of instantaneous values will 'seen' through filters remembering approximately the same past. This could be of importance if we for example were interested in measuring the covariance $\langle uv \rangle$; as we have demonstrated Kristensen and Lenschow (1988) in the case of two first-order filters, the measured covariance between two output gets contributions not only from the cospectrum (the 'in-phase' spectrum) but also from the quadrature-spectrum (the 'out-of-phase' spectrum) when there is a mismatch between the filter characteristics.

Cup anemometer as trigger

If we are only interested in the mean-wind direction and the mean velocity, the most practical way to measure these is to use the anemometer only as a trigger to read off ϕ. For example, we could let our measuring system read off ϕ once for every resolution, corresponding the wind way $2\pi\ell$ in the direction ϕ, i.e. the length of the column of air which has blown through the anemometer in the meantime. If we do not want to use such a small temporal resolution, we could let every second or tenth resolution trigger the read-off.

Mean wind vector

We store all these direction measurements during the averaging period T, e.g. 10 minutes. Let ϕ_n be measurement number n of the total number N. Then the number pair

$$\left\{ \begin{array}{c} U \\ \\ V \end{array} \right\} = \frac{2\pi\ell}{T} \left\{ \begin{array}{c} \sum_{n=1}^{N} \cos(\phi_n) \\ \sum_{n=1}^{N} \sin(\phi_n) \end{array} \right\} \tag{233}$$

is, by definition, the horizontal mean velocity vector, because it corresponds to the displacement of an air parcel in the period T (if the windfield were only a function of time and not space). The mean wind speed becomes $\sqrt{U^2+V^2}$ and the mean wind direction can be determined as

Mean wind direction

$$\langle\phi\rangle = \arctan\left(\frac{\langle\sin(\phi)\rangle}{\langle\cos(\phi)\rangle}\right), \tag{234}$$

where

$$\left\{\begin{array}{c}\langle\cos(\phi)\rangle\\ \\ \langle\sin(\phi)\rangle\end{array}\right\} = \frac{1}{N}\left\{\begin{array}{c}\sum_{n=1}^{N}\cos(\phi_n)\\ \\ \sum_{n=1}^{N}\sin(\phi_n)\end{array}\right\}. \tag{235}$$

As a bonus, the wind direction variance can be obtained by expanding $\langle\cos(\phi)\rangle^2$ and $\langle\sin(\phi)\rangle^2$ in the deviation $\delta\phi$ from $\langle\phi\rangle$. A simple analysis shows

Direction variance

$$\langle\delta\phi^2\rangle = 1 - \langle\cos(\phi)\rangle^2 - \langle\sin(\phi)\rangle^2 + \text{ terms of order } \langle\delta\phi^2\rangle^2 \text{ and higher.} \tag{236}$$

In other words, due to the linearity of the cup anemometer calibration it is possible in a simple way to obtain three mean quantities, wind speed, wind direction and wind-direction variance—quantities important in e.g. dispersion measurements.

The wind speed, averaged over the n'the revolution of duration Δt_n, is $2\pi\ell/\Delta t_n$. If Δt_n is recorded together with ϕ_n it is possible also to compute the variance of the wind speed $\langle u^2\rangle$.

Wind speed variance

The reason we avoid v-bias is that now only the high wave-number part of the $\tilde{v}$ is 'experienced' by the anemometer. Pasquill and Smith (1983) have a straightforward derivation of an expression for the variance which is left after a temporal average of duration T has been removed [see also Kaimal *et al.* (1989)]. Their result applies to our case; we just have to think in terms of a spatial line average of length $2\pi\ell$, corresponding to one revolution of the rotor.

v-bias reduction

After removal of the low wave-number variance the residual v variance is

$$\langle v^2\rangle = \int_{-\infty}^{\infty}\{1-\mathrm{sinc}^2(\pi k\ell)\}F_v(k)dk, \tag{237}$$

where we have used the notation

$$\mathrm{sinc}(\xi) = \frac{\sin(\xi)}{\xi} \tag{238}$$

and $F_v(k)$ is the spectrum of $\tilde{v}$.

The situation is described in Figure 15. The integrand is the product of the functions $F_v(k)$ and the function $1-\mathrm{sinc}^2(k\ell/2)$. The reason they intersect way out in the inertial subrange is that ℓ is much smaller than the scale $\mathcal{L}_v$ of the lateral velocity component; as pointed out this length scale is of the order z_i, the depth of the boundary layer.

In the inertial subrange the spectrum $F_v(k)$ is given by (Lumley and Panofsky, 1964)

$$F_v(k) = \frac{1}{2}\left\{F_u(k) - k\frac{dF_u}{dk}\right\} = \frac{2}{3}\alpha_1\varepsilon^{2/3}|k|^{-5/3} \tag{239}$$

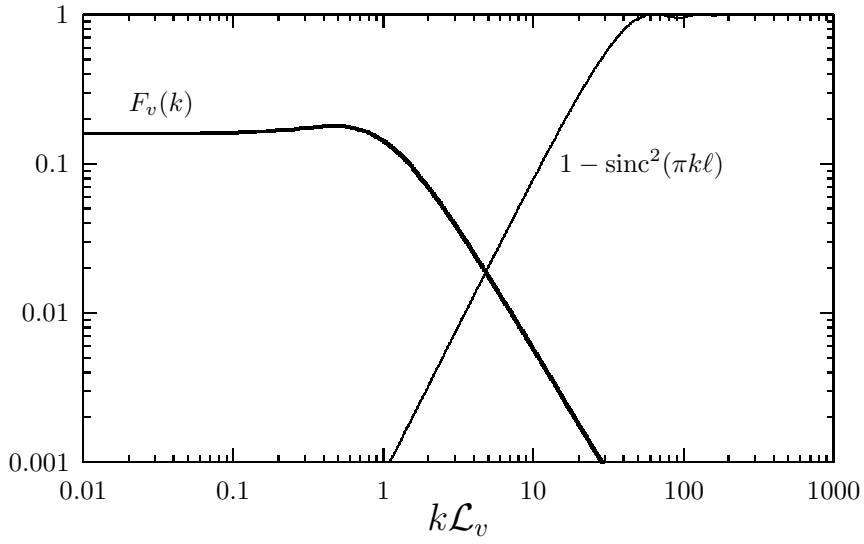

Figure 15. The spectrum $F_v(k)$ (thick line) of the lateral wind component $\tilde{v}$ and the function $1-sinc^2(\pi k\ell)$ (thin line).

and the *effective* v-bias now becomes

$$\begin{aligned}
\delta_v &= \frac{2}{3}\alpha_1\frac{\varepsilon^{2/3}}{2U^2}\int_{-\infty}^{\infty}\{1-\mathrm{sinc}^2(\pi k\ell)\}|k|^{-5/3}dk \\
&= \frac{2}{3}\alpha_1\frac{(\pi\varepsilon\ell)^{2/3}}{U^2}\int_0^{\infty}(1-\mathrm{sinc}^2(\xi))\xi^{-5/3}d\xi \\
&= \frac{4\pi}{3\sqrt{3}\Gamma(11/3)}\alpha_1\frac{(2\pi\varepsilon\ell)^{2/3}}{U^2}. \qquad (240)
\end{aligned}$$

Applying the diabatic profile functions (118) and (120) we get

$$\begin{aligned}
\delta_v &= \frac{4\pi}{3\sqrt{3}\Gamma(11/3)}\alpha_1\kappa^{4/3}\chi_u\left(\frac{z}{z_0},\frac{z}{L}\right)\left(\frac{2\pi\ell}{z}\right)^{2/3} \\
&\approx 0.34\,\chi_u\left(\frac{z}{z_0},\frac{z}{L}\right)\left(\frac{\ell}{z}\right)^{2/3}, \qquad (241)
\end{aligned}$$

an expression with very close resemblance to the u-bias in its dependence on the height z. It is not the distance constant ℓ_0 which enters to the power 2/3, but the calibration distance. This is typically 0.2 m so if $L=-10$ m, $z=10$ m and $z_0=0.1$ m we get $\delta_v\lesssim 1\%$. It can hardly be any larger so this is quite acceptable.

5 Gust Determination

In our article 'In Search of a Gust Definition' (Kristensen *et al.*, 1991) we have tried to give a practical definition of a gust. Traditionally a gust is defined as the

difference between the extreme value and the average value of the wind speed in a given time of interval T (Beljaars, 1987). This is in itself a reasonable definition, but the way it is determined is always from the preceeding period and thus contains very little predictive power; the gust in the following period will most certainly be different and it is impossible to tell, just from a gust determination from one period, with what probability the largest excursion in the following period will exceed this gust.

We start by pointing out that there are two different approaches in studying extreme excursions, which in our terminology are: the 'Rice Approach' (Rice, 1944 and 1945) and the 'Gumbel Approach' (Gumbel, 1958).

In both cases we imagine that we are dealing with an infinite ensemble of records of duration T of the wind speed with the ensemble mean subtracted.

Rice approach

In the Rice approach we ask for the average frequency $\eta_{\mathcal{U}}$ with which the level $\mathcal{U}$ is exceeded. We determine that by counting, in each realization, the number of excursions of $\tilde{u}$ beyond $\mathcal{U}$. If this is $N_i(\mathcal{U})$ in realization number i then the average number of excursions is

$$N(\mathcal{U}) = \lim_{M\to\infty} \frac{1}{M} \sum_{i=1}^{M} N_i(\mathcal{U}). \tag{242}$$

The rate of excursions becomes

$$\eta(\mathcal{U}) = \frac{N(\mathcal{U})}{T}. \tag{243}$$

If we assume that the individual excursions are statistically independent in each individual realization, then the excursions will be Poisson distributed, i.e. the probability for n excursions will be

$$P_{\mathcal{U}}[n] = \frac{e^{-N(\mathcal{U})}}{n!} N^n(\mathcal{U}). \tag{244}$$

In particular, the probability for no excursions beyond $\mathcal{U}$ ($n = 0$) becomes

$$P_{\mathcal{U}}[0] = e^{-N(\mathcal{U})}. \tag{245}$$

This number is also the fraction of realizations in which the level $\mathcal{U}$ is not exceeded.

Gumbel approach

In the Gumbel approach we only record the maximum value $\mathcal{U}_i$ of $\tilde{u}(t)$ in each of the M realizations. We can then determine the probability $P(< \mathcal{U})$ that the maximum value does not exceed the level $\mathcal{U}$ by introducing the index function

$$B_i(\mathcal{U}) = \begin{cases} 1 \text{ for } & \mathcal{U}_i \le \mathcal{U} \\ 0 \text{ for } & \mathcal{U}_i > \mathcal{U} \end{cases} \tag{246}$$

for each value of $\mathcal{U}$ to obtain

$$P(< \mathcal{U}) = \lim_{M\to\infty} \frac{1}{M} \sum_{i=1}^{M} B_i(\mathcal{U}). \tag{247}$$

Often the left-hand side of $P(<\mathcal{U})$ is approximated by the first of the so-called three asymptotes (Gumbel, 1958):

$$P(<\mathcal{U}) = \exp\left(-\exp\left(-C\frac{\mathcal{U}-[\mathcal{U}]}{\langle\mathcal{U}\rangle-[\mathcal{U}]}\right)\right), \tag{248}$$

where

$$C = 0.5772156649\ldots \tag{249}$$

is the Euler constant, $\langle\mathcal{U}\rangle$ the mean of the maxima and $[\mathcal{U}]$ the position of the maximum of the probability density function corresponding to (248):

$$p(\mathcal{U}) = \frac{C}{\langle\mathcal{U}\rangle-[\mathcal{U}]}\exp\left(-C\frac{\mathcal{U}-[\mathcal{U}]}{\langle\mathcal{U}\rangle-[\mathcal{U}]}\right)\exp\left(-\exp\left(-C\frac{\mathcal{U}-[\mathcal{U}]}{\langle\mathcal{U}\rangle-[\mathcal{U}]}\right)\right). \tag{250}$$

The Gumbel probability density function is always skew; if $\langle\mathcal{U}\rangle = [\mathcal{U}]$ it degenerates into a Dirac delta function.

Rice and Gumbel approaches are equivalent

We saw that the probability that the level $\mathcal{U}$ is not exceeded is given by (245). If the level is $\mathcal{U}$ is not exceeded the maximum value will not exceed this level either.

In the Gumbel approach we determined the probability (248) that the maximum value of $\tilde{u}(t)$ does not exceed $\mathcal{U}$. If the maximum value does not exceed $\mathcal{U}$, the time series cannot exceed $\mathcal{U}$ in its entire duration.

We thus conclude

$$P(<\mathcal{U}) = P_{\mathcal{U}}[0] \tag{251}$$

or, identifying (245) and the approximation (248),

$$N(\mathcal{U}) = \exp\left(-C\frac{\mathcal{U}-[\mathcal{U}]}{\langle\mathcal{U}\rangle-[\mathcal{U}]}\right). \tag{252}$$

We see that Rice approach and the Gumbel approach are equivalent. This was also pointed out by Davenport (1964). If we know the average frequency of excursions beyond any level $\mathcal{U}$ we can determine the probability function for the maximum values and, if this function is known then the average frequency of excursions beyond any level is known.

Here we have, in order to be specific, chosen the asymptotic extreme-probability function (248). This is by no means necessary to obtain the general conclusion (251). However, (248) is widely used because it is simple and believed to be reasonably accurate for most applications.

Further, it leads to a natural definition of a gust: *Gust definition*

> The gust is the wind-speed deviation from the mean which, on average, is exceeded once during the reference period T.

Since (252) gives us the average number of excursions beyond $\mathcal{U}$, we can determine the gust by setting the left-hand side of (252) equal to one. We conclude that the gust in our approximation becomes equal to the most probable value, the mode $[\mathcal{U}]$, of the Gumbel probability density function (250). With this definition we can, with the aid of (244), assign probabilities as follows: *Gust probabilities*

No excursion:	$P_{[\mathcal{U}]}[0] = e^{-1}$	$\sim 37\%$
At least one excursion:	$1 - e^{-1}$	$\sim 63\%$

The Rice-theory (Rice, 1944 and 1945) and its applications have been discussed in detail by Panofsky and Dutton (1984) under the name *exceedance statistics*.

The joint probability density $P(u, \dot{u})$ of the fluctuating part of the velocity $u(t)$ and its time derivative $\dot{u}$ contains the information about the rate of excursions $\eta_{\mathcal{U}}$. If $u(t)$ is measured continuously in time this rate becomes for a stationary time series *Excursion rate*

$$\eta_{\mathcal{U}} = \int_0^\infty \dot{u} P(\mathcal{U} - U, \dot{u}) d\dot{u}. \tag{253}$$

In other words, the number of times $\tilde{u}(t)$ exceeds $\mathcal{U}$ per unit time is equal to the average of the *positive* values of the time derivative $\dot{u}$ or, as the derivation of (253) by e.g., Panofsky and Dutton (1984) shows, to the average rate of up-crossings of the level $\mathcal{U}$.

In the period T, $\tilde{u}(t)$ will, on average, be larger than $\mathcal{U}$ in the total amount of time

$$\Theta_{\mathcal{U}} = T \int_{\mathcal{U}-U}^\infty du \int_{-\infty}^\infty P(u, \dot{u}) d\dot{u} \tag{254}$$

and since the average number of times $\mathcal{U}$ is exceeded in the same period of time is $\eta_{\mathcal{U}} T$, the *average duration* of one excursion beyond $\mathcal{U}$ can be estimated as *Excursion duration*

$$\vartheta_{\mathcal{U}} \approx \frac{\Theta_{\mathcal{U}}}{\eta_{\mathcal{U}} T} = \frac{\displaystyle\int_{\mathcal{U}}^\infty du \int_{-\infty}^\infty P(u, \dot{u}) d\dot{u}}{\displaystyle\int_0^\infty \dot{u} P(\mathcal{U} - U, \dot{u}) d\dot{u}}. \tag{255}$$

The joint probability density contains, as we see, all the important information about the gust. In Kristensen *et al.* (1991), we simply assumed that u and $\dot{u}$ have a joint-Gaussian probability density *Joint-Gaussian statistics*

$$P(u, \dot{u}) = \frac{1}{2\pi \sqrt{\langle u^2 \rangle} \sqrt{\langle \dot{u}^2 \rangle}} \exp\left(-\frac{u^2}{2\langle u^2 \rangle} - \frac{\dot{u}^2}{2\langle \dot{u}^2 \rangle} \right), \tag{256}$$

and obtained the following simple expressions for $\eta_{\mathcal{U}}$ and $\vartheta_{\mathcal{U}}$

$$\eta_{\mathcal{U}} = \frac{1}{2\pi}\frac{\sqrt{\langle \dot{u}^2\rangle}}{\sqrt{\langle u^2\rangle}}\exp\left(-\frac{(\mathcal{U}-U)^2}{2\langle u^2\rangle}\right) \tag{257}$$

and

$$\vartheta_{\mathcal{U}} = \pi\frac{\sqrt{\langle u^2\rangle}}{\sqrt{\langle \dot{u}^2\rangle}}\exp\left(\frac{(\mathcal{U}-U)^2}{2\langle u^2\rangle}\right)\operatorname{erfc}\left(\frac{\mathcal{U}-U}{\sqrt{2}\sqrt{\langle u^2\rangle}}\right), \tag{258}$$

where

$$\operatorname{erfc}(x) = \frac{2}{\sqrt{\pi}}\int_x^\infty e^{-t^2}dt \tag{259}$$

is the complementary error function. In the limit when the excursion is very large, i.e. when $\mathcal{U}-U \gg \sqrt{\langle u^2\rangle}$, we get the simple result

$$\vartheta_{\mathcal{U}} \approx \sqrt{2\pi}\frac{\sqrt{\langle u^2\rangle}}{\sqrt{\langle \dot{u}^2\rangle}}\frac{\sqrt{\langle u^2\rangle}}{\mathcal{U}-U}, \tag{260}$$

which has the straightforward interpretation that the average duration of an excursion is inversely proportional to the deviation from the mean.

Cup-anemometer gust

With the assumption (256) the whole problem reduces to determining the ratio between the variances $\langle u^2\rangle$ and $\langle \dot{u}^2\rangle$ of u and $\dot{u}$. We must remember, however, that the wind speed is observed through the filter of the cup anemometer so the gust should really be determined in terms of s, i.e. we must determine the variances $\langle s^2\rangle$ and $\langle \dot{s}^2\rangle$.

We consider the cup anemometer a first-order, linear filter, described by the equation

$$\dot{s} + \frac{s}{\tau_0} = \frac{1}{\tau_0}\frac{u}{\ell}. \tag{261}$$

Equation (261) is the same as (28), with the assumption that the cup anemometer has up-down symmetry, i.e. $\mu_1 = 0$.

Multiplying (261) by s and τ_0 and averaging, we get

$$\langle s^2\rangle = \frac{1}{\ell}\langle su\rangle = \frac{1}{\ell^2}\int_{-\infty}^{\infty}\frac{S_u(\omega)}{1+\omega^2\tau_0^2}d\omega, \tag{262}$$

where we have used (73) and the fact that $\langle s\dot{s}\rangle = 0$.

Multiplying (261) by $\dot{s}$ and averaging, we obtain $\langle \dot{s}^2\rangle$ as follows

$$\langle \dot{s}^2\rangle = \frac{\langle \dot{s}u\rangle}{\ell\tau_0}. \tag{263}$$

Employing (261) once more to eliminate $\dot{s}$ on the right-hand side, provides the result

$$\begin{aligned}\langle \dot{s}^2 \rangle &= \frac{1}{\ell\tau_0}\left\{\left\langle \frac{u}{\ell\tau_0}u\right\rangle - \left\langle \frac{s}{\tau_0}u\right\rangle\right\} \\ &= \frac{1}{\ell^2\tau_0^2}\int_{-\infty}^{\infty} S_u(\omega)d\omega - \frac{1}{\ell^2\tau_0^2}\int_{-\infty}^{\infty}\frac{S_u(\omega)}{1+\omega^2\tau_0^2}d\omega \\ &= \frac{1}{\ell^2}\int_{-\infty}^{\infty}\frac{\omega^2 S_u(\omega)}{1+\omega^2\tau_0^2}d\omega. \end{aligned} \tag{264}$$

We see that the variance of the time derivative s is proportional to the variance of the velocity after first-order high-pass filtering with the time constant τ_0.

In Kristensen *et al.* (1991) we generalized these results by including another low-pass filter, a simple running-means filter, applied to the output of the cup anemometer. The reason for this is that it is common practice in airports to define the gust as extreme excursions of the wind speed as seen through a filter with a fixed averaging time τ_{rm}, which is usually about 3 s. The typical value of $\tau_0 = \ell_0/U$ is 0.1 to 0.4 s and the effect of the cup anemometer low-pass filter is hardly felt after this heavy-handed running-means filtering. In the sense that turbulence is less of a temporal than a spatial structure through which we can consider ourselves to be probing with the mean wind velocity U in the mean-wind direction, it would give a better representation of the turbulence structure if temporal averaging is avoided entirely, so that the turbulence we 'see' through the cup-anemometer signal becomes independent of U and is just a line averaging along the mean wind direction. Here we will therefore just consider the signal s without auxiliary filtering and apply Taylor's hypothesis to reformulate (263) and (264) with the result

$$\langle s^2 \rangle = \frac{1}{\ell^2}\int_{-\infty}^{\infty}\frac{F_u(k)}{1+k^2\ell_0^2}dk \tag{265}$$

and

$$\langle \dot{s}^2 \rangle = \frac{U^2}{\ell^2}\int_{-\infty}^{\infty}\frac{k^2 F_u(k)}{1+k^2\ell_0^2}dk. \tag{266}$$

When we derived the equation for the u-bias in subsection 2.7 we assumed that distance constant was much smaller than the turbulence length scale of $\tilde{u}$, i.e. $\ell_0 \ll \mathcal{L}_u$ and were able to derive a quite accurate analytical expression for the u-bias. The reason was that only that part of the spectrum $F_u(k)$ for which $|k| \gtrsim 1/\ell_0$ contributes to the u-bias. Since (266) shows that exactly the same integral enters in the determination of $\langle \dot{s}^2 \rangle$, this quantity becomes to the same accuracy

$$\langle \dot{s}^2 \rangle = \frac{\pi}{\sqrt{3}}\alpha_1(\varepsilon\ell_0)^{2/3}\frac{U^2}{\ell^2\ell_0^2} \tag{267}$$

It it is much more difficult to evaluate (265) because contributions from arbitrarily large eddies enter the integral. In Kristensen *et al.* (1991) we neglected this problem by only discussing the case of neutral stratification and assuming that the low-pass filtering (in wave-number domain) takes place so far out in the inertial subrange that it does not cause any loss of variance. This implied that we could use the simple result

$$\langle s^2 \rangle = 4.77\frac{u_*^2}{\ell^2}, \tag{268}$$

consistent with the spectrum for $\tilde{u}$ under neutral conditions in the surface layer by Kaimal *et al.* (1972).

Under the same conditions

$$\varepsilon = \frac{u_*^3}{\kappa z} \tag{269}$$

and (267) becomes

$$\langle \dot{s}^2 \rangle = \frac{\pi}{\sqrt{3}} \alpha_1 \kappa^{-2/3} \frac{U^2}{\ell^2 \ell_0^2} \left(\frac{\ell_0}{z} \right)^{2/3} u_*^2 \approx 1.87 \frac{U^2}{\ell^2 \ell_0^2} \left(\frac{\ell_0}{z} \right)^{2/3} u_*^2. \tag{270}$$

The ratio between $\sqrt{\langle \dot{u}^2 \rangle}$ and $\sqrt{\langle u^2 \rangle}$, entering (257) and (258), should really be $\sqrt{\langle \dot{s}^2 \rangle / \langle s^2 \rangle}$ and this ratio becomes

$$\frac{\sqrt{\langle \dot{s}^2 \rangle}}{\sqrt{\langle s^2 \rangle}} = 0.626 \frac{U}{\ell_0} \left(\frac{\ell_0}{z} \right)^{1/3}. \tag{271}$$

Equation (268) is an overestimation because the observation time T may not be large compared to the integral time scale $\mathcal{T}_u$. We can use the simple spectral model (A.2) in Appendix A to estimate this overestimation. We are not in this case interested in the dissipation range at all so we simplify (A.2) accordingly:

$$F_u(k) = \frac{1}{2} \alpha_1 \varepsilon^{2/3} \begin{cases} {\mathcal{L}'_u}^{5/3} & \text{for } 0 \le |k| \le {\mathcal{L}'_u}^{-1} \\ k^{-5/3} & \text{for } {\mathcal{L}'_u}^{-1} \le |k| < \infty \end{cases}. \tag{272}$$

The length scale $\mathcal{L}'_u$ is not quite equal to the real length scale , determined by (82) and $\mathcal{L}_u = U\mathcal{T}_u$. In Appendix A we show

$$\mathcal{L}'_u = \frac{5}{\pi} \mathcal{L}_u \approx 8z. \tag{273}$$

With the spectrum (272) we get

$$\begin{aligned} \langle \ell^2 s^2 \rangle &= \int_{-\infty}^{\infty} \left\{ 1 - \mathrm{sinc}^2 \left(\frac{\omega T}{2} \right) \right\} S_u(\omega) d\omega \\ &= \int_{-\infty}^{\infty} \left\{ 1 - \mathrm{sinc}^2 \left(\frac{kUT}{2} \right) \right\} F_u(k) dk \\ &\approx \langle u^2 \rangle - \frac{\alpha_1}{2} (\varepsilon \mathcal{L}'_u)^{2/3} \frac{\mathcal{L}'_u}{UT} \int_{-\infty}^{\infty} \mathrm{sinc}^2(\xi) d\xi \\ &= \langle u^2 \rangle - \pi \alpha_1 (\varepsilon \mathcal{L}'_u)^{2/3} \frac{\mathcal{L}'_u}{UT} \end{aligned} \tag{274}$$

Using (269) for ε and

$$\langle u^2 \rangle = 4.77 u_*^2, \tag{275}$$

corresponding to neutral stratification, (268) must be replaced by

$$\langle s^2 \rangle \approx 4.77 \frac{u_*^2}{\ell^2} \left\{ 1 - 22 \frac{z}{UT} \right\}. \tag{276}$$

If $z = 10$ m and $UT = 3000$ m, corresponding to a typical length of a runway in the airport, the value of (268) is about 7% too large. This means that (271) will be underestimated by about 3.5%. On the other hand, if $U = 10$ m s^{-1} and $T = 180$ s as convention sometimes dictates, then the corresponding numbers are 12% and 6%, respectively. These numbers may not be insignificant, so in order to investigate this problem any further it is necessary to use a more realistic and detailed spectral expression than (272).

Experimental verification

Here we will just point out that we used the result (271) with success (Kristensen *et al.*, 1991) in a case where the cup-anemometer signal was subjected to a running averaging over the time τ_{rm}. We found the gust $[\mathcal{U}]$ well predicted by the dimensionless expression

$$\mu \equiv \frac{[\mathcal{U}] - U}{\langle u^2 \rangle^{1/2}} = \sqrt{2 \ln \left(0.1483 \left\{ \frac{U \tau_{rm}}{z} \right\}^{1/3} \frac{T}{\tau_{rm}} \right)}, \tag{277}$$

which shows that the gust, not surprisingly, is proportional to the root-mean-square of u.

We used a stationary time series of $\tilde{u}$ of total duration 20 hours with a mean $U \approx 12$ m s^{-1}. Varying T from 120 s to 1800 s and using $\tau_{rm} = 1$, 2 and 3 s, we found that the two ways of defining a gust—the 'Rice Approach' and the 'Gumbel Approach'—agreed well within 4% and that the prediction (277) in all cases agreed with these gusts within 12%, but that the agreement was typically within 8%.

The reason that the cup-anemometer's own low pass filter does not affect (277), i.e. that ℓ_0 does not appear in the equation, is that $\ell_0/U \lesssim 0.2$ s$\ll \tau_{rm}$, so that the low-pass filtering is completely dominated by the running-means filter.

If there had been no filtering of the raw cup-anemometer signal, the gust expression would have been

$$\mu = \sqrt{2 \ln \left(0.0997 \left\{ \frac{\ell_0}{z} \right\}^{1/3} \frac{UT}{\ell_0} \right)}. \tag{278}$$

We believe that a gust prediction based on an equation like (278), possibly modified to account for a non-Gaussian probability density for u, is superior to a prediction based on the largest excursion from the previous period. Our method of prediction takes a lot more information into account than just the largest excursion. Another advantage is that it eliminates the effect of discrete sampling—the fact that statistically we are certain to miss some of the largest excursions. The effect of the discrete sampling is that in the mean the gust will be underestimated (Beljaars, 1987). The variance, on the other hand, is not systematically affected by the discrete sampling.

Discrete sampling

Let us think about this for a moment: why is it that $\langle u^2 \rangle$ is not affected by the discrete sampling and yet the statistics of the extremes is? What is different between discrete and continuous sampling? The answer is that $\tilde{u}$ has the possibility to cross any given level $\mathcal{U}$ unnoticed between samplings, which are separated in time by the interval Δt. This will reduce the apparent number of excursions and also the gust obtained by recording the largest value in each reference period. We expect this effect to be an increasing function of the ratio between $\Delta t = 2\pi\ell/U$ and the time constant ℓ_0/U (or τ_{rm}).

Reduction of gust rate and gust magnitude

It is possible to estimate how much the gust is reduced by discrete sampling as

compared to continuous sampling as is shown in Appendix B. The apparent gust rate $\eta'_{\mathcal{U}}$ is shown by a heuristic proof to be smaller than $\eta_{\mathcal{U}}$ by the factor

$$\frac{\eta'_{\mathcal{U}}}{\eta_{\mathcal{U}}} = \sqrt{1 - 1.70 \left(\frac{\ell}{\ell_0}\right)^{2/3}}, \tag{279}$$

shown in Figure 16. The apparent dimensionless gust μ' becomes

$$\mu' \approx \mu - \frac{0.85}{\mu} \left(\frac{\ell}{\ell_0}\right)^{2/3}. \tag{280}$$

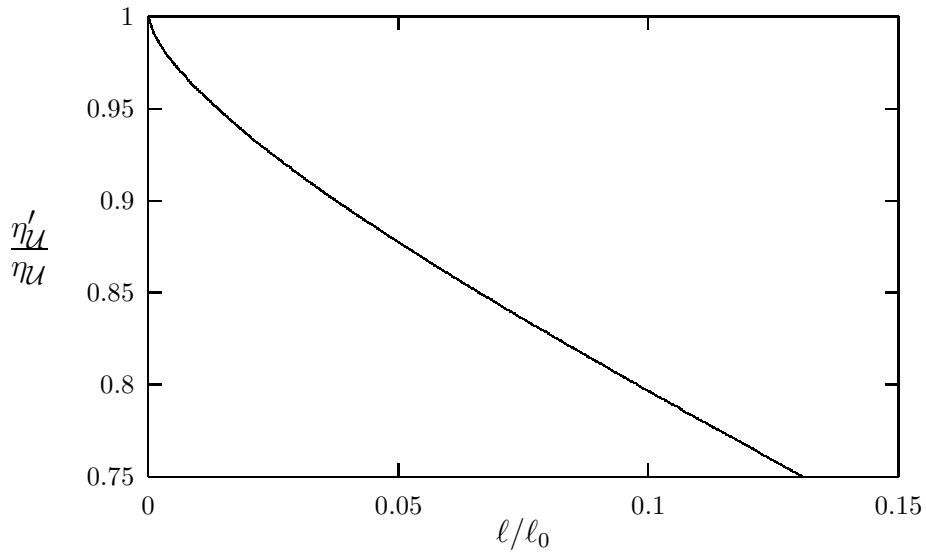

Figure 16. The gust reduction factor (279) due to the discrete sampling of the cup anemometer.

The Risø-70 cup anemometer has $\ell = 0.2$ m and $\ell_0 \approx 1.7$ m which means that if we measured gust with this instrument by detecting the largest value in each reference period we would estimate an excursion rate which would be systematically about 16% too small. A typical value of μ is 2.5 and we see that the gust correspondingly will be reduced by less than 0.5%.

The two equations (279) and (280) can of course also be formulated in the time domain for a time series subjected to a first-order low-pass filtering with a time constant τ_0 and sampled equidistantly in time with the separation Δt. In this case ℓ/ℓ_0 must be replaced by $\Delta t/(2\pi\tau_0)$. They confirm our intuition that this ratio must be small compared to one to obtain trustworthy values of $\eta_{\mathcal{U}}$ and μ; it means that the signal must be 'calmed down' in order that it should not cross the level $\mathcal{U}$ unnoticed.

6 Conclusions

The nonlinear dynamics of sensors for atmospheric measurements has been the main theme in this work. Many sensors have nonlinear dynamics, but historically

the cup anemometer has attracted considerable attention because of the so-called overspeeding. Here, this instrument has therefore been given most attention.

In the discussion of nonlinear sensor dynamics I have used the adjectives *linear/nonlinear* and *first-order/second-order* as qualifiers of different concepts. Perhaps it would be useful at this point to repeat the most important definitions I have used.

Let us consider a sensor or a system with one input $\tilde{x}$ and one response $\tilde{y}$. We assume that the connection between $\tilde{x}$ and $\tilde{y}$ is determined by an ordinary differential equation in $\tilde{y}$. The order of this differential equation is the order of the system. A general system of order n obeys the equation

$$\frac{d^n\tilde{y}}{dt^n} = F\left(\tilde{y}, \frac{dy}{dt}, \ldots, \frac{d^{n-1}\tilde{y}}{dt^{n-1}}, \tilde{x}\right). \tag{281}$$

Here the function F is the forcing, which can be linear or nonlinear in its n variables. If just one of the $n(n+1)/2$ second derivatives of F is different from zero, the system is nonlinear.

A nonlinear system may or may not have a linear, steady-state calibration. The calibration is obtained by keeping the input $\tilde{x} = X$ constant until the response $\tilde{y} = Y$ has become constant and all its derivatives are zero. The condition

$$F(Y, 0, \ldots, X) = 0 \tag{282}$$

implies the steady-state relation

$$Y = Y(X) \tag{283}$$

between X and Y. This relation is the calibration. If the second derivative of $Y(X)$ with respect to X is zero for all values of X, the system has a linear calibration. If the system is linear, (282) is a linear equation in X and Y and the calibration (283) is then also linear. However, we cannot a priori say that the calibration is nonlinear if the system is nonlinear.

The differential equation (281) will often be nonlinear and so complicated that it is not possible to obtain an exact solution. We therefore try to extract information about the system by applying a perturbation technique. In the neighborhood of the calibration point $(\tilde{y}, \tilde{x}) = (Y(X), X)$, we express the function F as a power series in all its n variables. A first-order perturbation equation includes only variables up to the power one. Similarly, a second-order perturbation equation includes terms of no higher order than two. We do not go beyond second order.

With all these concepts in place, we note that a cup anemometer, exposed only to a horizontal wind component of constant direction, is a nonlinear, first-order system with a linear calibration.

Using first- and second-order perturbation theory on the equation of motion of the cup anemometer, with the total horizontal and the vertical wind components as input, it is possible to determine the systematic error in the measured mean value due to turbulent fluctuations. This systematic error, or overspeeding, has been considered a serious drawback, which has recently become of importance, because climatological cup anemometer records of mean winds are used to assess the performance of modern wind turbines. The available wind energy is roughly proportional to the cube of the wind speed and thus a five percent overestimation

of the mean wind speed may lead to an expectation of an wind energy production which is perhaps 15 percent too high.

I have discussed four types of overspeeding: 1) the u-bias, which is caused by the response asymmetry to wind gusts and lulls and which is what is usually considered the 'real' overspeeding, 2) the v-bias, which is really the interpretation error one is guilty of, if one equates the mean of the horizontal wind speed and the magnitude of the mean horizontal wind velocity vector, 3) the w-bias caused by a nonideal angular response ($\mu_1 \neq 0$ or $\mu_2 \neq 0$) and often discussed in the literature together with the u-bias (MacCready, 1966, Kaganov and Yaglom, 1976, Busch and Kristensen, 1976, Wyngaard, 1981, Coppin,, 1982) and finally, 4) the stress-bias, which is caused by the stress correlation $\langle uw \rangle$ in connection with anemometer up-down asymmetry ($\mu_1 \neq 0$) and which, to my knowledge, has not been discussed before.

The simplest of the four biases are the v-bias and the w-bias. Neglecting the cup-anemometer offset speed U_0 and μ_1, they are $\langle v^2 \rangle / (2U^2)$ and $\mu_2 \langle w^2 \rangle / (2U^2)$, respectively. In other words, they are both proportional to the square of the relative turbulence intensities of the respective velocity components. The w-bias is seldom very large in the atmospheric surface layer since the proximity of the impenetrable boundary limits the horizontal scale of the turbulence of the vertical velocity fluctuations. The investigation here shows that it is probably always less than about one percent. There is no such geometrical limit to the scale of the lateral velocity fluctuations and, particularly in very unstable and very stable stratifications, the v-bias can be quite large—more than 10% according to e.g., Smith and Abbott (1961).

The u-bias and the stress-bias are similar in the sense that only the high wavenumber turbulence contributes. So even if the variance $\langle u^2 \rangle$ like $\langle v^2 \rangle$ can be large, the cup anemometer can faithfully follow the fluctuations of the longitudinal velocity component with wavelengths larger than the cup anemometer distance constant ℓ_0. The u-bias is approximately equal to the square of the relative turbulence intensity pertaining to wave numbers larger than $1/\ell_0$. The stress-bias is equal to μ_1 times the covariance of u and w from wave numbers larger than $1/\ell_0$ divided by the mean wind speed. The u bias is seldom more than a few percent and, depending on the value of the asymmetry coefficient μ_1, the stress-coefficient will usually be about 0.1% or less.

From these considerations it is clear to me that cup-anemometer overspeeding in the traditional sense, i.e. u-bias, together with the w-bias and the stress-bias can be neglected in most applications.

In these considerations I have presented the results in terms of a very simple equation for the forcing of the cup rotor. I assume that it is a second-order polynomial in the input and the output. With the observation that it can only have one positive root in order for the calibration to be unambiguous and that this root cannot be a double root if the time scale of the first-order response is finite, this polynomial can be expressed in terms of three positive length scales and the two dimensionless parameters μ_1 and μ_2, characterizing the response to the vertical wind component. The three length scales are the calibration length ℓ, the distance constant ℓ_0 and a length Λ, which determines whether or not the second-order mixed term $\langle su \rangle$ reduces or enhances the u-bias. If Λ is smaller than ℓ the covariance between $\langle su \rangle$ will counteract the overspeeding and enhance it if Λ is larger than ℓ. Unfortunately, I have not been able to provide a better physical interpretation of the length scale Λ. The model, which is in good agreement with the investigations by Wyngaard *et al.* (1974) and in fair agreement with the findings of

Coppin (1982), provides nice looking results in the form of equations for the four biases. However, the main result that 'overspeeding is overrated' is independent of this model. Only the assumption that the forcing is a second-order polynomial is necessary to maintain that the distance constant is an instrument constant, i.e. independent of the wind speed.

Although the cup anemometer is a very prominent sensor in sofar as nonlinear forcing is concerned, there are many other sensors who have the same property and consequently will give systematically biased means. Restating the results obtained by us (Kristensen and Lenschow, 1988) and correcting the errors in this work, I have here discussed nonlinear forcing of first and second order.

The dynamic equation for the Pitot tube, like that for the cup anemometer, can be described by a first order, ordinary differential equation. The Pitot tube, therefore, is a first-order system. In contrast to the cup anemometer, it is characterized by a time constant rather than a distance constant.

As second-order systems we chose as examples the thrust anemometer and the CSIRO liquid water probe.

The first of these and the Pitot tube we have discussed in terms of two modes of operation: 1) detection and recording of the 'raw' output, the actual displacement of the thrust element and the pressure difference from the Pitot tube, and 2) on-line interpretation of the raw output as a wind speed by means of the static calibration, a process which is also called *linearization*. It turns out that the first will in general give higher bias of the mean (overspeeding) than the second. This can be understood immediately: the nonlinear calibration will cause the low frequency part of the variance to contribute in the first mode of operation whereas in the second mode of operation this contribution will be eliminated by high-pass filtering. When a sensor has a nonlinear *calibration* it is advisable to linearize the output before any other processing, such as averaging, is performed. This seems a trivial and obvious result which we could have derived by means of simple arguments. However, there is a continuation: we have found that even if we linearize there is a bias from the high-frequency part of the turbulence if the instrument has nonlinear *forcing*. In the case of the thrust anemometer the biases from the two modes of operation can be quite different: without linearization the bias on the mean can be as much as perhaps 10%, whereas linearization reduces the bias to less than 1%.

The CSIRO liquid water probe measures the mean with a negative bias because of nonlinear forcing. The signal is linearized, but it turns out from an analysis of aircraft data that the bias of the mean can be -10% if the amount of water is about 2 g m^{-3}, a value not uncommon in clouds. However, this result is somewhat speculative because it is assumed that the variance of the water concentration is proportional to the square of the mean concentration. More data analysis is needed to more correctly estimate the bias.

In sections 4 and 5 we return to cup-anemometer operation and application. I show that it is possible to reduce the v-bias by operating the cup anemometer together with a wind vane in a particular way, namely to let the cup anemometer pulse from each revolution trigger a recording of the wind direction. In this way the v-bias will also be small, equal to one-half the square of the turbulence intensity from wave numbers larger than $2\pi\ell$, where ℓ is the calibration distance. Usually this reduced bias will be no larger than about 1%. In this mode of operation the output will, after the averaging, provide the two components of the horizontal mean wind velocity and, as a by-product, also the lateral variance from the averaging period. It is a condition for this scheme to work that the cup-anemometer calibration is

linear and that the offset speed U_0 can be neglected.

If we also record the length of time of each revolution of the cup rotor we can also calculate the variance $\langle u^2 \rangle$ of the longitudinal velocity component. As we show in section 5, it is possible to apply this variance to obtain a prediction of the gust, which is defined as 'the wind-speed deviation from the mean which, on average, is exceeded once in the reference (averaging) period' (Kristensen *et al.*, 1991). We point out that this definition of the gust, under the assumption that the individual large excursions from the mean can be considered statistically independent, is identical to the most probable value of the largest excursion in a reference period. Traditionally the gust, e.g. in airports, is predicted by letting the largest excursion from the previous period predict the largest value in the following. By using the variance rather than the largest value for this prediction, we obtain a statistically more reliable value and, with our definition it is also possible to actually state the probability that the gust is exceeded at least once, exactly once, twice, any number of times or not at all. For example, the probability that the predicted gust value *is not* exceeded is 37%.

Acknowledgements

I would like to take this opportunity to express my gratitude toward my colleagues in the Department of Meteorology and Wind Energy at Risø National Laboratory for their patience and encouragement to complete this project. My friend Henk Tennekes of the Royal Netherlands Meteorological Institute (KNMI) graciously invited me to spend–'with no strings attached'–four wonderful months at KNMI to organize my ideas and put them into writing. In this period from the beginning of September 1991 until the middle of January 1992 Henk Tennekes and his colleagues have provided valuable assistance in selecting and arranging the material to be presented. Aad van Ulden offered many critical, but constructive comments which, in my own opinion improved the readability of the present report and Adri Buishand carefully checked my ideas concerning extreme statistics. Jon Wieringa was extremely helpful in my literature search and the librarians at KNMI as well as at Risø have gone out of their way to obtain copies of books and articles, often so old that they were difficult to locate. My colleague in the Computer Section Peter Kirkegaard with whom I have worked in many years has evaluated analytically several of the integrals and Anne Margrethe Larsen has lead me through the mysteries of obtaining a nice LaTeX layout. Finally, I am thankful to all my coauthors of the articles to be submitted together with this report for their inspiring cooperation. They are Niels E. Busch who himself was fascinated by the cup anemometer and taught me the basics, D.H. Lenschow of National Center for Atmospheric Research in Boulder, Colorado, who over the years of our friendship and cooperation has been extremely good at asking interesting questions, resulting in many joint papers, Ib Troen, Maria Casanova and Mike Courtney with whom I have enjoyed to be in team when obtaining an answer to the question about a rigorous definition of a gust.

Dansk Sammendrag

Vi har diskuteret ikke-lineær dynamik for målesinstrumenter, som anvendes i meteorologi. Der er mange instrumenter, som adlyder ikke-lineære dynamiske ligninger, men historisk har kopanemometret tiltrukket sig stor interesse på grund af den såkaldte "overspeeding", som er en systematisk fejl på den målte middelvindhastighed, der skyldes turbulente variationer af hastighedskomponenten i middelvindretningen. I denne rapport er det derfor også kopanemometret, der har fået den mest detaljerede behandling.

Dynamikken bliver beskrevet ved hjælp af en differentialligning i tiden, med input og output som afhængige variable. I tilfælde af kopanemometret er der to input, nemlig den horisontale og den vertikale projektion af vindhastighedsvektoren, som kaldes henholdsvis $\tilde{h}$ og $\tilde{w}$, og et output, koprotorens vinkelhastighed, $\tilde{s}$. Bevægelsesligningen er her af første orden og af formen

$$\dot{\tilde{s}} = F(\tilde{s}, \tilde{h}, \tilde{w}), \tag{284}$$

hvor funktionen F er kraftmomentet på koprotoren divideret med dennes inertimoment.

Ved hjælp af første-og anden ordens perturbationsregning på (284) finder vi, at der på den målte middelværdi er fire typer af systematiske fejl, som skyldes anemometrets ikke-lineære reaktion på turbulente fluktuationer. De fire fejl benævnes her: "u-bias", som er identisk med omtalte "overspeeding", "v-bias" og "w-bias", som skyldes fluktuationer i henholdsvis den laterale vindhastighedskomponent, d.v.s. vindretningen, og den vertikale vindhastighedskomponent, samt endelig "stress-bias", der optræder på grund af korrelationen mellem den longitudinale og den vertikale vindhastighedskomponent. Disse fire systematiske fejl kan udtrykkes ved hjælp af effektspektrene af de tre vindhastighedskomponenter, $\tilde{u}$, $\tilde{v}$ og $\tilde{w}$, krydsspektret mellem $\tilde{u}$ and $\tilde{w}$ samt egenskaberne ved funktionen F. Nærværende analyse viser, at u-bias og stress-bias begge er proportionale med den højfrekvente del af henholdsvis effektspektret af u og realdelen af krydspektret mellem u og w, mens v-bias og w-bias begge er proportionale med hele variansen af henholdsvis v og w.

Ved hjælp af en fænomenologisk model for koprotorens bevægelse under indflydelse af vindens tre komponenter bliver de fire systematiske fejl beregnet. Denne fænomenologiske model indeholder 5 instrumentkonstanter, nemlig kalibreringslængden ℓ, d.v.s. længden af den søjle af luft, der skal blæse gennem anemometret for at rotoren skal dreje en radian, længdekonstanten ℓ_0, som er længden af den søjle af luft, der skal blæse gennem anemometret for at rotoren skal have reageret med 63% af en pludselig ændring af vindhastigheden, endnu en længde Λ, for hvilken det ikke har været muligt at give en nem kvalitativ fortolkning, samt to dimensionsløse konstanter, μ_1 og μ_2, som karakteriserer anemometrets vertikalvinkel-følsomhed til første og anden orden i inklinationsvinklen. De tre længder ℓ, ℓ_0 og Λ er alle positive. De to konstanter μ_1 og μ_2 er begge nul, dersom kopanemometret har en "ideel" vertikalvinkel-følsomhed, d.v.s. er ufølsomt over for vindkomponenten langs koprotorens akse. Hvis μ_1 er nul, er vertikalvinkelfølsomheden symmetrisk, hvilket medfører, at stress-bias er nul.

Denne fænomenologiske model gør det muligt, under antagelse af Taylor's hypotese for "frossen turbulens" og med anvendelse af standardformlerne for de vertikale profiler af middelvindhastigheden, varianserne af u, v og w og den molekylære dissipationshastighed af turbulent kinetisk energi i det diabatiske, horisontalt homogene overfladegrænselag, at udtrykke de fire typer systematiske fejl ved hjælp af

de fem instrumentparametre samt de tre atmosfæriske længder, højden, z, ruhedslængde, z_0 og Monin-Obukhov længden, L. Da u-bias og stress-bias udelukkende skyldes den del af turbulensen, hvis bølgelængder er mindre end længdekonstanten, ℓ_0, er disse systematiske fejl i reglen ubetydelige, typisk henholdsvis 1% og 0.01%. Af de to øvrige systematiske fejl, v-bias og w-bias, er den første altid størst. Den er nemlig praktisk taget uafhængig af de fem instrumentkonstanter og lig med det halve af variansen på vindretningen, hvorimod w-bias er lig med det halve af variansen på vindens inklination, multipliceret med μ_2, som numerisk er typisk 1 eller mindre. Erfaringer fra målinger har vist, at vindretningsvariansen altid er større end inklinationsvariansen og, især under stærkt ustabile forhold, meget større. Således overskrider w-bias sjældent nogle få procent, mens v-bias forholdsvis nemt kan være 10%.

Teknikken til bestemmelse af bias på den målte middelværdi kan anvendes på andre typer instrumenter, både instrumenter, der, ligesom kopanemometret, adlyder en første-ordens differentialligning af typen (284), og instrumenter, der følger højere-ordens differentialligninger. Idet vi nu begrænser os til et enkelt input, $\tilde{x}$, kan vi generalisere (284) til ligningen for et n'te-ordens dynamisk system. Den n'te tidsafledede af output $\tilde{y}$ sættes lig med en funktion af $\tilde{x}$, $\tilde{y}$ og alle de tidsafledede af $\tilde{y}$ til og med orden $n-1$, d.v.s.

$$\frac{d^n\tilde{y}}{dt^n} = F\left(\tilde{y}, \frac{dy}{dt}, \ldots, \frac{d^{n-1}\tilde{y}}{dt^{n-1}}, \tilde{x}\right). \tag{285}$$

Ud fra denne ligning vil det være muligt at bestemme den systematiske fejl på middelværdien af $\tilde{y}$, som skyldes, at $\tilde{x}$ har variationer på tidsskalaer, som er små i forhold til filterkonstanten af måleinstrumentet, der, dynamisk set, er karakteriseret ved funktionen F.

Pitot-røret, der som anemometer er meget anvendt på fly og i vindtunneller, samt vindtryksanemometret og CSIRO-instrumentet til bestemmelse af tætheden af mikroskopiske dråber i skyer bliver anvendt som eksempler på endnu et første-ordens system (Pitot-røret) og to anden-ordens systemer. Undersøgelsen viser, naturligt nok, at hvis man lineariserer output $\tilde{y}$ med en opdateringsfrekvens, som er stor i forhold til den reciprokke reaktionstid for instrumentet, vil den systematiske fejl på middelværdien ikke få bidrag fra den del af variansen, der svarer til fluktuationer, som er langsommere end systemets reaktionstid. Den vil kun få bidrag fra den højfrekvente del af variansen og, helt generelt, være proportional med denne.

Vi vender tilbage til kopanemometret og viser, hvorledes det er muligt operationelt at reducere den problematiske v-bias til maksimalt omkring 1% ved at anvende en vindretningsføler. Ved nemlig at lade hver fulde omdrejning af koprotoren "trigge" en aflæsning af vindretningsføleren kan man beregne den såkaldte *vindvejsvektor* for en bestemt midlingstid. Vindvejsvektoren, som en den resulterende horisontale flytning af en hypotetisk luftpartikel, som hele tiden bevæger sig i overensstemmelse med den vindhastighedsvektor, som kopanemometret måler, indeholder information om både vindens middelretning-og størrelse. Som en ekstragevinst kan man også let beregne vindretningsvariansen ved denne teknik.

Til sidst bliver det diskuteret, hvorledes en præcis definition af et vindstød kan bringes i anvendelse, og hvorledes kopanemometret kan bruges til vindstødsbestemmelse.

References

Beljaars, A.C.M. (1987). The Influence of Sampling and Filtering on Measured Wind Gusts. *J. Atmos. Oceanic Technol.*, **4**, 613-626.

Bradley, S.G. and King, W.D. (1979). Frequency Response of the CSIRO liquid water probe. *J. Appl. Meteorol.*, **18**, 361-366.

Brazier, C.E. (1914). Recherches expérimentales sur les moulenets anémometrique. *Ann. Bur. Centr. Météorol. France*, 157-300; Thèse Fac. Sc. Univ. Paris (1921), ed. Gaurthier-Villars.

Brevoort, N.J. and Joyner, U.T. (1935). Aerodynamic Characteristics of Anemometer Cups. *NACA Tech. Note*, No. 489, 1-7.

Businger, J.A., Wyngaard, J.C., Izumi, Y. and Bradley, E.F. (1971). Flux-Profile Relationships in the Atmospheric Surface Layer. *J. Atmos. Sci.*, **28**, 181-189.

Busch, N.E. (1965). A Micrometeorological Data-Handling System and some Preliminary Results. Risø Report R-99, 92 pp.

Busch, N.E. and Kristensen, L. (1976). Cup Anemometer Overspeeding. *J. Appl. Meteorol.*, **15**, 1328-1332.

Busch, N.E., Christensen, O., Kristensen, L., Lading, L. and Larsen, S.E. (1980). Cups, Vanes, Propellers and Laser Anemometers. *Air-Sea Interaction—Instruments and Methods.* F. Dobson, L. Hasse and R. Davis, Eds., Plenum Press, NY, 11-46.

Carl, M.D., Tarbell, T.C. and Panofsky, H.A. (1973). Profiles of Wind and Temperature from Towers over Homogeneous Terrain. *J. Atmos. Sci*, **30**, 788-794.

Clough, T.W. and Penzien, J. (1975). *Dynamics of Structures*, pp. 293-307, McGraw-Hill Inc., NY.

Coppin, P.A. (1982). An Examination of Cup Anemometer Overspeeding. *Meteorol. Rdsch.*, **35**, 1-11.

Davenport, A.G. (1964). Note on the Distribution of the Largest Value of a Random Function with Application to Gust Loading. *Proc. Inst. Civ. Eng. (London)*, **28**, 187-196.

Feynman, R.P., Leighton, R.B. and Sands, M. (1964). *The Feynman Lectures on Physics*, **2**. Addison-Wesley Inc., Reading, MA.

Frenzen, P. and Hart, L.H. (1983). A Further Note on the Kolmogorov-von Kármán Product and the Values of the Constants. *Proc. Sixth Symp. on Turbulence and Diffusion*, March 22-25, Boston, MA, 24-27.

Frenzen, P. (1988). Fast Response Cup Anemometers for Atmospheric Turbulence Research. *Proc. Eighth Symp. on Turbulence and Diffusion*, April 25-29, San Diego, CA, 112-115.

Freymuth, P. (1977). Further Investigation of the Nonlinear Theory for Constant-Temperature Hot-Wire Anemometers. *J Phys E: Sci. Instrum.*, **10**, 710-713.

Gradshteyn, I.S. and Ryzhik, I.M. (1980). *Table of Integrals, Series, and Products.* Academic Press, NY, 1160 pp.

Gumbel, E.J.: 1958, *Statistics of Extremes.* Columbia University Press, New York, 375 pp.

Haugen, D.A., Kaimal, J.C. and Bradley, E.F. (1971). Surface Layer Stress and Heat Flux. *Quart. J. Roy. Meteorol. Soc.*, **97**, 168-180.

Izumi, Y. and Barad, M.L. (1970). Wind Speeds as Measured by Cup and Sonic Anemometers and Influenced by Tower Structure. *J. Appl. Meteorol.*, **9**, 851-856.

Kaganov, E.I. and Yaglom, A.M. (1976). Errors in Wind Speed Measurements by Rotation Anemometers. *Boundary-Layer Meteorol.*, **10**, 15-34.

Kaimal, J.C., Wyngaard, J.C., Izumi, Y. and Coté, O.R. (1972). Spectral Characteristics of Surface Layer Turbulence. *Quart. J. Roy. Meteorol. Soc.*, **98**, 563-589.

Kaimal, J.C., Wyngaard, J.C., Haugen, D.A., Coté, O.R., Izumi, Y, Caughey, S.J. and Readings, C.J. (1976). Turbulence Structure in the Convective Boundary Layer. *J. Atmos. Sci.*, **33**, 2152-2169.

Kaimal, J.C., Clifford, S.F. and Lataitis, R.J. (1989). Effect of Finite Sampling on Atmospheric Spectra. *Boundary-Layer Meteorol.*, **47**, 337-347.

King, W.D., Parkin, D.A. and Handsworth, R.J. (1978). A Hot-Wire Liquid Water Device Having fully Calculable Response Characteristics. *J. Appl. Meteor.*, **17**, 1809-1813.

Knollenberg, T.G. (1981). Techniques for Probing Cloud Microstructure. *Clouds: Their Formation, Optical Properties and Effects*. P.V. Hobbs and A. Depak, Eds., Academic Press, NY, 15-89.

Kondo, J., Naito, G. and Fujinawa, Y. (1971). Response of Cup Anemometer in Turbulence. *J. Meteorol. Soc. Japan*, **49**, 63-74.

Kristensen, L. and Lenschow, D.H. (1988). The Effect of Nonlinear Dynamic Forcing Response on Measured Means. *J. Atmos. Oceanic Technol.*, **5**, 34-43.

Kristensen, L., Lenschow, D.H., Kirkegaard, P. and Courtney, M.S. (1989). The Spectral Velocity Tensor for Homogeneous Boundary-Layer Turbulence. *Boundary-Layer Meteorol.*, **47**, 149-193.

Kristensen, L., Casanova, M., Courtney, M.S. and Troen, I. (1991). In Search of a Gust Definition. *Boundary-Layer Meteorol.*, **55**, 91-107.

Larsen, S.E. and Busch, N.E. (1974). Hot-wire Measurements in the Atmosphere. Part I: Calibration and Response Characteristics. *DISA Information*, **16**, 15-34.

Lenschow, D.H. (1986). Aircraft Measurements in the Boundary Layer. *Probing the Atmospheric Boundary Layer*. D.H. Lenschow, Ed., Amer. Meteor. Soc., Boston, MA, 39-55.

Lumley, J.L. and Panofsky, H.A. (1964). *The Structure of Atmospheric Turbulence*. Interscience Publishers, NY, 239 pp.

MacCready, P.B., Jr. (1965). Dynamic Response Characteristics of Meteorological Sensors. *Bull. Am. Met. Soc.*, **46**, 533-538.

MacCready, P.B., Jr. (1966). Mean Wind Speed Measurements in Turbulence. *J. Appl. Meteorol.*, **5**, 219-225.

Middleton, W.E.K. and Spilhaus, A.F. (1953). *Meteorological Instruments*, third ed.. University of Toronto Press, Canada, 286 pp.

Norman, J.M., Perry, S.G. and Panofsky, H.A. (1976). Measurement and Theory of Horizontal Coherence at a Two-Meter Height. *Proc. Third Symp. on Atmospheric Turbulence, Diffusion and Air Quality*, October 19-22, Raleigh, NC, 26-31.

Panofsky, H.A. and Dutton, J.A. (1984). *Atmospheric Turbulence*. John Wiley & Sons, NY, 397 pp.

Pasquill, F. and Smith, F.B. (1983). *Atmospheric Diffusion* (3rd Edition). Ellis Horwood Ltd., Chichester, England, 437 pp.

Patterson, J. (1926). The Cup Anemometer. *Trans. Roy. Soc. Canada*, Ser. III, **20**, 1-54.

Rice, S.O. (1944, 1945). Mathematical Analysis of Random Noise. *Bell Syst. Tech. J.*, **23**, 282-332, **24**, 46-156.

Robinson, S.K. (1991). Coherent Motions in the Turbulent Boundary Layer. *Annu. Rev. Fluid Mech.*, **23**, 601-639.

Smith, F.B. and Abbott, P.F. (1961). Statistics of Lateral Gustiness at 16 m Above the Ground. *Quart. J. Roy. Meteorol. Soc.*, **87**, 549-561.

Smith, S.D. (1980). Dynamic Anemometers. *Air-Sea Interaction — Instruments and Methods.* F. Dobson, L. Hasse and R. Davis, Eds., Plenum Press, NY, 65-80.

Sommerfeld, A. (1964). *Mechanics of Deformable Bodies*, **2**. Academic Press Inc., NY, 396 pp.

Stearns, S.D. and David, R.A. (1988). *Signal Processing Algorithms.* Prentice-Hall, Inc., NJ, 349 pp.

Tennekes, H. and Lumley, J.L. (1972). *A First Course in Turbulence.* MIT Press, Cambridge, MA, 300 pp.

Tennekes, H. (1981). Similarity Relations, Scaling Laws and Spectral Dynamics. *Atmospheric Turbulence and Air Pollution Modelling.* F.T.M. Nieuwstadt and H. van Dob, Eds., Reidel Publishing Company, Dordrecht, Holland, 37-68.

Wieringa, J. (1980). A Revaluation of the Kansas Mast Influence on Measurements of Stress and Cup Anemometer Overspeeding. *Boundary-Layer Meteorol.*, **18**, 411-430.

Wieringa, J. (1982). Reply. *Boundary-Layer Meteorol.*, **22**, 251-255.

Wyngaard, J.C. and Coté, O.R. (1972). Cospectral Similarity in the Atmospheric Surface Layer. *Quart. J. Roy. Meteorol. Soc.*, **98**, 590-603.

Wyngaard, J.C., Bauman, J.T. and Lynch, R.A. (1974). Cup Anemometer Dynamics. *Proc. Instrument Society of America*, Pittsburgh, PA, May 10-14, 1971, **1**, 701-708.

Wyngaard, J.C. (1981). Cup, Propeller, Vane, and Sonic Anemometers in Turbulence Research. *Annu. Rev. Fluid Mech.*, **13**, 399-423.

Wyngaard, J.C., Businger, J.A., Kaimal, J.C. and Larsen, S.E. (1982). Comments on 'A Revaluation of the Kansas Mast Influence on Measurements of Stress and Cup Anemometer Overspeeding'. *Boundary-Layer Meteorol.*, **22**, 245-250.

Zhang, S.F, Oncley, S.P. and Businger, J.A. (1988). A Critical Evaluation of the von Kármán Constant from a New Atmospheric Surface Layer Experiment. *Proc. Eighth Symp. on Turbulence and Diffusion*, April 25-29, San Diego, CA, 148-150.

A Spectral Corrections to u-bias

The spectrum for wave numbers numerically smaller than $2\pi/\mathcal{L}_u$ is in general not too well known; it is different in different situations. However, since it is finite and since in our bias calculation it gets multiplied by k^2 before integration, its detailed behavior in this wave-number region is not important and we will just let it be constant. For very high wave numbers the spectrum will fall off much more rapidly than described by (109). In the dissipation range, i.e. in the range where $|k|$ is equal to or larger than the reciprocal of the Kolmogorov length scale

$$\eta = \left(\frac{\nu^3}{\varepsilon}\right)^{1/4}, \tag{A.1}$$

$\nu \sim 1.5\ 10^{-5}$ m^2 s^{-1} being the kinematic viscosity of air, we can safely set the spectrum equal to zero.

We use a composite spectrum of the form

$$F_u(k) = \frac{1}{2}\alpha_1\varepsilon^{2/3}\begin{cases} {\mathcal{L}'_u}^{5/3} & \text{for } 0 \le |k| \le {\mathcal{L}'_u}^{-1} \\ k^{-5/3} & \text{for } {\mathcal{L}'_u}^{-1} \le |k| < \eta^{-1} \\ 0 & \text{for } \eta^{-1} \le |k| < \infty \end{cases}, \tag{A.2}$$

to determine the order of magnitude of the overestimation in (111).

The quantity $\mathcal{L}'_u$ is not quite the same as the integral length scale $\mathcal{L}_u$ as we can see from the following argument. The value of $F_u(0)$ is proportional to $\mathcal{L}_u$ since, according to (69), (82) and Taylor's hypothesis

$$\begin{aligned} F_u(0) &= \frac{1}{U}S_u(0) = \frac{1}{U}\frac{1}{2\pi}\int_{-\infty}^{\infty} R_u(\tau)d\tau \\ &= \frac{1}{\pi}\langle u^2\rangle\frac{\mathcal{T}_u}{U} = \frac{\langle u^2\rangle\mathcal{L}_u}{\pi} \end{aligned} \tag{A.3}$$

so that

$$\langle u^2\rangle = \frac{\pi F_u(0)}{\mathcal{L}_u} = \frac{\pi}{2}\alpha_1(\varepsilon\mathcal{L}'_u)^{2/3}\frac{\mathcal{L}'_u}{\mathcal{L}_u}. \tag{A.4}$$

On the other hand, the variance is equal to the area under the spectrum, i.e.

$$\langle u^2\rangle = \int_{-\infty}^{\infty} F_u(k)dk = \frac{5}{2}\alpha_1(\varepsilon\mathcal{L}'_u)^{2/3}\left\{1 - \frac{3}{5}\left(\frac{\eta}{\mathcal{L}'_u}\right)^{2/3}\right\}. \tag{A.5}$$

Equations (A.4) and (A.5) imply

$$\mathcal{L}'_u = \frac{5}{\pi}\mathcal{L}_u\left\{1 - \frac{3}{5}\left(\frac{\eta}{\mathcal{L}'_u}\right)^{2/3}\right\} \approx \frac{5}{\pi}\mathcal{L}_u, \tag{A.6}$$

since $\mathcal{L}'_u \sim z$ and

$$\eta \sim \left(\frac{u_* z}{\nu}\right)^{-3/4} z \sim 10^{-4} z. \tag{A.7}$$

$$\begin{aligned}
\delta_u &= \alpha_1 \frac{\ell}{\ell+\Lambda} \frac{\varepsilon^{2/3}}{U^2} \left\{ \int_0^{{\mathcal{L}'_u}^{-1}} \frac{k^2\ell_0^2}{1+k^2\ell_0^2} {\mathcal{L}'_u}^{5/3} dk + \int_{{\mathcal{L}'_u}^{-1}}^{\eta^{-1}} \frac{k^2\ell_0^2}{1+k^2\ell_0^2} k^{-5/3} dk \right\} \\
&= \alpha_1 \frac{\ell}{\ell+\Lambda} \frac{(\varepsilon\ell_0)^{2/3}}{U^2} \left\{ \int_0^\infty \frac{\xi^{1/3}}{1+\xi^2} d\xi + \left(\frac{\mathcal{L}'_u}{\ell_0}\right)^{5/3} \int_0^{\ell_0/\mathcal{L}'_u} \frac{\xi^2}{1+\xi^2} d\xi \right. \\
&\qquad \left. - \int_0^{\ell_0/\mathcal{L}'_u} \frac{\xi^{1/3}}{1+\xi^2} d\xi - \int_{\ell_0/\eta}^\infty \frac{\xi^{1/3}}{1+\xi^2} d\xi \right\} \\
&\approx \alpha_1 \frac{\ell}{\ell+\Lambda} \frac{(\varepsilon\ell_0)^{2/3}}{U^2} \left\{ \frac{\pi}{\sqrt{3}} - \frac{5}{12} \left(\frac{\ell_0}{\mathcal{L}'_u}\right)^{4/3} - \frac{3}{2} \left(\frac{\eta}{\ell_0}\right)^{2/3} \right\}.
\end{aligned} \tag{A.8}$$

The u-bias will therefore with $\ell_0 = 2$ m and $z = 5$ m, say, have to be corrected down from $\pi/\sqrt{3} \approx 1.81$ to $\pi/\sqrt{3} - 0.0144 \approx 1.80$—a correction we hardly need to worry about.

The ratio between $\mathcal{L}'_u$ and η is proportional to the Reynolds number

$$Re = \frac{u_* z}{\nu} \tag{A.9}$$

to the power 3/4. As we see, it is the ratio between the numerically highest and lowest wave numbers between which the longitudinal velocity spectrum is given by the equation (109). This is three orders of magnitude or more in the surface layer and the spectrum in the dissipation is seldom of practical interest. Figure 17 shows our spectral model (without the dissipation range).

B Discrete Rice Theory

We consider the time series $\tilde{u}(t) = U + u$ being sampled with the temporal resolution Δt.

If $u_0 \equiv u(n\Delta t) < \mathcal{U} - U$ and $u_1 \equiv u((n+1)\Delta t) > \mathcal{U} - U$ we know that the level $\mathcal{U}$ has been up-crossed at least once in the period from $n\Delta t$ to $(n+1)\Delta t$. If we call the probability for this event $\mathrm{Prob}(u_0 < \mathcal{U} - U, u_1 > \mathcal{U} - U)$ then the lower limit of the average number of times the level $\mathcal{U}$ has been exceeded in the period of time $T = N\Delta t$ is $N\mathrm{Prob}(u_0 < \mathcal{U} - U, u_1 > \mathcal{U} - U)$ and the corresponding lower limit of the average rate becomes

$$\begin{aligned}
\eta'_{\mathcal{U}} &= \frac{N}{T} \mathrm{Prob}(u_0 < \mathcal{U} - U, u_1 > \mathcal{U} - U) \\
&= \mathrm{Prob}(u_0 < \mathcal{U} - U, u_1 > \mathcal{U} - U)/\Delta t.
\end{aligned} \tag{B.1}$$

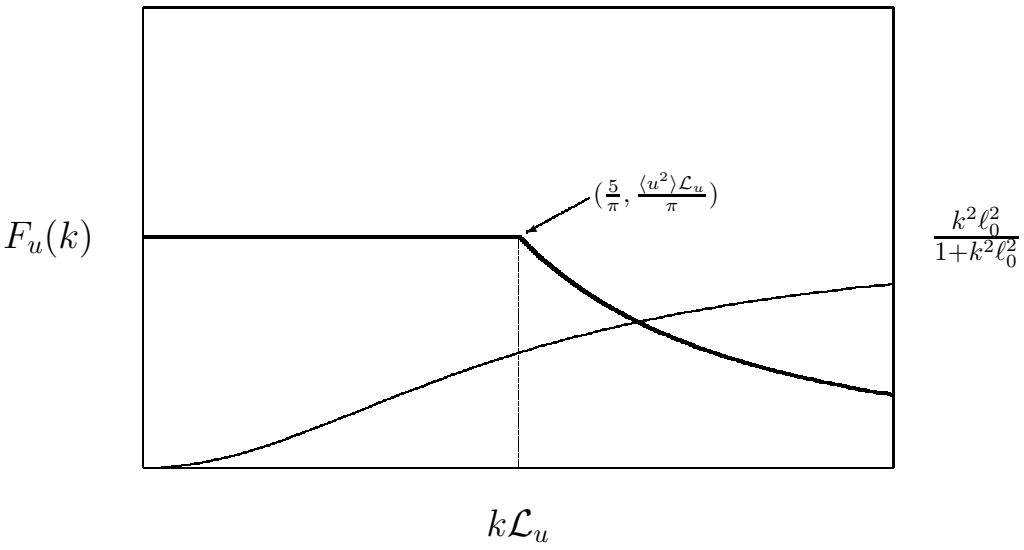

Figure 17. The simple spectrum (A.2) (thick line) and the u-bias high-pass filter (thin line). Note that the axes are linearly scaled.

When the temporal resolution becomes extremely good, i.e. when $\Delta t \to 0$, then $\eta'_{\mathcal{U}}$ becomes the true excursion rate beyond $\mathcal{U}$, viz.

$$\lim_{\Delta t \to 0} \eta'_{\mathcal{U}} = \eta_{\mathcal{U}}. \tag{B.2}$$

Let $\tilde{P}(u_0, u_1)$ be the joint probability density of u_0 and u_1. Then

$$\text{Prob}(u_0 < \mathcal{U} - U, u_1 > \mathcal{U} - U) = \int_{-\infty}^{\mathcal{U}-U} du_0 \int_{\mathcal{U}-U}^{\infty} du_1 \tilde{P}(u_0, u_1). \tag{B.3}$$

We introduce the transformation

$$\left.\begin{array}{rcl} u_c &=& \frac{1}{2}(u_0 + u_1) \\ \Delta u &=& u_1 - u_0 \end{array}\right\} \Longleftrightarrow \left\{\begin{array}{rcl} u_0 &=& u_c - \Delta u/2 \\ u_1 &=& u_c + \Delta u/2 \end{array}\right. \tag{B.4}$$

of the integration variables, and since the Jacobian is one, we can reformulate (B.3) in the following way:

$$\text{Prob}(u_0 < \mathcal{U} - U, u_1 > \mathcal{U} - U) = \int_0^{\infty} d\Delta u \int_{\mathcal{U}-U-\Delta u/2}^{\mathcal{U}-U+\Delta u/2} du_c P(u_c, \Delta u), \tag{B.5}$$

where

$$P(u_c, \Delta u) \equiv \tilde{P}(u_c - \Delta u/2, u_c + \Delta u/2). \tag{B.6}$$

For small values of Δt the jump Δu will usually be small compared to u_c when $u_c \sim \mathcal{U} - U$. Stated differently, the probability density $P(u_c, \Delta u)$ in this domain is relatively small when $\Delta u \gtrsim u_c$. Therefore we can approximate the last integral in (B.5) by $\Delta u P(\mathcal{U} - U, \Delta u)$ so that

$$\text{Prob}(u_0 < \mathcal{U} - U, u_1 > \mathcal{U} - U) \approx \int_0^{\infty} \Delta u P(\mathcal{U} - U, \Delta u) d\Delta u. \tag{B.7}$$

Inserting (B.7) in (B.1), the rate $\eta'_{\mathcal{U}}$ becomes

$$\eta'_{\mathcal{U}} = \frac{1}{\Delta t}\int_0^\infty \Delta u P(\mathcal{U}-U,\Delta u)d\Delta u. \tag{B.8}$$

We see that in the limit $\Delta t \to 0$ (B.8) becomes identical to (253).

We note that u_c and Δu as defined by (B.4) are uncorrelated. If $\tilde{P}(u_0,u_1)$ were joint Gaussian then $P(u_c,\Delta u)$ would also be joint Gaussian and, since u_c and Δu are uncorrelated, they would in this case also be statistically independent. This means that $P(u_c,\Delta u)$ could be written as a product of two probability densities as

$$P(u_c,\Delta u) = P_1(u_c)P_2(\Delta u). \tag{B.9}$$

If we assume that (B.9) is true in general we can determine $\eta'_{\mathcal{U}}$ for any probability density of u_c and in particular allow for the possibility that u_c has a large positive skewness and $P_1(u_c)$ a correspondingly 'long tail to the right'.

However, in order to be specific we will adopt the idea of Beljaars (1987) and calculate $\eta'_{\mathcal{U}}$ with $\tilde{P}(u_0,u_1)$ being joint Gaussian, i.e.

$$\tilde{P}(u_0,u_1) = \frac{\exp\left(-\dfrac{u_0^2-2\rho_u u_0 u_1+u_1^2}{2\langle u^2\rangle(1-\rho_u^2)}\right)}{2\pi\langle u^2\rangle\sqrt{1-\rho_u^2}}, \tag{B.10}$$

where

$$\rho_u = \rho_u(\Delta t) = \frac{\langle u_0 u_1\rangle}{\langle u^2\rangle} = \frac{R_u(\Delta t)}{R_u(0)} \tag{B.11}$$

is the correlation between u_0 and u_1.

Since

$$\langle \Delta u^2\rangle \equiv \langle (u_1-u_0)^2\rangle = 2\langle u^2\rangle(1-\rho_u), \tag{B.12}$$

$P(u_c,\Delta u)$ becomes

$$P(u_c,\Delta u) = \frac{\exp\left(-\dfrac{u_c^2}{(1+\rho_u)\langle u^2\rangle}\right)}{\sqrt{(1+\rho_u)\pi\langle u^2\rangle}}\ \frac{\exp\left(-\dfrac{\Delta u^2}{2\langle \Delta u^2\rangle}\right)}{\sqrt{2\pi\langle \Delta u^2\rangle}}. \tag{B.13}$$

Inserting (B.13) in (B.8), we get

$$\begin{aligned}\eta'_{\mathcal{U}} &= \frac{\sqrt{\langle \Delta u^2\rangle}}{\Delta t}\ \frac{\exp\left(-\dfrac{(\mathcal{U}-U)^2}{(1+\rho_u)\langle u^2\rangle}\right)}{\sqrt{(1+\rho_u)2\pi^2\langle u^2\rangle}} \\ &\approx \frac{\sqrt{\langle \Delta u^2\rangle}}{\Delta t}\ \frac{\exp\left(-\dfrac{(\mathcal{U}-U)^2}{2\langle u^2\rangle}\right)}{2\pi\sqrt{\langle u^2\rangle}}.\end{aligned} \tag{B.14}$$

With the assumption that $P(u_c, \Delta u)$ is given by (B.13), we can actually quantify the condition that (B.7) is a good approximation to (B.5) by calculating a correction factor to (B.14). We proceed as follows:

Let

$$x = \frac{\mathcal{U} - U}{\sqrt{(1+\rho_u)\langle u^2\rangle}} \tag{B.15}$$

and

$$\epsilon = \frac{\Delta u}{\sqrt{(1+\rho_u)\langle u^2\rangle}}. \tag{B.16}$$

Then

$$\begin{aligned}
\int_{\mathcal{U}-U-\Delta u/2}^{\mathcal{U}-U+\Delta u/2} P_1(u_c)du_c &= \int_{\mathcal{U}-U-\Delta u/2}^{\mathcal{U}-U+\Delta u/2} \exp\left(-\frac{u_c^2}{(1+\rho_u)\langle u^2\rangle}\right) \frac{du_c}{\sqrt{(1+\rho_u)\pi\langle u^2\rangle}} \\
&= \frac{1}{\sqrt{\pi}} \int_{x-\epsilon/2}^{x+\epsilon/2} e^{-t^2} dt \\
&= \frac{1}{2}\{\mathrm{erfc}(x-\epsilon/2) - \mathrm{erfc}(x+\epsilon/2)\}.
\end{aligned} \tag{B.17}$$

Expanding (B.17) in power series of ϵ, we get

$$\int_{\mathcal{U}-U-\Delta u/2}^{\mathcal{U}-U+\Delta u/2} P_1(u_c)du_c \approx \frac{e^{-x^2}}{\sqrt{\pi}}\epsilon\left\{1 + (2x^2-1)\frac{\epsilon^2}{12}\right\}. \tag{B.18}$$

Instead the first line of (B.14), evaluation of (B.5) yields

$$\begin{aligned}
\eta'_{\mathcal{U}} &= \frac{\sqrt{\langle \Delta u^2\rangle}}{\Delta t} \frac{\exp\left(-\dfrac{(\mathcal{U}-U)^2}{(1+\rho_u)\langle u^2\rangle}\right)}{\sqrt{(1+\rho_u)2\pi^2\langle u^2\rangle}} \\
&\quad \times \left\{1 + \frac{1}{6}\left(2\frac{(\mathcal{U}-U)^2}{(1+\rho_u)\langle u^2\rangle} - 1\right)\frac{\langle \Delta u^2\rangle}{(1+\rho_u)\langle u^2\rangle}\right\}.
\end{aligned} \tag{B.19}$$

We see immediately that the correction factor is close to one if the following two conditions are fulfilled:

$$\frac{\langle \Delta u^2\rangle}{(1+\rho_u)\langle u^2\rangle} = 2\frac{1-\rho_u}{1+\rho_u} \ll 1 \tag{B.20}$$

and

$$2\frac{1-\rho_u}{1+\rho_u}\,\frac{(\mathcal{U}-U)^2}{(1+\rho_u)\langle u^2\rangle} \ll 1. \tag{B.21}$$

Assuming that $U\Delta t$ is much smaller than length the scale $\mathcal{L}_u$, we may use the spectrum (109) to obtain an approximate expression for ρ_u. The result is

$$\rho_u = \rho_u(\Delta t) \approx 1 - \frac{3}{4}\Gamma\left(\frac{1}{3}\right)\alpha_1\frac{(\varepsilon U\Delta t)^{2/3}}{\langle u^2\rangle}. \tag{B.22}$$

Under neutral conditions the expressions (120) with (128) and (275) apply and (B.22) can be written in the form

$$1 - \rho_u \approx 0.43 \left(\frac{U\Delta t}{z} \right)^{2/3}. \tag{B.23}$$

If Δt is set equal to the time for one revolution of a cup anemometer rotor with the calibration distance ℓ, then $U\Delta t = 2\pi\ell$ and (B.23) becomes

$$1 - \rho_u \approx 1.5 \left(\frac{\ell}{z} \right)^{2/3}. \tag{B.24}$$

The Risø cup anemometer has $\ell = 0.2$, which means that for $z = 10$ m, $1 - \rho_u$ will be about 0.11. Setting $\mathcal{U} - U$ equal to 2 standard deviations, say, the correction factor in (B.19) becomes 1.06.

Assuming that $1 - \rho_u$ is small compared to one, we can expand (B.19) in powers of this quantity. The result to first order is

$$\begin{aligned} \eta'_{\mathcal{U}} &\approx \frac{\sqrt{\langle \Delta u^2 \rangle}}{\Delta t} \frac{\exp\left(-\dfrac{(\mathcal{U} - U)^2}{2\langle u^2 \rangle} \right)}{2\pi\sqrt{\langle u^2 \rangle}} \\ &\quad \times \left\{ 1 - \frac{1}{6} \left(\frac{(\mathcal{U} - U)^2}{\langle u^2 \rangle} - 1 \right) (1 - \rho_u) \right\}. \end{aligned} \tag{B.25}$$

We see that to the first order in $1 - \rho_u$ the correction factor is one if $\mathcal{U} - U$ is exactly one standard deviation.

Returning to the approximation (B.14) and comparing this result with (257), we see that the expressions for $\eta_{\mathcal{U}}$ and $\eta'_{\mathcal{U}}$ are nearly the same and, in fact, become identical in the limit $\Delta t \to 0$. Instead of $\sqrt{\langle \dot{u}^2 \rangle}$, we must determine $\sqrt{\langle \Delta u^2 \rangle}/\Delta t$ in order to evaluate $\eta'_{\mathcal{U}}$.

Using (B.12), we get

$$\begin{aligned} \langle \Delta u^2 \rangle &= 2\{R_u(0) - R_u(\Delta t)\} \\ &= 2 \int_{-\infty}^{\infty} \{1 - \cos(\omega \Delta t)\} S_u(\omega) d\omega \\ &= \Delta t^2 \int_{-\infty}^{\infty} \operatorname{sinc}^2 \left(\frac{\omega \Delta t}{2} \right) \omega^2 S_u(\omega) d\omega. \end{aligned} \tag{B.26}$$

In (B.26) we are considering the unfiltered signal, but if we take the filtering by the cup anemometer into account we see that the result means that (264) and (266) in the case of discrete sampling must be replaced by

$$\begin{aligned} \frac{\langle \Delta s^2 \rangle}{\Delta t^2} &= \frac{1}{\ell^2} \int_{-\infty}^{\infty} \operatorname{sinc}^2 \left(\frac{\omega \Delta t}{2} \right) \frac{\omega^2 S_u(\omega)}{1 + \omega^2 \tau_0^2} d\omega \\ &= \frac{U^2}{\ell^2} \int_{-\infty}^{\infty} \operatorname{sinc}^2(\pi k \ell) \frac{k^2 F_u(k)}{1 + k^2 \ell_0^2} dk, \end{aligned} \tag{B.27}$$

where ℓ is the calibration distance given by (4).

Assuming the spectrum (109), we get instead of (267)

$$\frac{\langle \Delta s^2 \rangle}{\Delta t^2} = \frac{\alpha_1}{2} (\varepsilon \ell_0)^{2/3} \left(\frac{U}{\pi \ell^2} \right)^2 I\left(2\pi \frac{\ell}{\ell_0} \right), \tag{B.28}$$

where

$$I(x) = \int_0^\infty \{1 - \cos(xs)\} \frac{s^{-5/3}}{1+s^2} ds. \tag{B.29}$$

Kristensen *et al.* (1991) found

$$\begin{aligned} I(x) &= \frac{\pi}{\sqrt{3}} \{\cosh(x) - 1\} \\ &\quad - \frac{9\sqrt{3}\,\pi^{3/2}}{10\Gamma(1/3)\Gamma(5/6)} \left(\frac{x}{2} \right)^{8/3} {}_1F_2\left(1; \frac{7}{3}, \frac{11}{6}; \left[\frac{x}{2} \right]^2 \right), \end{aligned} \tag{B.30}$$

where ${}_1F_2(a; b, c; z)$ is one of the generalized hypergeometric functions (Gradshteyn and Ryzhik, 1980).

For $x \lesssim 1$, $I(x)$ can be approximated by

$$I(x) \approx \frac{\pi x^2}{2\sqrt{3}} \left\{ 1 - \frac{27\sqrt{\pi}\, 2^{-5/3}}{10\Gamma(1/3)\Gamma(5/6)} x^{2/3} \right\} \approx \frac{\pi x^2}{2\sqrt{3}} \{1 - 0.50\, x^{2/3}\} \tag{B.31}$$

with the consequence that (B.28) becomes

$$\frac{\langle \Delta s^2 \rangle}{\Delta t^2} \approx \frac{\pi}{\sqrt{3}} \alpha_1 (\varepsilon \ell_0)^{2/3} \frac{U^2}{\ell^2 \ell_0^2} \left\{ 1 - 1.70 \left(\frac{\ell}{\ell_0} \right)^{2/3} \right\}. \tag{B.32}$$

In other words, $\eta_{\mathcal{U}}$ is reduced by the factor

$$\frac{\eta'_{\mathcal{U}}}{\eta_{\mathcal{U}}} = \sqrt{1 - 1.70 \left(\frac{\ell}{\ell_0} \right)^{2/3}}. \tag{B.33}$$

Replacing $\sqrt{\langle \dot{s}^2 \rangle}$ by $\sqrt{\langle \Delta s^2 \rangle / \Delta t^2}$ in (271), the apparent dimensionless gust μ' can be expressed in terms of the real dimensionless gust μ given by (278) as

$$\mu' \approx \mu - \frac{0.85}{\mu} \left(\frac{\ell}{\ell_0} \right)^{2/3}. \tag{B.34}$$

Strictly speaking, the results (B.33) and (B.34) are based on the assumption that the cup-anemometer rotor turns with a constant angular velocity when the wind speed is constant. As I pointed out in subsection 2.8 this is usually not the case. Therefore, we will usually average the cup-anemometer signal over at least one full revolution. If we want to have the best possible temporal resolution, we average over just one revolution and consequently the low-pass filter will be given by (136), i.e.

$$H(k) = \frac{\mathrm{sinc}^2(\pi k \ell)}{1 + k^2 \ell_0^2},$$

which I repeat here for convenience.

As a consequence, the expressions for $\langle \dot{s}^2 \rangle$ and $\langle \Delta s^2 \rangle / \Delta t^2$ should be modified accordingly.

The first will now be given by (B.28), i.e.

$$\frac{\langle \Delta s^2 \rangle}{\Delta t^2} = \frac{\alpha_1}{2} (\varepsilon \ell_0)^{2/3} \left(\frac{U}{\pi \ell^2} \right)^2 I\left(2\pi \frac{\ell}{\ell_0} \right), \tag{B.35}$$

where $I(x)$ is given by (B.30), whereas $\langle \Delta s^2 \rangle / \Delta t^2$ becomes

$$\frac{\langle \Delta s^2 \rangle}{\Delta t^2} = \alpha_1 (\varepsilon \ell_0)^{2/3} \left(\frac{U}{\pi \ell^2} \right)^2 \left(2\pi \frac{\ell}{\ell_0} \right)^{-2} J\left(2\pi \frac{\ell}{\ell_0} \right), \tag{B.36}$$

where

$$J(x) = \int_0^\infty \{1 - \cos(xs)\}^2 \frac{s^{-11/3}}{1+s^2} ds. \tag{B.37}$$

This integral can also be evaluated analytically as

$$\begin{aligned} J(x) &= \frac{\pi}{\sqrt{3}} \{\cosh(x) - 1\}^2 \\ &\quad - \frac{162\sqrt{3}\pi^{3/2}}{385\Gamma(1/3)\Gamma(5/6)} \left\{ \frac{x^{14/3}}{4} {}_1F_2\left(1; \frac{10}{3}, \frac{17}{6}; x^2 \right) \right. \\ &\qquad \left. - \left(\frac{x}{2} \right)^{14/3} {}_1F_2\left(1; \frac{10}{3}, \frac{17}{6}; \left[\frac{x}{2} \right]^2 \right) \right\} \end{aligned} \tag{B.38}$$

For $x \lesssim 1$, $J(x)$ is given approximately by

$$\begin{aligned} x^{-2} J(x) &\approx \frac{\pi x^2}{4\sqrt{3}} \left\{ 1 - \frac{486\sqrt{\pi}(1 - 2^{-8/3})}{385\Gamma(1/3)\Gamma(5/6)} x^{2/3} \right\} \\ &\approx \frac{\pi x^2}{4\sqrt{3}} \{1 - 0.62\, x^{2/3}\}. \end{aligned} \tag{B.39}$$

The modified equations for $\eta'_{\mathcal{U}} / \eta_{\mathcal{U}}$ and μ' now become

$$\frac{\eta'_{\mathcal{U}}}{\eta_{\mathcal{U}}} = \sqrt{1 - 0.425 \left(\frac{\ell}{\ell_0} \right)^{2/3}} \tag{B.40}$$

and

$$\mu' = \mu - \frac{0.21}{\mu} \left(\frac{\ell}{\ell_0} \right)^{2/3}. \tag{B.41}$$

Bibliographic Data Sheet **Risø–R–615(EN)**

Title and author(s)

The Cup Anemometer—and Other Exciting Instruments

Leif Kristensen

ISBN	ISSN
87–550–1796–7	0106–2840

Dept. or group	Date
Meterology and Wind Energy	April 1993

Groups own reg. number(s)	Project/contract No.

Pages	Tables	Illustrations	References
83		17	55

Abstract (Max. 2000 char.)

Nonlinear sensor dynamics is discussed in terms of differential equations in time with the input signal and the response as dependent variables. The cup anemometer response to the turbulent wind is analyzed in detail. Applying second-order perturbation theory, the so-called overspeeding, which is a bias in the measured mean wind speed due to fluctuations in the longitudinal wind component, is evaluated in terms of a phenomenological model of the wind forcing of the cup rotor. It is shown how the fluctuation in the other wind components give rise to three other types of bias and it is concluded that the positive bias in the mean wind speed due to wind-direction fluctuations is always largest and much larger than the overspeeding and can be as much as 18% whereas the overspeeding only in extreme cases exceeds about 2%. The differential equation describing the cup-anemometer dynamics is of only first order. However, the technique of evaluating the bias on the mean is generalized to apply to sensors with nonlinear dynamics and obeying second-order differential equations. It is then demonstrated how the bias in the mean due to random fluctuations can be determined for three other sensor, namely the Pitot tube, the thrust anemometer and the CSIRO liquid water probe. The last instrument will always have a negative bias. Returning to the discussion of the cup anemometer, it is shown how this instrument can be used together with a wind vane to reduce the bias due to wind direction fluctuations. Finally it is discussed how a precise definition of a gust can be implemented and how gusts can be determined by means of a cup anemometer.

Descriptors INIS/EDB

ANEMOMETER; EXTREME-VALUE PROBLEMS; HOT WIRE ANEMOMETERS; NONLINEAR PROBLEMS; PERTURBATION THEORY; PITOT TUBES; TURBULENCE; VELOCITY; WIND

Available on request from:
Information Service Department, Risø National Laboratory
(Afdelingen for Informationsservice, Forskningscenter Risø)
P.O. Box 49, DK–4000 Roskilde, Denmark
Phone (+45) 46 77 46 77, ext. 4004/4005 · Fax (+45) 46 77 40 13